ANALYSIS OF NMDA RECEPTOR REGULATED GENE EXPRESSION

Alison Jane Begg

A Thesis Submitted For The Degree Of Doctor Of Philosophy
The University of Edinburgh
2004

DECLARATION

I declare that the work presented in this thesis is my own, except where noted in the text and as detailed below.

Kevin Robertson (Scottish Centre for Genomic Technology and Informatics, University of Edinburgh) labelled RNA samples and performed subsequent microarray hybridisations in accordance with Affymetrix protocols.

Marie Craigon (Scottish Centre for Genomic Technology and Informatics, University of Edinburgh) performed the liquid handling of oligonucleotides and set up the spotting of custom microarrays. She used SpotCheck for quality control assessment of the spotted arrays.

Alan Ross (Scottish Centre for Genomic Technology and Informatics, University of Edinburgh) labelled and hybridised RNA samples to custom microarrays using QIAGEN RLS protocols.

Alison J. Begg

ACKNOWLEDGEMENTS

Firstly, I would like to thank my supervisor, Seth Grant, for all his support and advice over the course of my PhD. In addition, massive thanks to all members of the Grant Lab, past and present, for always giving me help when I've needed and providing me with plenty entertainment along the way. In particular, thanks to Doug for teaching me beginner's molecular biology, for being there when all we had to listen to was Moby and all his help throughout. Also, cheers to Nobby Hennakao, for his steady dissecting hands, Kris, for her motivational chats and help through all the cultures, Paul, for letting me in on the magic of multi-electrode arrays, Bence, for all the tomfoolery (complete with sound effects) and Karen and Jane for always keeping me in line.

Thank you to the other members of the Neuroscience Division who've given me advice and assistance, and also to Peter Ghazal and everyone at the SCGTI who helped me with the microarray work, particularly Kevin Robertson for knowing all things Affymetrix!

On the social side, 3 cheers to those of you who had to share an office with me. You kept me bordering on sanity and taught me valuable life lessons - I now know all I will ever need to about backgammon strategy and that coffee and chunky kit kats can cure anything! Outwith the realms of science, I'd like to thank my friends and flatmates for always providing me with amusement and suitable distractions from the lab. A special 'Big Up' to the Nairn crew (particularly the Dream Team), Anna and Sonia for all the good times and for being there when the going got tough.

Finally, Mum, Dad, Karen, Dr Fish and associated pets – **hooooooge** thanks for all your support throughout my career as a student. I know you look forward to me joining the 'real world', where I can set about following Karen's advice - *"You don't need a job, Alison....just get a dog"*.

ABBREVIATIONS

4AP	4-amino pyridine
ADG	Activity dependent gene
AMPA	α-amino-3-hydroxy-5-methylisoxazole-4-propionic acid
AP1	Activator protein 1
APV	Amino-5-phosphonovalerate
BLAST	Basic Local Alignment Search Tool
CaMKII	Calcium/calmodulin dependent kinase II
CaMKIV	Calcium/calmodulin dependent kinase IV
CBP	CREB binding protein
cDNA	Complimentary DNA
CRE	cAMP response element
CREB	cAMP response element binding protein
C_t	Cycle threshold
DIV	Days *in vitro*
DNA	Deoxyribonucleic acid
ERK	Extracellular signal regulated kinase
EST	Expressed sequence tag
GABA	γ-aminobutyric acid
IEG	Immediate early gene
IRES	Internal ribosome entry site
LTP	Long term potentiation
MAGUK	Membrane associated guanylate kinase
MEA	Multi electrode array
MECS	Maximal electro convulsive seizures
NMDA	N-methyl-D aspartate
NRC	NMDA receptor complex
PKA	Protein kinase A
PSD95	Postsynaptic density protein 95
PTZ	Pentylenetetrazole
QRT-PCR	Quantitative reverse transcription- polymerase chain reaction
RNA	Ribonucleic acid
RT-PCR	Reverse transcription- polymerase chain reaction
SCGTI	Scottish Centre for Genomic Technology and Informatics
SRE	Serum response element
SRF	Serum response factor
TCF	Ternary complex factor
TTX	Tetrodotoxin
UTR	Untranslated region
VDCC	Voltage dependent calcium channel

ABSTRACT

The N-methyl-D-aspartate (NMDA) subtype of glutamate receptors is central in spatial learning, pathological conditions such as neuropathic pain and stroke and is required for experimental paradigms of synaptic plasticity e.g. long term potentiation. These diverse and sustained cellular effects are accompanied by coordinated changes in gene expression and transcription has been shown essential in NMDA receptor dependent phenomena. The NMDA receptor is found bound to an intracellular complex of proteins that includes molecules with known involvement in signalling pathways downstream of receptor activation, including ones that can modulate gene expression.

Mutation of two NMDA receptor complex proteins, PSD95 and SynGAP, results in altered phenotypes in NMDA dependent phenomena. As components of the receptor complex, necessary for NMDA mediated signalling, mutation of these proteins may alter pathways that regulate gene expression.

Affymetrix microarray analysis of RNA from PSD95$^{-/-}$ forebrain and SynGAP$^{+/-}$ hippocampi, compared to wildtype samples, revealed significant changes, greater than 1.5 fold, in a limited numbers of genes. Of the 12000 transcripts analysed 0.22% were significantly altered in PSD95 mutant tissue and 0.35% were significantly changed in SynGAP mutant tissue. The genes altered in each genotype were distinct apart from an overlap of 3 genes that were similarly found at lower levels in PSD95$^{-/-}$ forebrain and SynGAP$^{+/-}$ hippocampi.

To study activity regulated gene expression an *in vitro* method of NMDA receptor stimulation was sought. NMDA and bicuculline treatment of primary cultured cortical neurons proved ineffective methods of inducing activity dependent gene induction as measured by *cfos* expression. However, AP5 treatment of primary cultured neurons was found to decrease activity dependent gene expression. Electrophysiological analysis of the cultures revealed that bicuculline treatment had no significant effect on culture activity, where as AP5 treatment caused a significant decrease in neuronal activity.

Microarrays are useful technique as they allow the simultaneous analysis of many transcripts. Custom microarray chips can be advantageous as they allow specification of the genes that are represented on the arrays, unlike in commercial systems. A custom chip was designed, containing approximately 250 genes of interest. Oligonucleotides, 55 base pairs in length, were designed specifically for these target genes and printed onto slides along with control probes. The slides were validated and hybridised with RNA from PSD95$^{-/-}$ and matched wild type forebrain.

CHAPTER 1

INTRODUCTION AND AIMS

1. INTRODUCTION AND AIMS

Sensing patterns of neuronal firing is fundamental to nerve function. Trains of stimulatory input potentially cause long lasting changes in neuronal properties. Understanding how a post synaptic cell detects activity and couples this to downstream effecter pathways is essential to appreciating how the brain transmits the information essential to it's function.

Ligand gated ion channels respond *in vivo* to particular neurotransmitters causing the channels to open, allowing the movement of ions. The influx of ions to the neuron can initiate signal transduction pathways with wide ranging targets that can lead to prolonged effects within the cell. These pathways include ones that can alter the neuron at a transcriptional level, regulating gene expression. Thus, changing levels of mRNA can be used to study postsynaptic cellular signalling response to stimulatory input.

The rapid advancement of molecular biological techniques has changed the way signal transduction can be studied, with technologies being developed that enable a global view of cell activity and behaviour. Microarray based techniques are being used, with increasing popularity, to simultaneously analyse the levels of thousands of RNAs. This 'snapshot' of transcriptional activity of cells under given conditions can be exploited to study effects such as differential gene expression in different tissues, cellular response to particular stimuli and changes in gene expression in diseased or mutated tissue.

Given that transcriptional analysis can be used to examine the regulation of gene expression in a neuron, microarrays could be employed to study activity of pathways stimulated by synaptic activity. Combining this with animals carrying mutations in molecules involved in signalling pathways allows the analysis of the contribution of these proteins to the regulation of gene expression.

1.1 THE NMDA RECEPTOR SIGNALING COMPLEX

1.1.1 Function and Structure of the NMDA Receptor

Ionotrophic glutamate receptors are responsible for the majority of excitatory transmission in the central nervous system (CNS). There are 3 classes of ligand gated ion channels that respond *in vivo* to glutamate in the CNS; α-amino-3-hydroxy-5-methylisoxazole-4-propionic acid (AMPA), N-methyl-D-aspartate (NMDA) and kainate receptors. The NMDA receptor is found, predominantly, at postsynaptic sites in the CNS. It plays a role in behavioural tasks such as spatial learning, has function in pathological conditions such as neuropathic pain and is required for experimental paradigms of synaptic plasticity, e.g. long term potentiation (LTP) (Collingridge *et al.*, 1983; Morris *et al.*, 1986; Mayer *et al.*, 1999).

The NMDA receptor subunits were cloned in the early 1990s (Moriyoshi *et al.*, 1991; Kutsuwada *et al.*, 1992; Meguro *et al.*, 1992). The receptor is made up of at least one obligatory NR1 subunit and at least 2 NR2(A-D) subunits and is thought to be tetrameric in structure. The receptor is cation selective and, in particular, it is its permeability to Ca^{2+} ions that is important in the activation of signalling pathways within the neuron.

The NMDA receptor is critical for viability and animals that constitutively lack the NR1 or NR2B subunits die neonatally (Forrest *et al.*, 1994; Kutsuwada *et al.*, 1996). Animals lacking the NR2A receptor subunit are viable, but have reduced LTP in the hippocampus and impaired spatial learning (Sakimura *et al.*, 1995). By restrictive knockout of the NR1 subunit in the CA1 region it has been demonstrated that NR1 is required for CA1 LTP and spatial memory (Tsien *et al.*, 1996). In addition, it has been demonstrated that over expression of the NR2B subunit can improve performance in spatial learning tasks (Tang *et al.*, 1999).

1.1.2 Composition of the NRC

The intracellular C termini of NMDA receptor subunits can bind postsynaptic proteins and many components of a NMDA Receptor Complex (NRC) have been isolated (Husi *et al.*, 2000). At least 77 proteins have been identified to be within the NRC and the proteins within the complex have potentially many more binding partners.

Proteins of the NRC can be classified by their function. The key components are the subunits of the NMDA receptor and metabatropic glutamate receptor. The NMDA receptor subunits can directly bind adaptor proteins such as PSD95, SAP102 and Yotiao. These molecules have specific domains to facilitate protein-protein interaction and can act as scaffolding within the complex, with the potential to bind multiple proteins. Protein kinase A (PKA) subunits, protein kinase C isoforms and various other signalling proteins are found within the complex, including numerous molecules of the Ras-ERK pathways. Additionally, multiple cell adhesion and cytoskeletal proteins are present.

It is unlikely that the NRC exists as a static complex of bound proteins. It is more probable that NRCs are dynamic structures, the components of which can be determined by differential protein expression or response to synaptic input. With the numbers of proteins that have been identified as NRC components this could result in a wide variety of NRC structures, appropriate to different synaptic response, in various synapses across the nervous system.

1.1.3 Signalling Molecules Within the NRC

A complex of proteins, including structural, signalling and adaptor molecules, that can bind NMDA receptor subunits offers an attractive model for the organisation of postsynaptic signalling. It is hypothesised that the function of the NRC is to orchestrate the signalling pathways downstream of receptor activation. With

appropriate enzymes and substrates being brought within close proximity of each other, signal transduction could be coordinated, allowing specificity within the signalling network. This would enable effective transmission of a signal, initiated by receptor activation, within the neuron.

Components of several signalling pathways, essential to NMDA receptor mediated effects, have been identified as NRC proteins (see figure 1.1). For example, CaM Kinase II (CaMKII) and PKA, both critical for NMDA dependent phenomena such as LTP and hippocampal based learning (Silva *et al.*, 1992; Huang and Kandel, 1994; Bach *et al.*, 1995; Mayford *et al.*, 1996; Abel *et al.*, 1997) are found within the NRC. Another key pathway, downstream of NMDA receptor activity, with molecules within the NRC is the ras-ERK pathway.

The ras-ERK pathway is critical for NMDA receptor dependent effects. The key sequential kinase components of the pathway, [ras-raf-MEK-ERK], are all found within the NRC (Husi *et al.*, 2000). Additionally, SynGAP, a regulator of the pathway, is also found within the complex. A rasGAP (ras GTPase Activating Protein) protein, SynGAP promotes the hydrolysis of GTP, maintaining ras in an inactive, GDP bound state. As such, is thought to be a negative regulator of the ras-ERK kinase pathway (Kim *et al.*, 1998).

When CaMKII is active it inhibits the activity of SynGAP (Chen *et al.*, 1998), maintaining ras in an activated GTP bound state. It is hypothesised that, upon NMDA receptor mediated calcium entry to the cell, CaMKII becomes phosphorylated causing the inhibition of SynGAP. The removal of this negative regulation would act to initiate the ras-ERK Kinase pathway.

LTP stimulation and contextual learning activate the ras-ERK pathway (English and Sweatt, 1996; Atkins *et al.*, 1998) and MEK inhibition impairs the induction of LTP and causes deficits in spatial memory (Blum *et al.*, 1999; Adams and Sweatt, 2002).

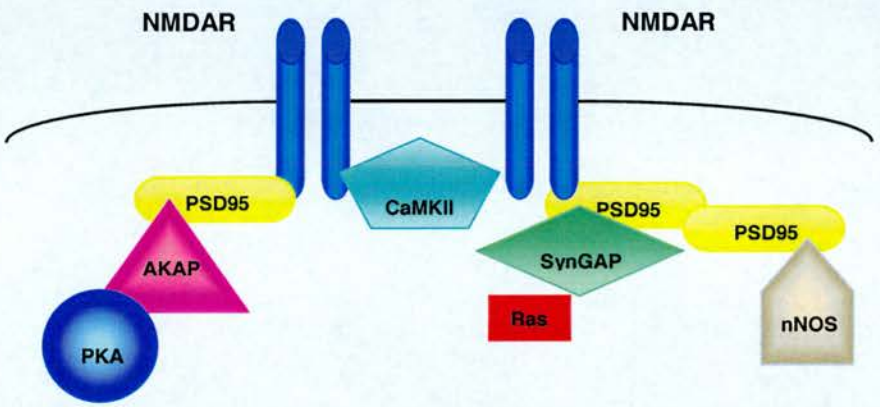

Figure 1.1 – Signalling Molecules Within The NRC. Schematic diagram shows the protein-protein interactions of signalling molecules within the NRC. CaMKII and PSD95 can both directly interact with the NMDA receptor. PKA, via AKAP, can interact with PSD95. SynGAP and nNOS both directly bind PSD95. SynGAP can act to regulate the ERK signalling pathway via Ras.

Mice lacking ERK2 die during development (Adams and Sweatt, 2002), however mice lacking ERK1 have reduced hippocampal LTP induced by theta burst stimulation, although LTP induced by 100Hz stimulation is as wild type (Mazzucchelli *et al.*, 2002). It is apparent that the ras-ERK pathway is critical for cellular response to stimulation at the NMDA receptor. The NRC may act to maintain the molecular components of the pathway in close proximity to each other and the receptor, ensuring effective activation of the Ras-ERK signalling pathway upon receptor stimulation.

1.1.4 Effects of Mutating NRC Proteins

The interest in NMDA receptor mediated effects has lead to a wide application of transgenic analysis in the research of learning and plasticity. This, combined with behavioural, molecular and electrophysiological studies, has helped elucidate the function of particular proteins involved in NMDA dependent phenomena, including learning and memory (reviewed by Matyina *et al.*, 2002). Phenotypes in NMDA receptor dependent effects are found in mice carrying mutations in NRC proteins. Mutations of two such proteins, PSD95 and SynGAP, are discussed further below.

1.1.3.1 PSD95

PSD95 was first identified enriched in rat brain post synaptic densities (Cho *et al.*, 1992) and was found to be a homolog of *Drosophila* suppressor gene, *dlg*, product (Woods and Bryant, 1991). It belongs to a family of proteins known as the MAGUKs (Membrane Associated GUanylate Kinases). MAGUKs share a common structure of 3 PDZ domains, 1GK and 1SH3 domain. These distinct binding domains enable protein-protein interactions, allowing the MAGUKs to function as adaptors within protein complexes.

PSD95 is expressed widely across the developing and adult brain (Fukaya *et al.*, 1999) (see figure 1.2A) and binds directly to NR2A and NR2B subunits (Kornau *et*

al., 1995; Niethammer *et al.*, 1996). Additional binding partners include other proteins found in the NRC, e.g. nNOS (Brenman *et al.*, 1996), and PSD95 is thought integral to the receptor complex in the hippocampus.

Migaud *et al.*, 1998 showed that mice carrying a mutant form of PSD95 have altered LTP and spatial memory. The mutation was generated by the introduction of a stop codon to the third PDZ domain resulting in the expression of a truncated protein, no longer localised to the post synaptic density or capable of binding NMDA receptor subunits. PSD95$^{-/-}$ mice have normal synaptic localisation of NMDA receptors and no alterations in NMDA currents. However, LTP induced at 100Hz is significantly enhanced in mutant cells. Indeed, across a range of stimulation frequencies, PSD95$^{-/-}$ hippocampal slices show increased potentiation as compared to wild type. PSD95$^{-/-}$ mice also have a marked impairment in the hidden platform transfer test of the Morris water maze, demonstrating a deficit in spatial memory (Migaud *et al.*, 1998).

The widespread expression of PSD95, localised with NMDA receptors, could indicate a role for the NMDA-PSD95 interaction in signalling pathways outwith the hippocampus. Indeed, Fagiolini *et al.*, 2003 showed that PSD95 mutant animals show impaired NMDA mediated plasticity in the visual cortex. Also, the animals do not develop hyperalgesia and allodynia in a model of neuropathic pain within the spinal cord (Garry *et al.*, 2003).

Published data shows mutation of PSD95 can impair NMDA receptor mediated phenomena in the hippocampus, cortex and spinal cord, showing the necessity of the NMDA receptor-PSD95 interaction across the nervous system. NMDA receptors are correctly localised and have wildtype currents in the hippocampus of PSD95$^{-/-}$ animals (Migaud *et al.*, 1998). This suggests that the mechanism of the mutant phenotypes is not due to changes in NMDA receptor expression or properties, but lies downstream of receptor activation.

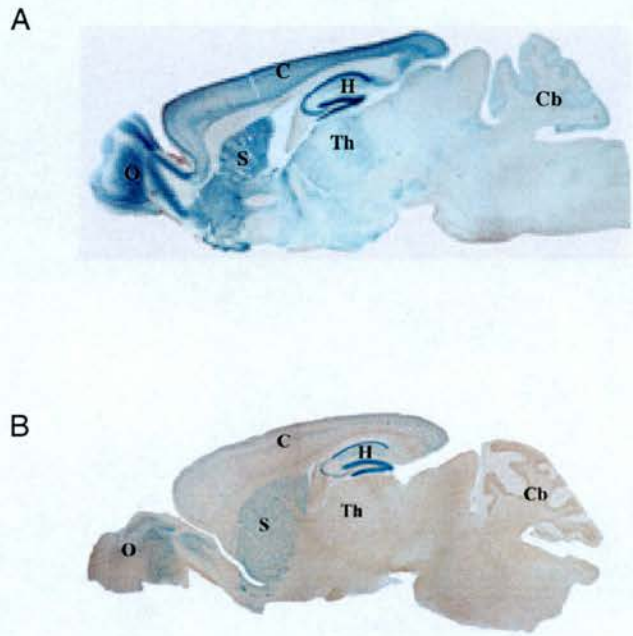

Figure 1.2 - Expression of PSD95 and SynGAP in the Adult Brain. Images show the expression of PSD95 (A) and SynGAP (B) in the adult brain. The images show the expression of β galactosidase, measured by LacZ staining, under the regulation of the PSD95 (**A**) and SynGAP (**B**) promoters. The olfactory bulb (O), striatum (S), cortex (C), hippocampus (H), thalamus (Th) and cerebellum (cb) are all indicated. The expression of PSD95 is widespread in the adult brain, the expression of SynGAP is more restricted, and is most highly seen in the hippocampus. (Images provided by Karen Porter).

1.1.3.2 SynGAP

As previously discussed, SynGAP is hypothesised to be a key regulator of the ras-ERK pathway, downstream of NMDA receptor activation. The expression of SynGAP in the brain is dynamic through development and overlaps, to degree, with the expression of PSD95. By adulthood, the expression of SynGAP is much more restricted than PSD95 and is highly enriched in the hippocampus, with lower expression in the cortex and amygdala (K. Porter, personal communication; see figure 1.2B).

Mice, homozygote for mutated SynGAP, die in early postnatal days suggesting a role for the protein in development (Komiyama *et al.*, 2002; Kim *et al.*, 2003). Due to the lethality of the mutation, there is a limit to the analysis that can be done on the homozygote animals, however analysis of SynGAP heterozygote mice does reveal phenotypes. SynGAP$^{+/-}$ hippocampal slices show diminished LTP, as compared to wildtype, after 100Hz stimulation. Also, NMDA stimulated SynGAP$^{+/-}$ hippocampal slices show higher levels of pERK than in wild type slices, consistent with the hypothesised action of SynGAP in the Ras-ERK pathway. SynGAP$^{+/-}$ animals have impaired performance in the Morris water maze, suggesting a hippocampal based deficit in learning and memory (Komiyama *et al.*, 2002). Additionally, animals carrying mutations in SynGAP fail to develop clear 'barrels', the discrete patterns, replicating the whisker pad, formed by layer IV granule cells, in the somatosensory cortex (P. Kind, personal communication).

Taken together, the data from PSD95 and SynGAP mutant animals demonstrate that the disruption of NRC proteins leads to the impairment of NMDA mediated effects downstream of receptor activity. The expression of PSD95 and SynGAP is overlapping in some areas of the brain (see figure 1.2) and in the hippocampus both are required for wildtype learning and plasticity. However, in other areas of the

brain the molecules act in independent NMDA receptor mediated phenomena. For example, SynGAP is not expressed in the spinal cord. Also, despite PSD95 expression in the cortex, $PSD95^{-/-}$ animals have no barrel cortex phenotype like that of the $SynGAP^{+/-}$ animals (P. Kind, personal communication).

It is apparent that PSD95 and SynGAP are required for overlapping and distinct neuronal functions. Thus, it appears that various molecules and signalling pathways are key for the various NMDA dependent phenomena in different parts of the CNS. This would be consistent with the hypothesis that the NRC is a highly dynamic structure, with its components altering depending on NMDA receptor function, in a given brain region.

1.2 ACTIVITY DEPENDENT TRANSCRIPTION

NMDA receptor signalling has various downstream effector targets, one of which is transcription. There is a great deal of evidence of activity regulated gene expression, i.e. synaptic activity can trigger signalling pathways that regulate expression of transcripts known as activity dependent genes (ADGs). NMDA receptor activity is critical for the regulation of particular genes following synaptic stimulation and alterations in gene expression could be required to facilitate long term cellular changes in response to stimulatory input. Indeed, transcriptional inhibitors block the maintenance of NMDA receptor dependent late phase hippocampal LTP (Nguyen *et al.*, 1994).

1.2.1 Activity Dependent Genes

Table 1.1 details genes known to be regulated by NMDA receptor activity in the hippocampus or cortex and shows examples of the stimulation protocols used to establish them as ADGs.

GENE	TISSUE SOURCE	STIMULATION	REFERENCE
Activin βA	Rat	MECS induction, *in vivo* LTP	Andreasson and Worley, 1995
	Rat	Kainate treatment, PTZ treatment, *in vivo* LTP	Inokuchi *et al.*, 1996
Arc/Arg3.1	Rat	MECS induction, *in vivo* LTP	Lyford *et al.*, 1995
Arcadlin	Rat	MECS induction, *In vivo* LTP	Yamagata *et al.*, 1999
BDNF	Rat	Seizure induction	Springer et al., 1994
	Rat	*In vivo* LTP	Dragunow *et al.*, 1993
Cfos	1° cerebellar granule cells	NMDA treatment of cells	Szekely *et al.*, 1987
	1° hippocampal rat cells	Glutamate treatment of cells	Bading *et al.*, 1995
	Rat	Quinolinic acid to striatum	Shan *et al.*, 1997
Cjun	1° hippocampal rat cells	Glutamate treatment of cells	Bading *et al.*, 1995
	1° cerebellar granule cells	Glutamate treatment of cells	Szekely *et al.*, 1990
Cns-1	Differentiating 1° cerebellar cells (rat)	NMDA treatment of cultured cells	Bulleit *et al.*, 1994
Cox-2	Rat	MECS induction, *in vivo* LTP	Yamagata *et al.*, 1993
Egr1/krox24/zif268	Rat	*In vivo* LTP	Cole *et al.*, 1989
	1° cerebellar granule cells	Glutamate treatment of cells	Szekely *et al.*, 1990
	1° hippocampal rat cells	Glutamate treatment of cells	Bading *et al.*, 1995
	Rat	MECS induction, *in vivo* LTP	French *et al.*, 2001
Egr2/krox 20	Rat	Kainate treatment, *In vivo* LTP	Inokuchi *et al.*, 1996
Egr3	Rat	MECS induction	Yamagata *et al.*, 1994
Egr4	Rat	Kainate treatment	Honkaniemi and Sharp, 1999
FosB	1° hippocampal rat cells	Glutamate treatment of cells	Bading *et al.*, 1995
GDH	Rat	Induced by Morris water maze training	Cavallaro *et al.*, 1997
GR33	Rat	*In vivo* LTP	Smirnova *et al.*, 1993
Homer/Vesl	Rat	Kainate treatment, *in vivo* LTP	Kato *et al.*, 1997
	Rat	MECS induction, *in vivo* LTP	French *et al.*, 2001

CONTINUED OVER PAGE

TABLE CONTINUED

IAP	Rat	Induced by avoidance training, NMDA injection to DG	Huang *et al.*, 1998
JunB	1^{o} hippocampal rat cells	Glutamate treatment of cells	Bading *et al.*, 1995
	1^{o} cerebellar granule cells	Glutamate treatment of cells	Szekely *et al.*, 1990
Narp	Rat	MECS induction, *in vivo* LTP	Tsui *et al.*, 1996
Neuritin	Rat / 1^{o} hippocampal and cortical rat cells	Kainate treatment / NMDA treatment of cells	Naeve *et al.*, 1997
NR2a	1^{o} cerebellar Granule Cells (rat)	KCl and NMDA treatment of cultured cells	Bessho *et al.*, 1994
Nur77	1^{o} hippocampal rat cells	Glutamate treatment of cells	Bading *et al.*, 1995
	Rat	Mechanical injury, *In vivo* LTP	French *et al.*, 2001
	Mouse	MECS induction	French *et al.*, 2001
Pim1	Rat	PTZ treatment, Kainate treatment, *in vivo* LTP	Konietzko *et al.*, 1999
Pip92	Mouse / H19-7 cells (rat)	Convulsive dosage NMDA / NMDA treatment of cells	Chung *et al.*, 2000
Presenilin-1	SK-N-SH human neuroblastoma cells	NMDA treatment of cells	Mitsuda *et al.*, 2001
Rheb	Rat	MECS induction, *in vivo* LTP	Yamagata *et al.*, 1994
RYR2	Rat	Induced by Morris water maze training	Cavallaro *et al.*, 1997
Somatostatin	1^{o} hypothalamic Cells (rat)	NMDA treatment of cells	Rage *et al.*, 1993
TPA	Rat	Metrazol induced seizure, kindling, *in vivo* hippocampal LTP	Qian *et al.*, 1993
TrkB	Rat	*In vivo* LTP	Dragunow *et al.*, 1997

Table 1.1 – Activity Regulated Genes. Table details genes regulated by NMDA receptor activity and how they have been shown to be activity regulated, with references.

1.2.1.1 Studying Activity Dependent Gene Expression

NMDA receptor regulated gene expression can be analysed in a variety of ways. The NMDA receptor can be specifically activated in order to induce transcription downstream of receptor activity. Many different approaches, both *in vivo* and *in vitro,* have been used to analyse the expression of activity dependent genes following NMDA receptor stimulation.

In vivo stimulation assays include the induction of LTP by trains of high frequency in anaesthetised or awake rats (Inokuchi *et al.*, 1996; Matsuo *et al.*, 1998; Konietzko *et al.*, 1999; Matsuo *et al.*, 2000; Qian *et al.*, 2000). The induction of gene expression following seizure is also commonly studied. Seizures can be induced in several ways and activity dependent genes have been studied following electrical stimulation (Yamagata *et al.*, 1994; Yamagata *et al.*, 1999), perfusion or injection of NMDA receptor agonist (Shan *et al.*, 1997; Chung *et al.*, 2000), perfusion or injection of other convulsive drugs (e.g. kainate, metrazol) (Nedivi *et al.*, 1993; Qian *et al.*, 1993; Kato *et al.*, 1997; Naeve *et al.*, 1997; Konietzko *et al.*, 1999) or mechanical injury (Dragunow *et al.*, 1996). However, seizures will likely cause activity of several receptor types, thus genes that are regulated by NMDA receptor activity would have to be identified by pharmacological isolation. Activity regulated genes have also been studied following the performance of animals in behavioural learning tasks such as spatial learning in the Morris water maze, fear conditioning and inhibitory avoidance tasks (Huang *et al.*, 1998; Guzowski *et al.*, 2001; Cavallaro *et al.*, 2002; Leil *et al.*, 2002; Ressler *et al.*, 2002).

The most common *in vitro* method of NMDA receptor stimulation is the pharmacological treatment of cultured neurons. This can be done using NMDA, glutamate or by cell depolarisation using KCl (Bading *et al.*, 1995, Bessho *et al.*, 1994).

Other methods include the electrical stimulation of brain slices (Cole *et al.*, 1989) or chemical stimulation of immortalised neuronal cell lines (Jung *et al.*, 1998).

A variety of techniques have been employed to analyse changing RNA levels in response to stimulation. Methods such as northern blotting, *in situ* hybridisation and RT-PCR, have been used in studies that have focused on the expression of one transcript or a limited number of genes in response to stimuli (Qian *et al.*, 1993; Bading *et al.*, 1995; Kato *et al.*, 1997; Chung *et al.*, 2000). However, several studies have used more widespread approaches to identify novel and candidate activity regulated genes. (Nedivi *et al.*, 1993) generated a subtracted cDNA library from the dentate gyrus of rats that have been injected with kainate. 52 'candidate plasticity genes' were reported, 40% of which were dependent on NMDA receptor activity. Differential display has been used to identify cDNAs regulated by LTP *in vivo*. The expression of 80 bands, out of an approximated 70000, was found modulated by LTP (Matsuo *et al.*, 1998).

More recently microarray analysis has been employed to identify activity regulated genes. 140 genes, of approximately 1300 screened, have been found significantly altered in the hippocampus following learning in the Morris Water Maze. These genes encoded a wide variety of neuronal proteins including receptor subunits, ion channels, signalling enzymes, cytoskeletal molecules, transcription related proteins and other synaptic molecules (Cavallaro *et al.*, 2002). Another study identified transcripts induced in the CA1 region of the hippocampus following electrically evoked seizure (French *et al.*, 2001). Of the 9000 genes screened, 14 candidate activity regulated genes were identified. However, of these, only one, *nur77*, could be confirmed induced by *in situ* hybridisation. Given the number of activity regulated genes previously identified, it could have been expected that microarray analysis would detect more than one seizure induced gene. This result may reflect the method used for the study, that is, extending analysis of seizure induced gene

expression to areas of the hippocampus beyond the CA1 region may have identifited more activity regulated genes.

1.2.1.2 Immediate Early Genes

ADGs are split, broadly, into two groups, immediate early gene (IEGs) and late response genes, based on their temporal profiles and sensitivity to protein synthesis inhibitors. It has been estimated that between 30 and 40 IEGs exist (Lanahan and Worley, 1998). IEGs are rapidly and transiently expressed following synaptic activity. For example, *in vitro* studies have detected IEG (*cfos, junB, egr1* and *nur77)* expression 15 minutes after glutamate treatment of primary cultured hippocampal neurons. The expression peaked between 30 and 60 minutes post stimulation and levels were basal by 4 hours (Bading *et al.*, 1995). *In vivo* studies during consolidation of fear conditioning found similar temporal profiles of the expression for *cfos* and *egr1* (Ressler *et al.*, 2002).

IEGs are expressed without requirement for *de novo* protein synthesis and, as such, their expression is controlled by constitutive transcription factors. Many of the well-characterised IEGs encode transcription factors. It is hypothesised that, once expressed, the encoded transcription factors act to regulate the expression of late response genes.

1.2.1.2.1 Inducible Transcription Factors

Inducible transcription factors are made up of 3 major families; fos, jun and egr. The fos family consists of *cfos, fosB, Fra-1* and *Fra-2.* The most studied of these is *cfos.* In 1987 it was demonstrated, for the first time, that specifically activating NMDA receptors, in cultured rat cerebellar granule cells, could induce *cfos* (Szekely *et al.*, 1987). Since then the induction of *cfos* has been studied in many NMDA receptor dependent paradigms of synaptic plasticity *in vivo,* such as LTP (Cole *et al.*, 1989; Dragunow *et al.*, 1989) and chemical induced seizure (Murphy *et al.*, 1991; Shan *et al.*,

1997), and *in vitro,* such as studies of glutamate stimulation of hippocampal neurons (Bading *et al.*, 1995).

Jun family products include *junD, cjun* and *junB.* Proteins from this family have been shown regulated by NMDA receptor activity in several *in vivo* and *in vitro* studies (Cole *et al.*, 1989; Szekely *et al.*, 1990; Murphy *et al.*, 1991; Bading *et al.*, 1995). Activator protein 1 (AP1) can be formed by *jun* family product homodimerisation or *jun/fos* heterodimerisation via shared leucine zipper motifs (Gentz *et al.*, 1989). AP1 can bind gene promoter regions to modulate transcription and its DNA binding activity is increased in cerebellar neurons following glutamate treatment (Szekely *et al.*, 1990). Thus IEGs induced by NMDA receptor treatment could act together to regulate transcription of target genes.

The egr family of IEGs are zinc finger transcription factors. *Egr1, egr2, egr3* and *egr4* can all be induced by synaptic activity (Yamagata *et al.*, 1994; Bading *et al.*, 1995; Inokuchi *et al.*, 1996; Honkaniemi and Sharp, 1999). Apart from their common zinc finger domain, the egr family share little homology and, as such, are hypothesised to regulate the expression of various targets. *Egr1 (zif268/krox24)* has been the most studied and is readily induced by *in vivo* and *in vitro* stimulation methods (Szekely *et al.*, 1987; Cole *et al.*, 1989; Bading *et al.*, 1995; French *et al.*, 2001).

Another zinc finger transcription factor that can be regulated by NMDA receptor activity is *nur77. Nur77* was first identified as a growth factor inducible immediate early gene, (Ryseck *et al.*, 1989) and subsequent studies found it induced by *in vitro* and *in vivo* stimulation of the NMDA receptor (Bading *et al.*, 1995; French *et al.*, 2001). *Nur77* encodes a protein with similarities to the steroid/thyroid hormone receptor family and, as such, has been hypothesised to act as a ligand activated transcription factor (Ryseck *et al.*, 1989). Indeed, *nur77* has been found to act, *in vitro,* as a transcriptional activator and a DNA recognition element, (5′ AAAGGTCA 3′), has been identified (Wilson *et al.*, 1991).

1.2.1.2.2 Other Immediate Early Genes

Many of the IEGs that have been identified encode transcription factors. However, there are several IEGs that encode proteins with other potential roles in synaptic plasticity. Examples of such are *narp, arcadlin* and *arg3.1*.

Narp is a secreted molecule regulated by synaptic activity (Tsui *et al.*, 1996) that belongs to the pentraxin family, a group of proteins that can self-multimerize (Gewurz *et al.*, 1995). Narp can cluster AMPA receptors and the enrichment of the molecule at pre and postsynaptic sites suggests it may play a role in formation of, and plasticity at, synapses (O'Brien *et al.*, 1999). Arcadlin is a cadherin protein that can be induced in the hippocampus by seizure or long term potentiation (Yamagata *et al.*, 1999). Cadherin molecules have been found localised to synaptic sites (Uchida *et al.*, 1996; Husi *et al.*, 2000). Cadherins are known to be involved in cell-cell interactions (Takeichi, 1991) and the regulation of such molecules by synaptic activity could underlie reorganisation at the synapse in response to stimulation. Another IEG that does not act as a transcription factor arg3.1 (also known as Arc) which is expressed and quickly distributed to the dendrites following synaptic stimulation (Link *et al.*, 1995; Lyford *et al.*, 1995), specifically localising to activated synapses (Steward and Worley, 2001). It is localised to dendrites in a pattern similar to F-actin and can interact with actin molecules (Lyford *et al.*, 1995). This is consistent with a role in activity regulated modulation of dendritic structure.

As discussed, several IEGs encode proteins that can be localised to the synapse. They have structural and adhesive properties that could be critical for synaptogenesis or for modulating synapse structure. The induction of these genes following synaptic activity is consistent with the hypothesis that NMDA receptor activity regulates the expression of molecules that are required for long term cellular response to synaptic input.

1.2.1.3 Late Response Genes

Late response genes have more prolonged profiles of expression compared to IEGs and are sensitive to translational inhibitors. It is hypothesised that the expression of these genes relies on the synthesis of induced transcription factors and that target genes encode proteins that are required to maintain the sustained effects of synaptic input.

Late response genes are not as well characterised as IEGs however some studies have tried to identify candidate late response genes. RNA fingerprinting of rat hippocampal samples found genes that were consistently upregulated in animals 6hrs after Morris water maze training. Two of these transcripts were identified to be glutamate dehydrogenase, key for the metabolism of glutamate, and ryanodine receptor type 2, an intracellular Ca^{2+} releasing channel (Cavallaro *et al.*, 1997).

A more recent publication used a combination of DAzLE (differential analysis of primary cDNA library expression) and cDNA microarrays to analyse genes regulated in cultured cortical neurons following NMDA treatment (Hong *et al.*, 2004). 661 genes were regulated by NMDA treatment, 5% of which had temporal profiles of expression consistent with immediate early genes. The remaining genes fitted profiles of prolonged expression of up to 24hrs post stimulation. The proteins encoded by the induced genes could be categorised by their function and included cytoskeletal and adhesion molecules, proteins involved in cell metabolism, receptor subunits, molecules involved in protein synthesis, intracellular signalling proteins and transcription factors. Comparison to genes induced by MECS stimulation found that 161 of 418 genes regulated by seizure were also regulated by NMDA treatment of the cortical neurons (Hong *et al.*, 2004).

1.2.2 Function of Activity Dependent Genes in NMDA Phenomena

Activity dependent genes encode proteins with a range of cellular functions many of which have been shown to be required for forms of synaptic plasticity and learning. Several studies of animals carrying mutations in ADGS have revealed phenotypes in NMDA receptor mediated phenomena. Jones *et al.*, 2001 demonstrated the requirement of egr1 in the maintenance of late LTP and long term memory, but not their short term counterparts, by analysis of $egr1^{-/-}$ mice. Analysis of animals lacking cfos in the brain has shown the transcription factor is required for LTP induction and spatial learning (Zhang *et al.*, 2002). In addition, hippocampal slices, from $Pim1^{-/-}$ animals, cannot maintain LTP beyond 2.5hrs (Konietzko *et al.*, 1999) and somatostatin knock out animals have reduced hippocampal short term plasticity and LTD, although LTP is not affected (Dutar *et al.*, 2002).

Other studies have used molecular and pharmacological approaches to reveal the role of ADGs in NMDA receptor dependent effects. For example, use of antisense has shown the requirement of arg3.1 for the maintenance, though not induction, of hippocampal LTP and for memory retention in Morris water maze (Guzowski *et al.*, 2000). Also, antisense of *IAP* (Integrin Associated Protein) reduces *in vivo* LTP, though has no effect on memory retention (Huang *et al.*, 1998). Blocking arcadlin, by use of an antibody, blocks hippocampal LTP in rats (Yamagata *et al.*, 1999) and the inhibition of COX by ibuprofen impairs the induction of LTP in anaesthetised rats and disrupts learning in the Morris Water Maze (Shaw *et al.*, 2003).

These studies demonstrate that genes induced by synaptic activity have a functional role in NMDA receptor dependent phenomena such as LTP and spatial learning, thus emphasising the significance of transcriptional regulation via NMDA receptor dependent signalling pathways.

1.2.3 Control of Activity Dependent Transcription

Neuronal gene expression can be activated by the entry of Ca^{2+} to the cell. Ca^{2+} enters the neuron by 2 principal methods; via the NMDA receptor upon receptor activation or via voltage dependent calcium channels (VDCC) following cell depolarisation. Intracellular signalling molecules respond to this, ultimately transmitting to the nucleus where the response is a change in gene expression.

Two transcription factor binding sites appear key in controlling gene expression in response to Ca^{2+} entry to the cell; the serum response element (SRE) and the cAMP response element (CRE). SRE and CRE binding sites are found in the promoters of many activity dependent genes (Montminy *et al.*, 1986; Chavrier *et al.*, 1989; Christy and Nathans, 1989; Rivera *et al.*, 1990; Gaiddon *et al.*, 1996).

1.2.3.1 Serum Response Element

The SRE binds various transcription factors including dimers of the serum response factor (SRF) and ternary complex factors (TCF), a family of transcription factors that includes Elk-1 and SAP1 (reviewed by Platenik *et al.*, 2000).

Glutamate treatment of cultured neurons and *in vivo* LTP initiate SRE mediated gene expression (Ghosh *et al.*, 1994; Xia *et al.*, 1996; Davis *et al.*, 2000). The *cfos* promoter contains both SRE and CRE binding sites (Berkowitz *et al.*, 1989; Rivera *et al.*, 1990) and, as such, manipulation of this promoter is often used to study the regulation of NMDA receptor mediated gene expression. NMDA mediated expression of *cfos*, in primary cultured neurons, has been shown to require an intact SRE binding site (Ghosh *et al.*, 1994; Xia *et al.*, 1996). SRE mediated transcription requires the binding of SRF, however maximal *cfos* induction occurs when both SRF and Elk-1 are bound (Xia *et al.*, 1996).

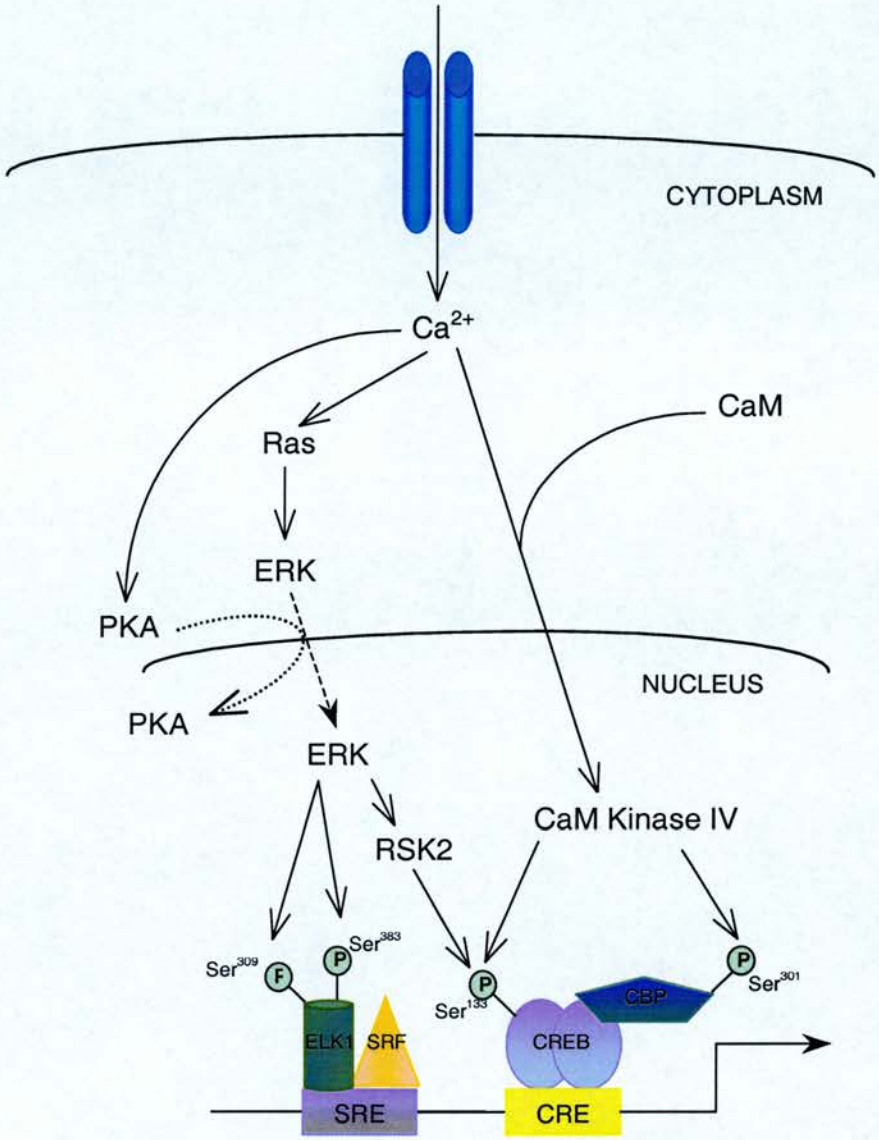

Figure 1.3 – NMDA Receptor Regulation of Gene Expression. Diagram shows hypothesised mechanisms of the regulation of SRE and CRE mediated gene expression following NMDA receptor stimulation. Calcium entry to the cell activates PKA, the Ras-ERK pathways and CaM Kinases. The Ras-ERK pathway can regulate the phosphorylation of ELK1 and CREB (via RSK2), with PKA potentially acting to aid the translocation of ERK to the nucleus. Activated CaM Kinase IV can act to phosphorylate CREB and CBP. Phosphorylation of Elk1 and binding of SRF can initiate SRE mediated transcription. The phosphorylation of CREB and CBP can initiate CRE mediated transcription.

Elk-1 is activated by phosphorylation at Ser^{383} and Ser^{389} (Marais *et al.*, 1993). It is hypothesised that the Ras-ERK pathway, in response to Ca^{2+} entry to the cell, phosphorylates Elk-1 at these sites, regulating activity dependent SRE mediated transcription. Phosphorylation of MAPK and Elk-1, which is rapidly induced by synaptic activity and regulates SRE mediated expression, is sensitive to inhibition of the Ras-ERK pathway (Xia *et al.*, 1996; Davis *et al.*, 2000). Figure 1.3 shows a model that includes the control of SRE mediated gene expression downstream of NMDA receptor activity.

1.2.3.2 cAMP Response Element

CRE mediated transcription is initiated by the binding of cAMP responsive element binging protein (CREB), which is active when phosphorylated at residue Ser^{113} (Gonzalez and Montminy, 1989). This phosphorylation site can be a target of protein kinases activated by Ca^{2+} entry to the cell (Dash *et al.*, 1991; Bading *et al.*, 1993; Impey *et al.*, 1996).

CREB dependent transcription has been shown to be required for long term memory in a variety of species, including *Aplysia, Drosophila* and mice (Bourtchuladze *et al.*, 1994; Yin *et al.*, 1994; Bartsch *et al.*, 1995). Mice lacking α and δ isoforms of CREB have been demonstrated to have impairments in hippocampal LTP and long term memory for cued and contextual conditioning, spatial learning and social transmission of food preference (Bourtchuladze *et al.*, 1994; Kogan *et al.*, 1997). Furthermore, an inducible CREB repressor protein has shown the requirement of CREB in the consolidation of new, and stability of reactivated, conditioned fear memories (Kida *et al.*, 2002).

However, some studies have failed to fully replicate the results of Bourtchuladze *et al.*, finding no impairment in LTP and spatial learning in the Morris water maze in mice lacking α and δ CREB isoforms (Gass *et al.*, 1998; Balschun *et al.*, 2003).

Analysis of mice lacking all isoforms of CREB in the brain similarly lacked LTP or spatial learning phenotypes, although the mutant animals did display more wall hugging behaviour in the Morris water maze than wild type controls (Balschun *et al.*, 2003). This suggests that the deficit in the CREB mutants previously seen could be due to the employment of inappropriate strategy in the water maze, as opposed to a spatial learning impairment.

The conflicting data from the studies of CREB mutants suggests that CREB plays a role in complex pathways involved in learning and memory processes. The differences seen in the studies could be due to differences in the genetic background of the animals and analysis of mutant CREB phenotypes could be confused by compensatory changes in the levels of other similar transcription factors (Hummler *et al.*, 1994). The role of CREB in LTP and behavioural learning is still to be clearly established and as such remains a focus of research.

1.2.3.2.1 Regulation of CRE Mediated Expression

A critical step in CRE mediated expression is the phosphorylation of CREB. Ser^{133} is the key regulation site of CREB and is phosphorylated by a variety of stimuli including KCl and glutamate treatment of cultured neurons, *in vitro* LTP and *in vivo* LTP (Ghosh *et al.*, 1994; Impey *et al.*, 1996; Davis *et al.*, 2000). CaMKIV, PKA and Ras-ERK pathways have all been shown capable to phosphorylating Ser^{133} in response to Ca^{2+} entry to the cell (Sun *et al.*, 1994; Xing *et al.*, 1998)

A proposed model of the regulation of CREB phosphorylation in response to synaptic activity involves two key pathways; CaM Kinases and Ras-ERK (Wu *et al.*, 2001; Hardingham and Bading, 2003) (see figure 1.3). CaM Kinases mediate a rapid initial phosphorylation of CREB at Ser^{133} in response to an increase of nuclear Ca^{2+} (Hardingham *et al.*, 1997). This localised increase of calcium is potentially facilitated by the translocation of calmodulin to the nucleus, in response to Ca^{2+} entry via the NMDA receptor or VDCC (Deisseroth *et al.*, 1998). CaM kinases I, II and IV are all

capable of phosphorylating CREB (Sheng *et al.*, 1991; Sun *et al.*, 1994), however CaMKIV is only one prominently expressed in the nucleus of hippocampal neurons (Bito *et al.*, 1996). As such, CaMKIV is most likely to be the enzyme mediating the CaM kinase dependent phosphorylation of CREB. Furthermore, animals lacking CaMKIV or expressing a dominant negative form of CaMKIV have impaired CREB phosphorylation and CRE mediated gene expression, as well as reduced hippocampal L-LTP (Ho *et al.*, 2000; Kang *et al.*, 2001).

Following the initial phosphorylation of CREB by CaM kinases, there is a long lasting phosphorylation of Ser^{133}, mediated by Ras-ERK pathway (Wu *et al.*, 2001). As discussed previously, the Ras-ERK pathway is activated following NMDA receptor stimulation. ERKs have no CREB kinase function, however, they can stimulate Rsk proteins that can phosphorylate CREB at Ser^{133} (Xing *et al.*, 1998). Depolarisation of cultured hippocampal neurons causes a robust increase in Rsk2 activity that is sensitive to MEK inhibitors (Impey *et al.*, 1998). Thus, Rsk2 is a good candidate for the CREB kinase that mediates prolonged phosphorylation of Ser^{133}, downstream of the Ras-ERK pathway.

There is also evidence that PKA, critical for L-LTP and hippocampal dependent long term memory (Huang and Kandel, 1994; Abel *et al.*, 1997), has a role in the regulation of CRE mediated transcription. Inhibition of PKA blocks the induction of CRE mediated expression in response to LTP and reduces phosphorylation of CREB in response to depolarisation in hippocampal neurons (Impey *et al.*, 1996; Impey *et al.*, 1998). It has long been accepted that there is crosstalk between the PKA and ERK signalling pathways (reviews by Stork and Schmitt, 2002). More specifically, PKA has recently been shown to be involved in the translocation of ERK to the nucleus in response to depolarisation of PC12 cell and hippocampal neurons (Impey *et al.*, 1998). Thus, the role of PKA in CRE mediated expression could lie in an interaction with the Ras-ERK pathway.

Sustained phosphorylation of CREB is necessary, but is not sufficient, to induce CRE mediated expression (Impey *et al.*, 1996). This suggests that there are additional regulation steps that are required before CRE mediated expression is initiated. One of these is the recruitment of CREB binding protein (CBP), a co-activator of transcription by phosphorylated CREB (Chrivia *et al.*, 1993). CBP recruitment can occur following CREB phosphorylation in response to synaptic activity (Hardingham *et al.*, 1999; Hu *et al.*, 1999). CBP is regulated by phosphorylation, which can be mediated by CaM Kinase IV (Chawla *et al.*, 1998; Impey *et al.*, 2002). This site of regulation has recently been identified as residue Ser^{301} (Impey *et al.*, 2002).

1.3 MEASURING GENE EXPRESSION BY MICROARRAY ANALYSIS

Many conventional methods of measuring RNA levels, such as northern blot, *in situ* hybridisation or RT-PCR, are restricted to studying limited numbers of genes at a time. Wider screens can be performed using subtractive hybridisation or differential display. The advent of microarray technology has offered a new method that enables large scale analysis, potentially genome wide, of RNA levels of annotated transcripts.

Microarrays can be used for the simultaneous analysis of thousands of transcripts. They are powerful, if expensive, tools that enable researchers to perform experiments to study known genes of interest as well as identify new genes that are important in the system being studied.

1.3.1 Overview of Technology

Although there are different microarray systems that can be used, their key principal remains constant. A labelled RNA or DNA sample in solution is hybridised to an ordered array of immobilised nucleic acid molecules (termed as probes). The amount of the bound sample at each probe is then determined by laser

scanning to give a quantitative measure of relative gene expression (Watson *et al.*, 1998; Harrington *et al.*, 2000).

There are 2 main types of arrays; ones that use oligonucleotide probes and those that use cDNA based probes (reviewed by Watson *et al.*, 1998; Schulze and Downward, 2001). Oligonucleotide based arrays can be manufactured by the spotting of short presynthesised oligonucleotides to the solid substrate of the array. Alternatively, as some commercial systems use, the oligonucleotides can be synthesised *in situ* on the slide surface. Using known sequence information, the probes are designed specific to each gene. This means they can be produced to distinguish between genes of high similarity or even differentiate splice variants, although factors such as the secondary structure of the oligonucleotides must be considered in the design process. However, a disadvantage of using oligonucleotide based arrays is that they rely on the availability of accurate sequence information.

Alternatively, cDNA based systems, using inserts from cDNA libraries or PCR products as probes, can be employed. Typically, these probes are longer than the oligonucleotides and are not restricted by a need for sequence information. Developing cDNA based arrays requires access to cDNA libraries and it is vital to ensure there is no cross contamination between clones.

1.3.2 Advantages and Applications of Microarrays

The great advantage of using microarrays is that they enable the simultaneous analysis of thousands of transcripts, allowing genome wide studies of transcription. The gene expression profile of a cell, or transcriptome, is a key in determining cellular function and behaviour. Where as the genome of a cell is a constant, the transcriptome is dynamic and can alter rapidly following stimulus. Microarray analysis can therefore provide a representation of cell or tissue activity at a given point in time, under particular conditions.

The potential of microarray technology is vast and can be applied to wide ranging studies of different cell types in a variety of conditions. For example, microarrays have been used to study transcriptional changes through yeast cell cycles (Cho *et al.*, 1998), the profile alterations in differentiating cells (Ma and Staudt, 2000; Tomczak *et al.*, 2004) or to reveal expression differences in healthy and diseased tissue (Kononen *et al.*, 1998; Brown *et al.*, 2001).

An advantage of using microarrays is that they can be used to perform unbiased wide screens. This may reveal new genes of interest in the particular system that is being investigated. These transcripts could then be more closely examined, using other techniques, to identify if they are of significant function. Changes revealed by microarrays can also be studied in a more global fashion, e.g. to reveal coregulated genes, which could give insight to the regulatory networks controlling transcription.

1.3.3 Challenges of Using Microarrays

As microarrays examine so many transcripts at once, experiments are susceptible to false positives, which could arise due to any disparities in sample preparation. Therefore, in order to obtain meaningful information from microarrays, a great deal of importance is placed on experimental design (reviewed by Yang and Speed, 2002). To be confident that results are real, experimental design should be kept simple with as few stages where variability could occur as possible. In order to validate results from microarray data, the detected patterns of gene expression should be confirmed by using an alternative method such as Northern blot or RT-PCR.

One of the greatest challenges of using microarray systems is the analysis of the data produced. With thousands of data points, a single experiment generates a vast amount of information. Specialised software is available to deal specifically with microarray data but analysis of an experiment can remain a daunting task.

However, the sheer volume of information can allow data to be studied in a variety of ways to extract meaningful information.

Using microarrays in the field of neuroscience has it's own particular challenges. The brain is complex, with heterogeneous cell populations, intricate developmental patterns and defined anatomical architecture. This offers practical problems as the isolation of desired tissues or cells must be precise, and at appropriate developmental stages, to avoid contamination from surrounding neuronal structures. However, the complexity of the central nervous system also means that it's understanding can be greatly enhanced by the successful application of microarray techniques. For example, microarrays have been used to analyse expression in the hippocampus through development and to analyse the differential of gene expression in different subregions of the hippocampus (Mody *et al.*, 2001; Lein *et al.*, 2004). Further application of microarray analysis across different brain structures at various developmental stages could provide insight to how differential gene expression correlates with the development of structure specific function. Microarray analysis has also been applied to analyse how particular areas of the brain following treatment, for example hippocampal gene expression has been analysed following ischemia, seizure and learning trials (French *et al.*, 2001; Jin *et al.*, 2001; Cavallaro *et al.*, 2002; Blalock *et al.*, 2003; Newton *et al.*, 2003). Microarrays offer the potential to further understanding as to how the various areas of the brain perform their specific functions in response to different input.

1.4 AIMS OF PROJECT

The NMDA receptor is crucial for learning and plasticity and the regulation of gene expression following receptor activation appears critical for mediating these effects. The isolation of the NRC and its proteins has identified molecules that potentially lie in pathways downstream of NMDA receptor activity, however, it has not been established which of these proteins contribute to the NMDA activated pathways that regulate transcription.

The aim of this project was to study the role of NRC proteins in the regulation of NMDA receptor regulated gene expression. To this end, and as described in this thesis, neuronal tissue carrying mutations in PSD95 and SynGAP was analysed by microarray. This large-scale analysis of gene expression could establish if disrupting the function of these NRC proteins can cause changes at a transcriptional level.

In order to develop techniques to analyse NMDA receptor mediate gene expression, *in vitro* methods of NMDA receptor stimulation have been studied and a custom microarray, with probes representing selected transcripts relevant to synaptic plasticity and learning, has been designed. A reliable method of NMDA receptor activation would enable the analysis of gene expression initiated by NMDA receptor stimulation in wild type and mutant cells and the custom array could enable the high throughput analysis of RNA levels.

CHAPTER 2

MATERIALS AND METHODS

2. MATERIALS AND METHODS

All general reagents were analytical grade or better from BDH, Fischer, Fluka or Sigma.

2.1 MOLECULAR BIOLOGY METHODS AND TECHNIQUES

Basic molecular biology techniques were performed as described in Sambrook and Russell (2000).

2.1.1 RNA Preparation

2.1.1.1 Details of Animals Used for Expriments

2.1.1.1.1 Generation of PSD95 Mutant Animals

The PSD95 mutant animals used for experiments in this thesis are as those detailed in Miguad *et al.*, 1998. A targetted mutation was introduced to the PSD95 gene by the insertion of a premature stop codon to the exon encoding the third PDZ domain of the protein. This insertion also introduced an IRES (internal ribosome entry site) driving the expression of a β-galactosidase reporter gene. The mutation left the gene sequence outwith the third PDZ domain intact.

2.1.1.1.2 Generation of SynGAP Mutant Animals

The SynGAP mutant animals used in this thesis are as those detailed in Komiyama *et al.*, 2002. A targetted mutation was introduced to the SynGAP gene by the insertion of a stop codon to the exon encoding the C2 domain of the protein. The insertion deleted the C2 and GAP domains of SynGAP and included an IRES driving the expression of a β-galactosidase reporter gene.

2.1.1.2 Dissection of Brain Tissue For Sample Preparation For Microarray Analysis

2.1.1.2.1 Dissection of PSD95$^{-/-}$ Forebrain

All mice used were female adults (at least 3 months old) on a C57/Black6 background. 3 wild type and 3 PSD95$^{-/-}$ animals were used. The animals were age matched and, where possible, litter matched.

Animals were killed by cervical dislocation (schedule 1 procedure, in accordance with UK Home Office regulations). The animals were then decapitated and brains removed from the skull. Dissections of the brains were performed on ice and tissue kept moist with chilled phospho-buffered saline (PBS) (GIBCO). The forebrains were separated from the cerebellum and brainstem and immediately frozen in liquid nitrogen. All dissections were performed consecutively, on the same day. RNA extraction was performed immediately after final dissection.

2.1.1.2.2 Dissection of SynGAP$^{+/-}$ Hippocampus

All mice used were female adults (at least 3 months old) on a C57/Black6 background. 3 wild type and 3 SynGAP$^{+/-}$ animals were used. The animals were age matched and, where possible, litter matched.

Animals were killed by cervical dislocation. The animals were then decapitated and brains removed from the skull. Dissections of the brains were performed on ice and the tissue kept moist with chilled PBS. The brains were hemisected and the hippocampi removed from each hemisphere. The hippocampi were immediately frozen in liquid nitrogen. All dissections were performed consecutively on the same day. RNA extraction was performed immediately after the final dissection.

2.1.1.3 Isolation of RNA from Tissue

RNA was extracted from animal tissue using QIAGEN RNeasy columns. Midi or Maxi kits were used based upon the weight of tissue, in accordance with manufacturers instructions (Midi for hippocampi, Maxi for forebrain). In all cases tissues was homogenised in the appropriate amount of QIAGEN RLT buffer for 1min. The protocols were then followed as per manufacturers instructions, including on the column DNase treatment performed using QIAGEN RNase-Free DNase set. RNA was eluted in 140µl (Midi kit) or 800µl (Maxi kit) DNase free water and stored at –80°C.

2.1.1.4 Isolation of RNA from Primary Cultured Neurons

RNA was isolated from primary cultured neurons using QIAGEN RNeasy mini kits according to manufacturers instructions. Cells were collected from 35mm dishes using 350µl QIAGEN RLT buffer and disrupted by application to QIAGEN QIAshredder homogeniser columns and 2mins centrifugation at 13500rpm. RNA extraction was then performed in accordance with QIAGEN RNeasy protocol. On the column DNase treatment was performed using QIAGEN RNase-Free DNase set. RNA was eluted in 40µl DNase free water and stored at –80°C.

2.1.1.5 Precipitation of RNA

To the RNA volume, 0.5 volumes 7.5M NH_4Ac and 2.5 volumes –20°C ethanol was added and vortexed. Samples were centrifuged at 12000g at 4°C for 20mins. Supernatant was removed and 0.5ml 80% -20°C ethanol was added to the pellet. Samples were centrifuged at 12000g at room temperature for 5mins. The ethanol was removed, 0.5ml 80% -20°C fresh ethanol was added and the samples centrifuged again at 12000g at room temperature for 5mins. Ethanol was removed, the pellets air dried and resuspended in 10µl RNase free H_2O. The concentration of samples was determined by spectrophotometry and RNA diluted to the appropriate concentration for specific protocol.

2.1.2 RNA Quality Analysis

2.1.2.1 RNA Formaldehyde Agarose Gel Electrophoresis

1µg RNA was made up to 5µl with DEPC treated H_2O and added to 11µl formamide, 4µl 12.3M formaldehyde and 5µl loading buffer (0.025% bromophenol blue, 0.025% xylene cyanol, 50% glycerol, 1mM EDTA pH8, 10% ethidium bromide). The reaction mixture was heated to 55°C for 15mins and run on a 1% RNA agarose gel (0.5g agarose, 5ml 10xMOPS buffer [0.4M MOPS, pH7, 0.1M sodium acetate and 0.01M EDTA], 9ml 12.3M formaldehyde made up to 50ml with DEPC H_20) at 80v for 1hr. Gels were visualised using Gene Genius Bioimager (SynGene) with GeneSnap software (SynGene).

2.1.2.2 Analysis by Agilent Bioanalyser

RNA was analysed using a Agilent 2100 Bioanalyser Nano Assay kit according to manufacturers instructions. Briefly, 1µl RNA 6000 Nano dye concentrate was added to 65µl RNA 6000 Nano filtered gel matrix. This was loaded into a RNA Nano chip. 5µl RNA 6000 Nano Marker was added to each sample well and the ladder well. 1µl RNA 6000 ladder (Ambion Inc.) was denatured at 70°C for 2mins and added to the ladder well of the Nano chip. RNA samples were heated to 70°C for 2mins and 1µl of each samples added to individual wells. The chips were vortexed at 2400rpm, inserted to the Agilent 2100 Bioanalyser and assays run using Agilent software.

2.1.3 PCR

2.1.3.1 cDNA 1st Strand Synthesis

First strand cDNA was made from 0.5µg RNA, using oligo dT primers, with RETROscript (Ambion Inc.). RNA was made up to 10µl with dH_2O and incubated with 2µl oligo dT for 3mins at 70°C. 4µl 10mM dNTPs, 2µl buffer, 1µl RNase Inhibitor and 1µl m-MLV reverse transcriptase was added and samples incubated for 1hr at 42°C. The enzyme was then heat inactivated at 92°C for 10mins.

2.1.3.2 RT-PCR

PCR reactions were performed using Promega Taq Polymerase in Storage Buffer A. Reaction mix, made up in 0.5ml thin walled tubes, consisted of 1µl cDNA, 4µl 2.5mM dNTPs, 2µl 10µM forward primer, 2µl 10µM reverse primer, 3µl 2.5mM $MgCl_2$, 5µl 10x reaction buffer, 0.5µl Taq polymerase (Promega) and 32.5µl dH_2O. PCR reactions were carried out using MJ Research DNA Engine Tetrad (GRI) in the following conditions: 94°C for 2mins, (94°C for 30s, 56°C for 30s, 72°C for 30s) x 30, 72°C 10mins, 4°C hold. Products were run out on a 4% agarose gel (3g NuSeive low melting point agarose [Cambrex BioScience], 1g agarose in 100ml TEA buffer [484µg tris base, 200µl 0.5M EDTA, 144µl glacial acetic acid made up to 100ml with dH_2O])

over 1hr at 110V. Gels were visualised using Gene Genius Bioimager (SynGene) with GeneSnap software (SynGene).

2.1.3.3 QRT-PCR

2.1.3.3.1 RT-PCR Reaction

QRT-PCR was carried out using the DNA Engine Opticon LightCycler (MJ Research). Reactions were set up as follows. For sample wells 2µl cDNA, 2.5µl primers (forward and reverse primers at 2.5µM) and 8µl H_2O were mixed with 12.5µl 2x Quantitect SYBR Green PCR Master Mix (QIAGEN), containing SYBR green dye, dNTPs and HotStarTaq DNA Polymerase. Wells for the standard curve for each primer pair were set up using 2µl of 1, 2, 4 and 8 fold dilutions of a standard cDNA from wild type forebrain RNA. These dilutions were attributed the values of 2000, 1000, 500 and 250 units to represent the amount of cDNA in the samples.

All reaction conditions were as follows: 95°C for 15s, (94°C for 15s, 55°C for 30s, 72°C for 30s) x 35, then melting curve run from 60°C to 90°C with a read every 1°C; with a hold for 1s between reads. The melting curves were examined to ensure each primer pair had only one double stranded product.

2.1.3.3.2 Data Analysis

The data generated from the lightcycler reactions was analysed in OpticonMonitor 2.0 software. Standard curves were established using the data from cDNA dilutions by plotting the log of cDNA quantity against the cycle number. The cycle threshold lines (C_T) are horizontal lines applied to an amplification plot (accumulated fluorescence vs. cycle number) at a particular fluorescence from which the cycle number for each samples is taken. C_T lines were placed where the r^2 value of the regression line through the standard curve was closest to one. Cycle numbers were then taken from all samples on the amplification plot through the set C_T line.

Against the standard curves, the relative amount of starting template in each sample was calculated from the cycle numbers.

The expression data was exported from OpticonMonitor 2.0 to Excel for analysis. Values for experimental genes were normalised to the levels of GAPDH control measured in each sample. For experiments comparing gene levels in wild type and mutant tissue, reactions in each sample were run in triplicate. The average values of transcript expression in each sample were used in t tests to compare expression in wildtype and mutant samples.

For experiments measuring gene expression in cultured neurons following drug treatment reactions were run in duplicate. The average value of transcript expression was used to calculate treated:untreated ratios. These values were used to assess the significance of changes by t test.

2.1.4 Microarray Hybridisation and Analysis

2.1.4.1 Affymetrix Hybridisation

Dr. Kevin Robertson at the Scottish Centre for Genomic Technology and Informatics (SCGTI) used the following Affymetrix protocols for hybridisation of Affymetrix U74av2 arrays. All reactions were carried out according to the manufacturers instructions (www.affymetrix.com/support/technical/manual/expression_manaul.affx) and the basics of the protocols are covered below.

2.1.4.1.1 Labelling of RNA

Briefly, the first strand cDNA synthesis from the RNA samples was performed with a SuperScript II kit (Invitrogen Life Technologies), using a GeneChip T7-$dT_{(24)}$ primer and 10μg starting material. Second strand synthesis was performed using *E. coli* DNA polymerase (Invitrogen Life Technologies), resulting in a double stranded cDNA product that was cleaned with a phenol-chloroform extraction, followed by ethanol precipitation.

An *in vitro* transcription reaction was performed on the double stranded cDNA with biotin labelled ribonucleases using T7 RNA polymerase and the Affymetrix EnzoBioArray High Yield RNA Transcription labelling kit. The resulting biotin labelled cRNA was fragmented for hybridisation. The cRNA was checked using the Agilent BioAnalyser to ensure the samples contained small fragments before proceeding to hybridisation.

2.1.4.1.2 Hybridisation

The hybridisation cocktail with final concentrations of 100mM MES, 1M Na^+, 20mM EDTA and 0.01% Tween was made up and contained the cRNA samples and additional spiked controls. OligoB2, which hybridises to a synthetic sequence spotted along the edges of the arrays, was included to align the array upon scanning. BioB, BioC and BioD oligos that hybridise to probes designed to *E. coli*

genes in the biotin pathway were included at 1.5pM, 5pM and 25pM to analyse the efficiency of the hybridisation reaction. The samples, in the hybridisation cocktail, were hybridised to the chips for 16hrs at 45°C at 60rpm.

2.1.4.1.3 Washing, Staining and Scanning

Following hybridisation, the arrays were stained with SAPE (streptavidin-phycoerythirin) and washed several times before scanning. Arrays were scanned with the Affymetrix GeneChip Scanner 2500.

2.1.4.1.4 Bioinformatic Analysis

Analysis was performed using the Affymetrix MAS 5.1 software in accordance with Affymetrix protocols (www.affymetrix.com/auth/support/downloads/manuals/mas_manuals.zip). All arrays were scaled to an average overall intensity of 100. Scatter plots and box and whisker plots of the data were produced in S-Plus software (Insightful Corporation) to confirm all arrays appeared to detect similar ranges of expression values.

To analyse the data further it was exported into Microsoft Excel and expression levels of each transcript compared, in wild type and mutant samples, by Welch t test to identify transcripts expressed at significantly altered levels in mutant tissue compared to wild type. Wild type gene expression in forebrain and hippocampal samples was compared by Welch t test to identify genes expressed at a significantly higher level in one tissue type compared to the other.

Chromosomal locations for genes were obtained from NetAffx (http://www.affymetrix.com/analysis/index.affx) and NCBI Entrez Gene (http://www.ncbi.nlm.nih.gov). Analysis of chromosomal clustering of significantly altered genes was performed by Chi square analysis. The observed frequency of genes per chromosome was compared to the expected frequency of genes per chromosome.

2.1.4.2 Custom Array Protocol 1

This following protocol was used for initial validation and hybridisation of custom arrays.

2.1.4.2.1 Labelling of RNA

25µg RNA, in 11µl DEPC water, was incubated at 70°C for 10mins with 4ul Oligo-dT (Invitrogen) then snap cooled on ice for 5mins. To this 6µl 5x first strand buffer (Invitrogen), 3µl 0.1M DTT, 0.6µl each of dATP, dTTP and dGTP, 3µl cy3 labelled dCTP (Amersham) and 2µl Superscript II (Invitrogen) was added. Samples were incubated at 42°C for 2hrs. 15µl 0.1M NaOH was then added and incubated for 10mins at 70°C before 15µl 0.1M HCl was added. 20µl COT1 human DNA was added. Samples were washed twice with H_2O through Microcon YM-30 columns (Milipore) and reduced to a volume of approximately 8µl then made up to 16µl with H_2O. To this 3.5µl 20xSSC (3M NaCl, 300mM sodium citrate) and 0.6µl 10% SDS was added and samples heated at 100°C for 2mins before incubation at 37°C for 30mins.

2.1.4.2.2 Slide and Coverslip Preparation

Slides, spotted with oligonucleotides, were prepared for hybridisation by incubation in a solution of 3g succinic anhydride in 175ml N-methyl-2-pyrolidinone (NMP) with 7.5ml of borate buffer (30.9g boric acid in 500ml H_2O, pH8) for 15mins with constant stirring. The slides were then put in boiled water for 2mins, before being cleaned by dunking in absolute alcohol.

Coverslips (Erie Scientific Company) were soaked in 0.1% SDS for 15mins, then rinsed in H_2O and soaked in 70% Ethanol for 5mins. The coverslips were dipped in acetone and left to air dry.

2.1.4.2.3 Hybridisation and Washes

Prepared slides were put in A1-biotech dual hybridisation chambers and coverslips placed over the area of the array. Labelled RNA samples were applied below the coverslips. 50µl 20xSSC was pipetted under the slides to prevent the chamber drying during hybridisation, the chambers were sealed and incubated overnight in hybridisation ovens at 50°C.

Slides were rinsed in 1xSSC/0.2% SDS (20xSSC, 10ml 10% SDS in 500ml) to remove coverslips and then washed in fresh 1xSSC/0.2% SDS for 5mins. Slides were washed for 5mins in 0.1xSSC/0.2% SDS then vigorously rinsed in 0.1xSSC. Slides were dried by 1mins spin at 1000rpm.

2.1.4.2.4 Scanning and Analysis

Arrays were scanned using Affymetrix 428 Array Scanner and QuantArray (GSI Lumonics) was used to extract intensity levels from the scanned images. Data from arrays was exported to Excel and thresholds of expression calculated as the average expression at the buffer spots plus 2 standard deviations of the buffer expression values. Box and whisker plots of the average expression values of genes of interest, positive controls, negative controls and buffer spots were generated in S-Plus.

2.1.4.3 Custom Array Protocol 2 - RLS

Alan Ross at the SCGTI, University of Edinburgh used the following protocols for hybridisation and analysis of the custom arrays.

2.1.4.3.1 Labelling of RNA

RNA labelling was performed using QIAGEN LabelStar kit. Briefly, RNA samples were concentrated to 2.27µg/µl and 2µl (4.54ug) of the samples were denatured. Reverse transcription reactions were performed using biotin-dUTP to label the cDNA. The labelled cDNA was cleaned using QIAGEN MiniElute columns.

2.1.4.3.2 Hybridisation and Washes

Slides were treated with HiLight Prehybridisation Solution (QIAGEN) at 42°C for 10mins and washed twice for 10s in deionised H_2O, then dried under N_2 gas. A hybridisation cocktail was made with HiLight Hybridisation Solution (QIAGEN), salmon sperm DNA and labelled cDNA and heated to 95°C. This mix was applied, under lifterslips, to the slides and hybridised overnight at 42°C.

Slides were washed twice for 10mins at 42°C with Wash Solution 1 (QIAGEN), then washed for 10mins at room temperature with Wash Solution 2 (QIAGEN) and finally washed twice for 1min at room temperature with Wash Solution 3 (QIAGEN).

2.1.4.3.3 HiLight Particle Binding and Wash

Following washing, slides were incubated at room temperature for 2mins in HiLight Blocking Buffer (QIAGEN). 30ul RLS particles and 15ul particle dilutent (QIAGEN) was added, under lifterslips, to each slide and incubated for 1hr at room temperature. Slides were washed over with Wash Solution 2, then washed 3 times for 1min at room temperature with Wash Solution 3. Finally, slides were rinsed with deionised H_2O and dried under N_2 gas.

2.1.4.3.4 Scanning and Analysis

Slides were scanned with HiLight reader (QIAGEN) and QuantArray was used to extract expression level data from the images. Data was exported into Excel and background expression, calculated as the mean expression at the buffer spots, was subtracted from expression levels. The 75th percentile expression value for each array and across all arrays was calculated. The average 75th percentile value for all arrays was divided by individual 75th percentile values for each array and used as a scaling factor. All expression values on each array were then multiplied by the appropriate scaling factor. Thresholds of expression level were set for individual

arrays using the 80th percentile value of the negative controls on each particular array.

Using Excel, the median values for transcripts on each array were used to calculate the average expression of genes in wildtype and mutant tissues. Box and whisker plots of the average expression values of genes of interest, positive controls and negative controls in wildtype and mutant tissues were generated in S-Plus. All expression values (3 per arrays) were used in t Tests to identify transcripts significantly altered in mutant tissue compared to wild type.

2.1.5 Oligonucleotide Design

2.1.5.1 Primer Design

cDNA sequences for target genes for RT-PCR were obtained from the National Centre for Biotechnology Information (NCBI) nucleotide site (http://www.ncbi.nlm.nih.gov/nucleotide). Using the Basic Local Alignment Search Tool (BLAST; http://www.ncbi.nlm.nih.gov/BLAST), intron and exon boundaries were identified by comparing cDNA sequence with mouse or, where this information was unavailable, human genomic sequence. RT-PCR primers were designed using online primer design programme Primer 3.0 (http://frodo.wi.mit.edu/cgi-bin/primer3/primer3_www.cgi) and positioned to span introns, with a bias to the 3'end of the sequence. The only exception was the primers designed to PSD95 which were not intron spanning as they were specifically designed to the 3' region of the gene where the probes on the Affymetrix U74A chip were positioned. All primers were chosen to give products of between 150 and 350 base pairs.

2.1.5.2 Custom Array Oligonucleotide Design

Oligonucleotides, 55 base pairs in length, were designed using Oligo 6 software (LifeScience). Target sequences for chosen genes of interest were obtained from www.ncbi.nlm.nih.gov/nucleotide. Where available, murine sequence was used and if not, rat sequence was used.

Target sequences were input to Oligo 6 and oligonucleotides were searched for. Melting temperature criteria was set between 90 °C and 100°C and oligonucleotides were searched for within 1000 bases of the 3′ end of the input sequences. Of the suggested oligonucleotides returned those with loop Δ G smaller than –3 kcal/mol were rejected. Oligonucleotides were chosen from those remaining to be, ideally, around 500 base pairs from the terminal polyA tail and with minimum secondary structure. For genes of high homology or to distinguish splice variants, similar sequences were compared pairwise using BLAST (www.ncbi.nlm.nih.gov/BLAST) to identify areas of diversity and oligonucleotides designed to the most 3′ of these areas.

The chosen 55mers were checked for homology to other sequences using nucleotide-nucleotide nBLAST (nr database). Any oligonucleotide with more than 15 contiguous base pairs common to a gene other than the one it was designed to was discarded and redesigned.

2.2 TISSUE CULTURE

2.2.1 Preparation of Surfaces For Plating Primary Cultured Neurons

Primary cultured neurons were grown on 6 well 35mm dishes, 1cm glass coverslips in 24 well 10mm dishes or multi electrode arrays (MEA) depending on the final use of the cells. Before incubation with cells all surfaces were treated with poly-D-lysine (Sigma), diluted to 0.01mg/ml in ice cold PBS (GIBCO), for 30mins and washed with

PBS. Laminin (Sigma) at approximately 5μg/ml was pipetted over surfaces and plates incubated at 37°C until use. Immediately before cell plating, laminin coated surfaces were washed with PBS.

2.2.2 Primary Culture of Cortical Neurons

Cortices were dissected from E17.5 mouse pups and cells disaggregated in approximately 2ml cold PBS. Any remaining clumps were allowed to settle over 5 minutes, the supernatent removed and made up to 10ml with Neurobasal with penicillin/streptomycin. Cells were centrifuged at 700rpm for 5 mins. The cell pellet was resuspended in Neurobasal with penicillin/streptomycin and spun again at 700rpm for 5mins. Cells were resuspended in Plating Media (2ml B27 (GIBCO), 0.25ml 200mM glutamine, 1ml penicillin/streptomycin per 100ml Neurobasal). Cells were counted and volume adjusted to give a final plating density of 1×10^5 cells/cm^2. The cells were plated on the poly-d-lysine/laminin coated substrates and incubated at 37°C 95% oxygen, 5% CO_2. The cells plated on 6 well plates were used for stimulation assays measuring gene expression, those plated on 1cm glass coverslips were used for immunofluorescent staining and those on MEAs were used for electrophysiological analysis.

2.2.3 Pharmacological Treatment of Cultured Neurons

2.2.3.1 NMDA Stimulation

Primary cultured E17.5 mouse cortical neurons were plated on 6 x 35mm well plates and grown for 10-12 DIV. 2hrs before stimulation, the wells were treated with 1μM tetrodotoxin (TTX) (TOCRIS) to reduce basal activity and cells incubated at 37°C. For stimulation, the media in the wells was replaced with Mg^{2+} free Locke's Solution (140mM NaCl, 3mM KCl, 15mM HEPES, 10mM Glucose, 2.5mM $CaCl_2$ and NaOH to pH to 7.4) containing 100μM NMDA and 10μM glycine for stimulation and incubated at 37°C. RNA was extracted 30mins post stimulation.

2.2.3.2 Bicuculline Stimulation

Primary cultured E17.5 mouse cortical neurons were plated on 6 x 35mm well plates and grown for 10-12 DIV. Plating media on was changed to 2.5ml stimulation media (per 100ml, 88ml SGG [5mM NaCl, 7.5% $NaHCO_3$, 3mM KCl, 1mM $MgCl_2$, 1mM $CaCl_2$, 1mM HEPES, 1mM glycine, 2.5mM glucose, 0.1mM Na Pyruvate, 0.5% phenol red], 10ml MEM, 0.5ml penicillin /streptomycin, 1.5ml 1xITS [insulin-transferrin-sodium selenite media supplement]) and cells incubated at 37°C for 24hrs before treatment. Stimulated wells were treated with 50µM bicuculline (TOCRIS) and unstimulated wells treated with media. For control purposes some wells were treated with 10µg/ml Actinomycin D or 50µM amino-5-phosphonovalerate (APV) (TOCRIS) 1 hour prior to bicuculline treatment. RNA was extracted from cells 1hr after bicuculline application.

2.2.3.3 APV Treatment

Primary cultured E17.5 mouse cortical neurons were plated on 6 x 35mm well plates and grown for 10-12 DIV. Plating media on was changed to 2.5ml stimulation media (as detailed above) and cells incubated at 37°C for 24hrs before treatment. Wells were treated with 50µM APV 1hr before RNA extraction.

2.2.4 Immunoflourescent Staining of Cultured Neurons

Primary cultured E17.5 mouse cortical neurons were grown on 1cm glass coverslips for staining. At DIV12, cells were washed with PBS and fixed for 10mins, on ice, with 500µl –20°C methanol. For the remainder of the protocol coverslips were kept in the dark at room temperature. The coverslips were washed with PBS and incubated in 500µl blocking buffer (tris buffered saline[TBS], 0.5% Tween, 5% goat serum) for 30mins. The coverslips were then incubated for 1hr with mouse MAP2B 1^0 antibody (Transduction Laboratories) diluted 1:100 in blocking buffer and then given 3 x 5min washes with TBS, 5% Tween. 2^o antibody, cy3-goat anti-mouse, (Jackson Laboratories) was diluted 1:200 in TBS, 5% Tween, and incubated on the

coverslips for 1hr. Coverslips were given 3 x 5min washes with TBS, 5% Tween. Coverslips were then dipped in dH_2O, air dried and mounted inverted onto glass slides with Fluromount mountant (Sigma). The slides were stored at 4°C.

2.2.5 DAPI Staining of Cultured Neurons

E17.5 mouse cortical neuron cultures were grown on 1cm glass coverslips for staining. At DIV12, cells were washed with PBS and fixed for 10mins, on ice, with 500ul –20°C methanol. The coverslips were kept in the dark at room temperature and 1ml 0.1µg/ml DAPI (4',6-diamidino-2-phenylindole), diluted in TBS, applied to each coverslip for 30mins. The coverslips were washed 3 x 5mins with TBS, dipped in dH_2O, air dried and mounted inverted onto glass slides with Fluromount mountant (Sigma). The slides were stored at 4°C.

2.3 ELECTROPHYSIOLOGY

2.3.1 Multi Electrode Array SetUp

Elecrophysiology experiments were conducted using Multi Channel Systems arrays. The Multi Electrode Arrays (MEA) were 8 x 8 grids of 30Ø diameter electrodes, set 200µm apart. Primary cultured cortical neurons were grown on the MEAs. For recording, MEAs were mounted in an amplifier and extracellular activity recorded in real-time using the MC_Rack software (Multi Channel Systems).

2.3.2 MultiElectrode Array Recording

Recordings were taken from primary cultured E17.5 cortical neurons, 10-13 DIV. Arrays were removed from the incubator and put into the recording equipment. The volume of the arrays is approximately 1ml and the cells were perfused with Mg^{2+} containing Locke's Solution (140mM NaCl, 3mM KCl, 15mM HEPES, 10mM Glucose, 2.5mM $CaCl_2$, 1mM $MgCl_2$ and NaOH to pH to 7.4) at a rate of 1ml/min. The perfusion and base plate of array were maintained at 30°C. Extracellular recordings, measuring spike rate, were performed continuously.

2.3.2.1 Bicuculline Treatment of Cultured Neurons

Perfusion with Locke's solution was maintained for at least 10mins to record control activity. 50μM bicuculline was added to the perfusion solution and activity recorded for at least 10mins. 50μM 4AP was then added to the Locke's/bicuculline solution and activity recorded for at least 10mins. The cells were then washed by perfusion with Locke's solution for at least 10mins and were then perfused with Locke's solution containing 1μM TTX. Activity was recorded throughout control, bicuculline treated, 4AP treated, wash and TTX periods.

2.3.2.2 APV Treatment of Cultured Neurons

Perfusion with Locke's solution was maintained for at least 10mins to record activity. 50μM APV was added to the perfusion solution and activity recorded for at least 10mins. Following a wash period by perfusion with Locke's solution, the cells were perfused with Locke's solution containing 1μM TTX. Activity was recorded throughout control, APV treatment, wash and TTX periods.

2.3.3 MultiElectrode Array Analysis

The recorded data was played back using Replayer function of the MC_Rack software. Channels from the arrays showing activity were chosen for analysis. Baseline noise levels were assessed as the signal recorded from TTX treat cells. Spike thresholds were set accordingly for each array to ensure spikes were counted, but background noise was disregarded. The data from the selected channels was replayed and Spike Detector recorded the spike rate vs. time.

The spike frequency data was imported to Excel and the average activity during different drug conditions calculated for each channel. Control activity at each channel was adjusted to 100 and all other activity measured at each channel normalised to this level. T tests were used to compare the activity on an array in conditions of drug treatment to control.

CHAPTER 3

GENE EXPRESSION IN PSD95$^{-/-}$ AND SYNGAP$^{+/-}$ TISSUE

3. GENE EXPRESSION IN PSD95$^{-/-}$ AND SYNGAP$^{+/-}$ TISSUE

The NRC contains signalling molecules that act in pathways that can regulate gene expression. However, it remains unclear what role many NRC molecules may play in controlling transcription. To examine this, gene expression was analysed in tissue from animals carrying mutations in PSD95 and SynGAP.

As discussed in the introduction, both PSD95$^{-/-}$ and SynGAP$^{+/-}$ animals have deficits in NMDA receptor dependent behavioural and electrophysiological paradigms (Migaud *et al.*, 1998; Komiyama *et al.*, 2002). As a structural component of the NRC, PSD95 could be hypothesised to have a role in regulating signalling downstream of the NMDA receptor. It's function, facilitating protein-protein interactions, could enable binding partners, involved in signalling, to be at a spatially advantaged position for effective signal transduction. Disruption of PSD95 could, therefore, interfere with multiple pathways downstream of NMDA receptor activity. The action of SynGAP as a GTPase activating protein means it could be involved in transcription via its role in the ras-ERK pathway.

To test whether mutations in these proteins cause transcriptional disruption, RNA levels in mutant and matched wild type tissues were assessed by microarray. The simultaneous analysis of thousands of transcripts revealed the global effect of PSD95 and SynGAP mutations on gene expression in neuronal tissue.

3.1 MICRORARRAY HYBRIDISATION AND QUALITY CONTROL

3.1.1 Isolation and Quality Assessment of RNA

Microarray analysis simultaneously assesses the levels of thousands of RNA transcripts. As such, the method is susceptible to false positive results. The dissection of tissue and subsequent RNA extraction was, therefore, performed to strict protocol criteria in order to minimise variation between samples.

Total RNA was isolated from the forebrains of 3 female adult PSD95$^{-/-}$ mice and 3 age and sex matched wild type animals. The forebrain was chosen for these samples as PSD95 is widely expressed in this area of the brain and to ensure adequate tissue for RNA isolation. RNA was also extracted from the hippocampi of 3 female adult SynGAP$^{+/-}$ animals and 3 age and sex matched wild type mice. For these samples the hippocampus was chosen as a source of RNA as SynGAP has a restricted expression pattern in the adult brain, but is highly expressed in this region (K. Porter, personal communication). Due to postnatal lethality of SynGAP$^{-/-}$ animals, heterozygotes were used.

Dissections of PSD95$^{-/-}$ and matched wildtype forebrains were performed consecutively, on the same day, and tissue immediately frozen in liquid nitrogen. Dissections of SynGAP$^{+/-}$ and matched wildtype hippocampi were performed similarly, on a different date, but at the same time of day as PSD95$^{-/-}$ samples. For both sets of samples, RNA isolation was performed on the same day as tissue dissection. Total RNA extraction, including DNase treatment, was performed on QIAGEN RNeasy spin columns and was eluted in 800µl (forebrain) or 140µl (hippocampi) DNase free water. RNA concentration was determined by taking A_{260} and A_{280} readings using a spectrophotometer (see table 3.1).

Sample	Genotype	A_{260}:A_{280}	Concentration (μg/ml)	Total RNA Extracted (μg)
PSD95 RNA Samples				
1	-/-	1.693	344	275.2
2	-/-	1.701	392	313.6
3	+/+	1.671	414	331.2
4	+/+	1.835	482	385.6
5	-/-	1.665	445	356.0
6	+/+	1.744	458	366.4
SynGAP RNA Samples				
1	+/+	2.038	64	8.96
2	+/+	2.046	72	10.02
3	+/+	1.807	80	11.23
4	+/-	1.905	76	10.67
5	+/-	1.885	78	10.98
6	+/-	1.668	109	15.32

Table 3.1 – A_{260}:A_{280} Ratios and RNA Concentrations. Genotypes of the samples are shown. A_{260}:A_{280} ratios and concentrations are taken from spectrophotometer readings. Total RNA extracted is calculated from concentration and volume of water for elution (800μl for PSD95 forebrains, 140μl for SynGAP hippocampi).

For microarray analysis, it is important that high quality starting material is used. For the PSD95 samples, the integrity of the RNA was assessed by running 1μg of each sample on an agarose gel and by use of the Agilent 2100 bioanalyser, a machine that uses 'lab-on-a-chip' technology to accurately analyse small amounts of RNA electrophoretically. Due to the limited amount of RNA extracted from hippocampi, the SynGAP RNA samples were analysed by Agilent bioanalyser alone. Figures 3.1 and 3.2 show this data for PSD95$^{-/-}$ and SynGAP$^{+/-}$ samples respectively.

Figure 3.1A is an image of an agarose gel showing the PSD95 samples to have the two expected bands of 18s and 28s ribosomal RNA. Figure 3.1B and figure 3.2 show the profiles of the samples generated by the Agilent 2100 bioanalyser for PSD95 and SynGAP samples. A marker added to each sample causes the initial peaks of each graph. The two peaks in the centre of the graphs represent the 18s and 28s ribosomal RNAs, the ratios of which can be calculated by comparing the areas under each respective peak. In all cases distinct ribosomal peaks were present, indicating the RNA is intact.

3.1.2 Microarray Hybridisation

Affymetrix U74Av2 GeneChip arrays were used to analyse the RNA extracted from PSD95 and SynGAP mutant brain tissue. These arrays contain oligonucleotide probe sets specific for approximately 12000 different transcripts. Around 6000 of these target known mouse genes present in the mouse Unigene database, build 74, and the remainder are specific to EST (expressed sequence tag) sequences. Samples from each animal were hybridised to individual chips (therefore, 12 arrays in total).

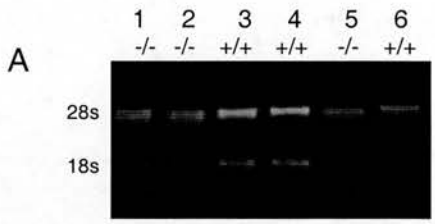

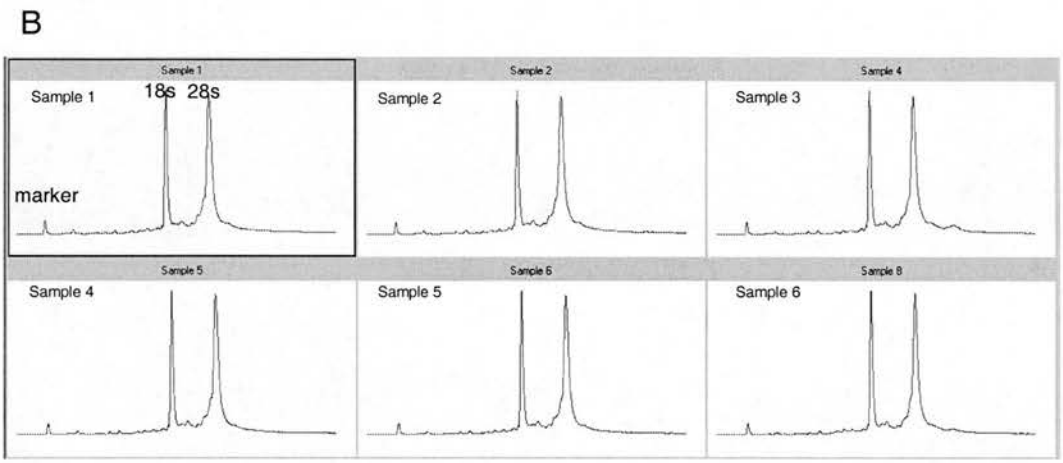

Figure 3.1 - Analysis of RNA Extracted from PSD95$^{-/-}$ and Wild Type Forebrains. A. Agarose gel showing the 18s and 28s ribosomal RNA bands of the RNA extracted from PSD95$^{-/-}$ and Wild Type forebrains. **B**. Graphs generated by Agilent Bioanalyser 2100. The two peaks in the graph represent the 18s and 28s ribosomal RNA.

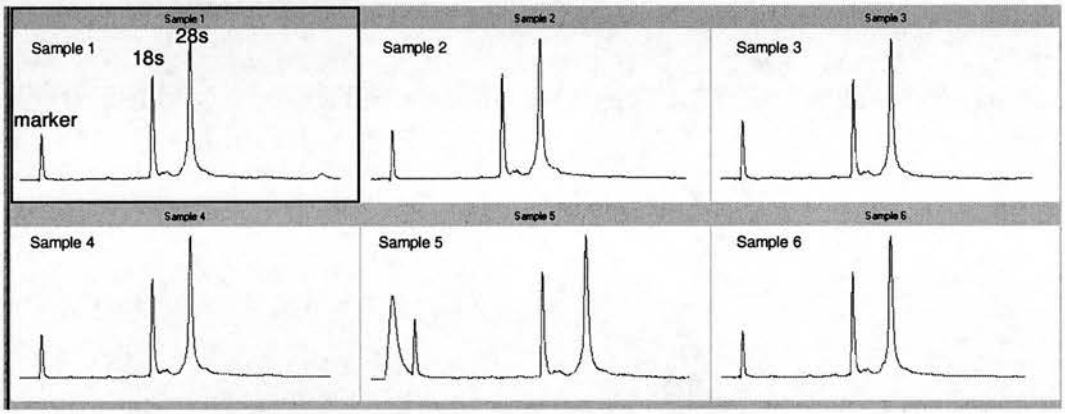

Figure 3.2 - Analysis of RNA Extracted from SynGAP$^{+/-}$ and Wild Type Hippocampi. Graphs generated by Agilent Bioanalyser 2100 for samples 1-6. The two peaks in the graph represent the 18s and 28s ribosomal RNA.

RNA labelling and hybridisation was carried out by Kevin Robertson at the Scottish Centre for Genomic Technology and Informatics (SCGTI), University of Edinburgh. RNA was prepared in accordance with Affymetrix protocols. Briefly, the RNA was primed with a primer encoding the T7 promoter with oligo-$dT_{(24)}$ used to initiate 1st strand synthesis from the polyA tails of mRNA. 1st strand cDNA synthesis was performed using reverse transcriptase (M-MLV). Using this template, second strand cDNA was synthesised by *E. coli* DNA polymerase. An *in vitro* transcription reaction was then performed by T7 RNA polymerase with biotin labelled ribonucleases. The labelled cRNA product was fragmented and hybridised to microarrays overnight. Following hybridisation the arrays were washed and stained with streptavidin phycoerythirin. The arrays were scanned using the Affymetrix GeneChip scanner 2500 and image analysis and quantitation undertaken using Affymetrix MAS 5.1 software according to standard Affymetrix protocols. Figure 3.3 shows examples of the scanned arrays. Figure 3.3A is an array hybridised with wild type forebrain sample and figure 3.3B is an array hybridised with sample from $SynGAP^{+/-}$ hippocampi.

Expression data from all arrays were normalised by scaling to an overall target intensity of 100. After normalisation, scaling factors for all the arrays were within an accepted range (i.e. within a 3 fold of each other). The result of normalisation was a spreadsheet of expression levels for all transcripts on the arrays, with a P (present), M (marginal) or A (absent) call as assigned by Affymetrix software. Absent transcripts have an expression below the threshold of detection and, if there is uncertainty about the presence of a transcript, it is called as marginal. The expression levels and presence/absence calls for all transcripts analysed in the PSD95 and SynGAP experiments are in Appendix 1 and Appendix 2 respectively.

A

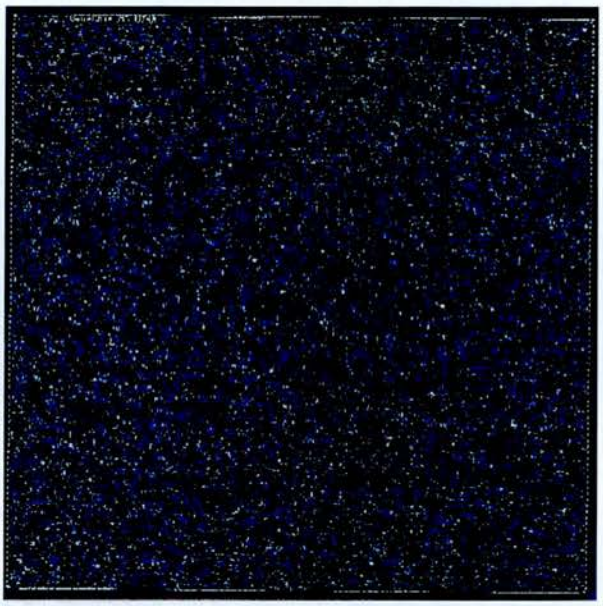

B

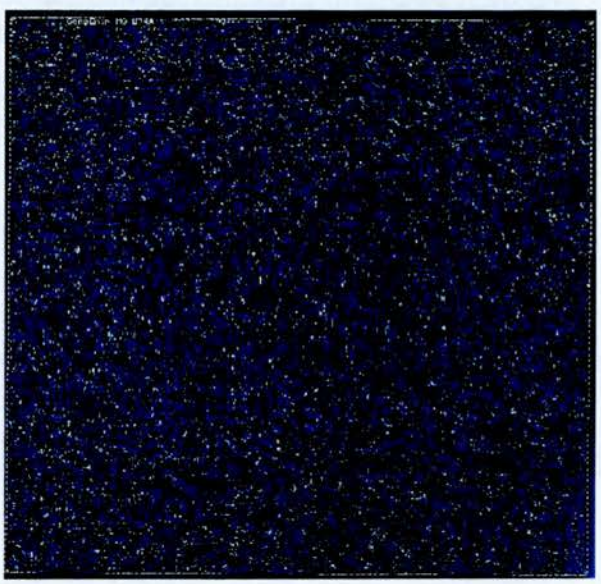

Figure 3.3 – Images of Scanned Arrays. Images show examples of scanned Affymetrix U74A arrays. **A** is an array hybridised with a sample from wild type forebrain used in the PSD95 experiment. **B** is an array hybridised with a sample from SynGAP$^{+/-}$ hippocampi. The colour intensity at a given spot is indicative of the amount of sample bound to that probe, with lighter colours representing increased amounts of binding.

3.1.3 Quality Control Data

3.1.3.1 Levels of Control Transcripts

The Affymetrix chips include several control probes, used to assess the quality of the reactions. Levels of positive control transcripts, βActin and GAPDH, were measured by oligonucleotides designed to 5′, mid and 3′ regions of the genes. The ratio of 3' and 5′ levels would ideally be close to 1 and it is recommended by Affymetrix that a ratio greater than 3 be considered unacceptable. As shown in table 3.2, for all 12 chips, βActin ratios range from 0.96 to 1.02 and those for GAPDH range from 0.96 to 1.01. These ratios indicate that the RNA used was undegraded and subsequent treatments were efficient.

To assess the quality of the hybridisations, the levels of spiked controls, at known concentrations, were measured. The spike with the lowest concentration, 'bioB' was detected present in all reactions (see table 3.2), indicating hybridisation, washing, staining and scanning were optimal.

Sample	βActin (3'/5')	GAPDH (3'/5')	BioB Level	BioB Call
PSD95 Arrays				
1. +/+	1.02	0.99	358.4	Present
2. +/+	1.03	0.99	333.3	Present
3. +/+	0.99	0.98	397.6	Present
4. -/-	1.02	0.99	288	Present
5. -/-	1.01	0.97	289.3	Present
6. -/-	1.01	1.01	312.2	Present
SynGAP Arrays				
1. +/+	0.96	0.99	169.1	Present
2. +/+	1.02	0.98	136.9	Present
3. +/+	0.98	0.96	172.5	Present
4. +/-	0.99	1.00	141.4	Present
5. +/-	0.98	0.95	167.7	Present
6. +/-	1.02	0.93	165.1	Present

Table 3.2 - Control Gene Ratios and Spiked Control Levels. Table shows the 3'/5' ratios of βActin and GAPDH transcripts for each sample array. Also, the levels of BioB, the spiked control of lowest concentration, and presence call are shown for each array.

3.1.3.2 Distribution of Transcript Expression Levels

To analyse the performance of the arrays, prior to data analysis, scatter plots were produced using Insightful SPLUS software (Insightful Corporation) (figures 3.4 and 3.5). To compare the range of expression and consistency of all arrays, the expression levels for all transcripts on each array were plotted against those of every other array. These plots show the data, from both the PSD95 and SynGAP experiments, have a symmetrical 'flared' distribution and a dynamic uninterrupted range of expression values from low to high signals. The symmetry of the plots, about the 45° line, indicates that the hybridisation of the arrays and subsequent normalisation of the data was consistent across all arrays. The flared distribution at lower levels occurs as a result of increased variation as signal levels decrease and is typical of data normalised in the manner described (K. Roberston, personal communication).

To further investigate the signal distribution across all arrays, a 'box-and-whiskers' representation of $\log_2$ expression levels was produced in SPLUS (figure 3.6). The plots show the lower quartile, median and upper quartile values for each array, as well as the range of expression values. After normalisation, the data from PSD95 and SynGAP experiments shows symmetry across all chips.

PSD 95 Data

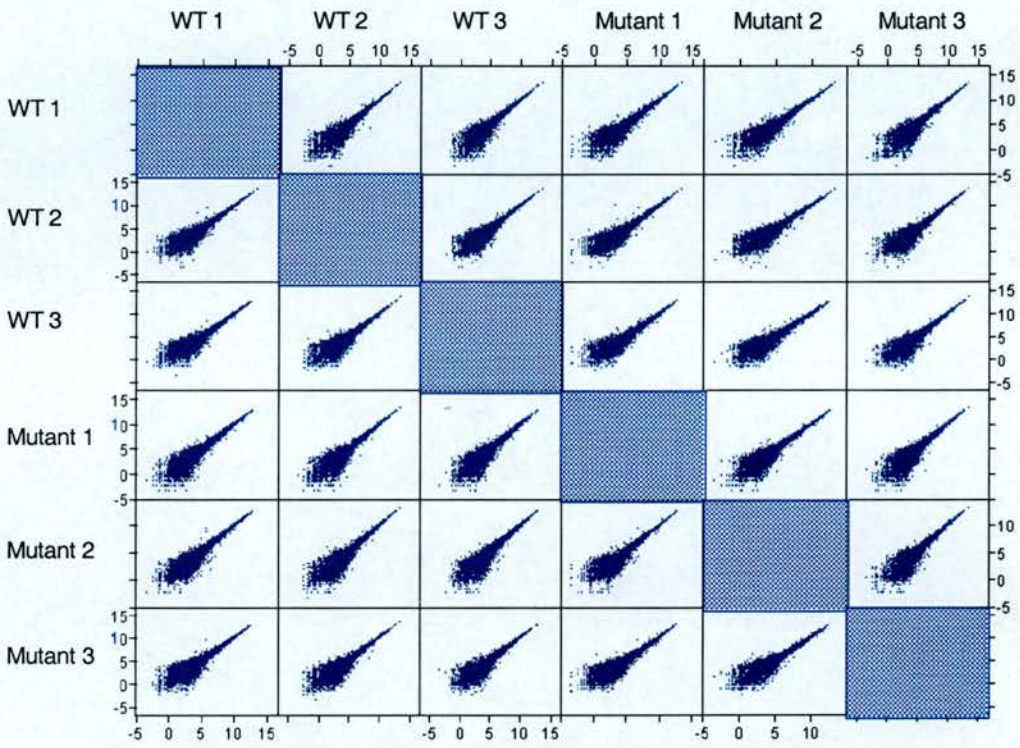

Figure 3.4 – Scatter Plots of Expression on All Arrays Against Each Other (PSD95 Experiment). Scatter plots are of the $\log_2$ expression levels of all transcripts on each array plotted against every other array. The plots show a symmetrical, flared distribution of expression.

SynGAP Data

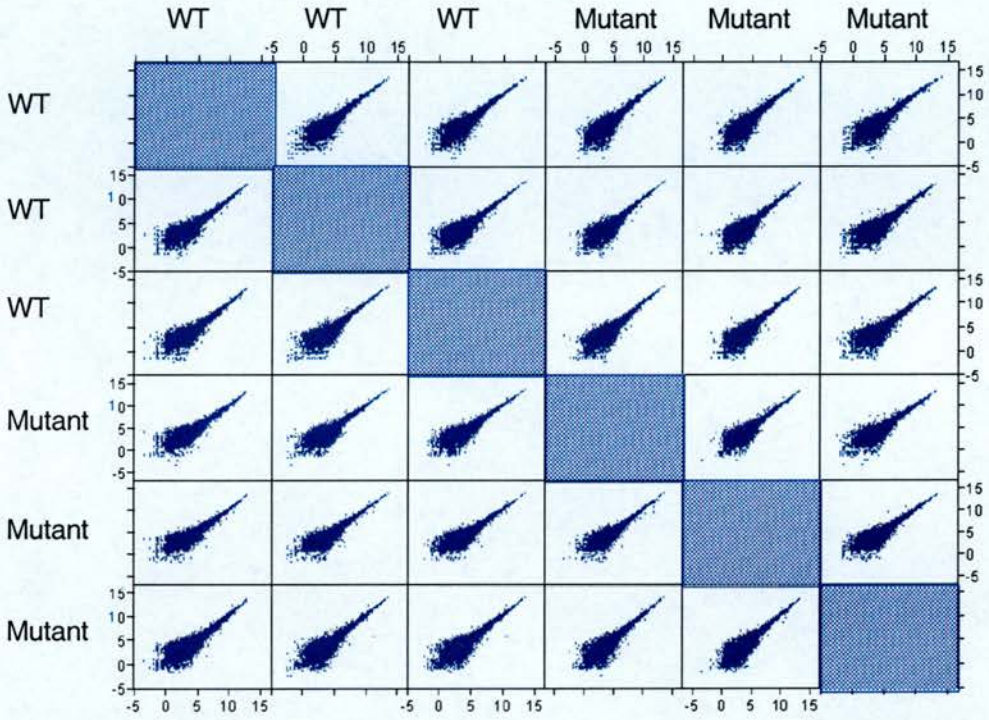

Figure 3.5 – Scatter Plots of Expression on All Arrays Against Each Other (SynGAP Experiment). Scatter plots are of the $\log_2$ expression levels of all transcripts on each array plotted against every other array. The plots show a symmetrical, flared distribution of expression.

PSD 95 Data

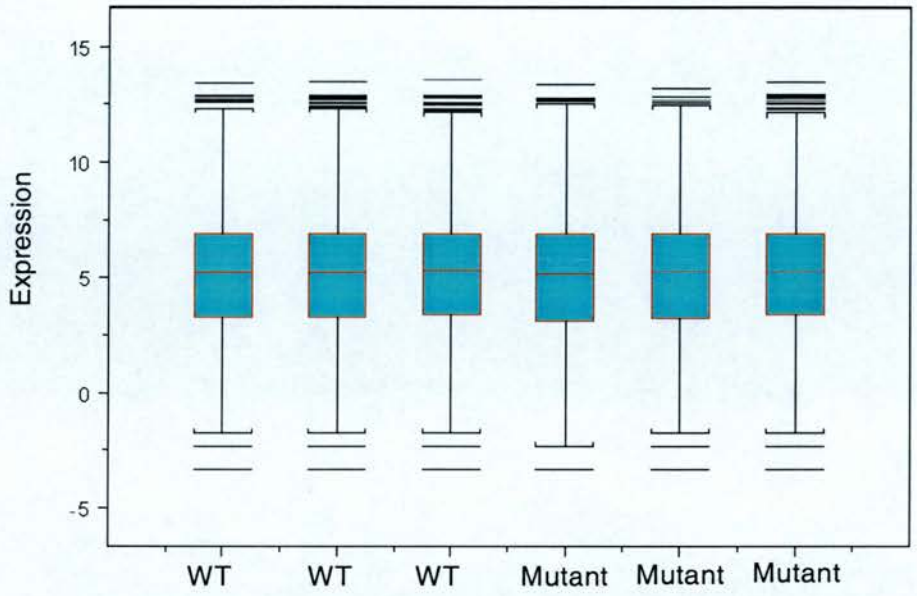

SynGAP Data

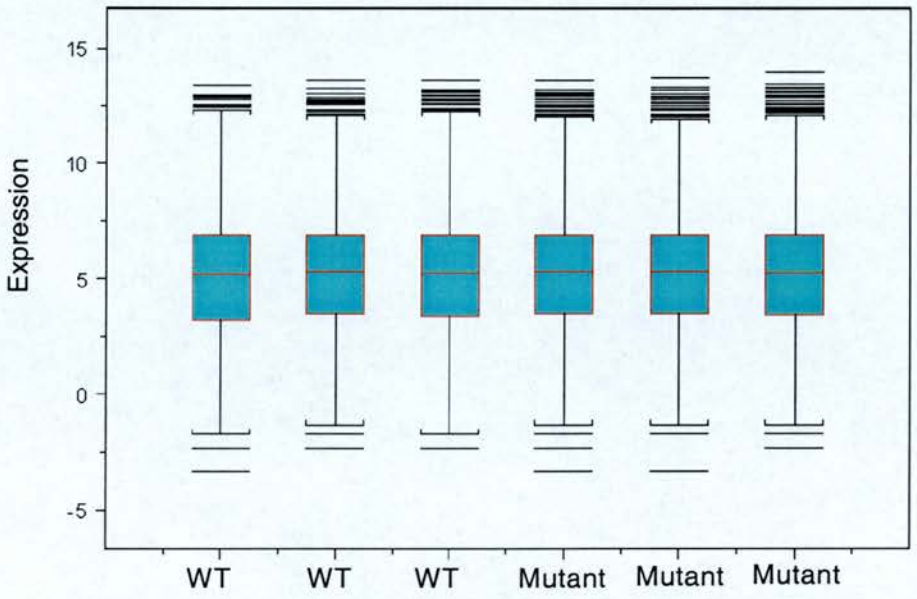

Figure 3.6 – Box and Whiskers Plots Of PSD95 and SynGAP Data. Plots illustrate the range of $\log_2$ expression values across each chip and show the lower quartile, median and upper quartile values for each array .

3.1.3.3 Numbers of Transcripts Detected

Affymetrix microarray chip reports contain information about the number of transcripts considered to be present, absent and marginal by Affymetrix MAS 5.1 software. Table 3.3 shows summary of this data for all arrays. It was found that, for the PSD95$^{-/-}$ chips (both mutant and wild type), an average of 5831 transcripts were detected present, 46.75% of the total probes present. 6333 transcripts (50.75% of the total probes) were called as absent. For the SynGAP$^{+/-}$ chips, on average, 5355 transcripts were present, 42.93% of the total on the array, and 6808 (54.58% of total probes) were absent.

Sample	# Present	% Of Total Probes	# Absent	% Of Total Probes	# Marginal	% Of Total Probes
PSD95 Samples						
1. +/+	5809	46.6	6336	50.8	328	2.6
2. +/+	5857	47.0	6304	50.5	312	2.5
3. +/+	5578	44.7	6587	52.8	308	2.5
4. -/-	6239	50.0	5917	47.4	317	2.5
5. -/-	5860	47.0	6314	50.6	299	2.4
6. -/-	5640	45.2	6541	52.4	292	2.3
Average	5831	46.75	6333	50.75	263	2.5
SynGAP Samples						
1. +/+	5752	46.1	6411	51.4	310	2.5
2. +/+	5420	43.5	6757	54.2	296	2.4
3. +/+	5472	43.9	6670	53.5	331	2.7
4. +/-	5178	41.5	6977	55.9	318	2.5
5. +/-	4991	40.0	7174	57.5	308	2.5
6. +/-	5317	42.6	6858	55.0	298	2.4
Average	5355	42.93	6808	54.58	310	2.5

Table 3.3 – Numbers of Detected Transcripts. Table shows the number of genes detected present, absent and marginal on each microarray and this represented as a % of the total probes on each chip. The average for each genotype set is also shown.

3.2 GENES SIGNIFICANLTY ALTERED IN MUTANT TISSUE

3.2.1 Analysis and Sorting of Data

Control data and analysis of expression distribution indicated that the labelling and hybridisation reactions were all successful. Thus, the data from these reactions were further analysed. To identify genes expressed at significantly different levels in mutant tissue, as compared to wild type, data was imported into Microsoft Excel and Welch t tests, which do not assume equal variance, were performed.

Figure 3.7 shows scatter plots of the PSD95$^{-/-}$ data. The graphs show, on a $\log_{10}$ scale, the average expression level in mutant tissue versus wild type expression for each probe on the Affymetrix array. Spots on the line at 45° that passes through the point of origin are unchanged in mutant tissue, the other two parallel 45° lines represent 2 fold changes up and down.

Figure 3.7A shows data from all transcripts on the array. The dots representing the transcripts are coloured according to their expression, ranging from blue at low levels to yellow at high levels. A greater deviation from the unchanged line is seen in transcripts of lower expression. This is due to the increased variability of measurements at extreme low levels. Figure 3.7B shows transcripts that were found expressed at significantly different levels in PSD95$^{-/-}$ tissue, compared to wild type ($p<0.05$, as measured by Welch t test). 644 transcripts were found differentially expressed with a p value less than 0.05.

Figure 3.8 shows scatter plots for the SynGAP$^{+/-}$ data in the same was as shown for the PSD95 data. For the SynGAP samples, 658 transcripts were found to have a p value of less than 0.05.

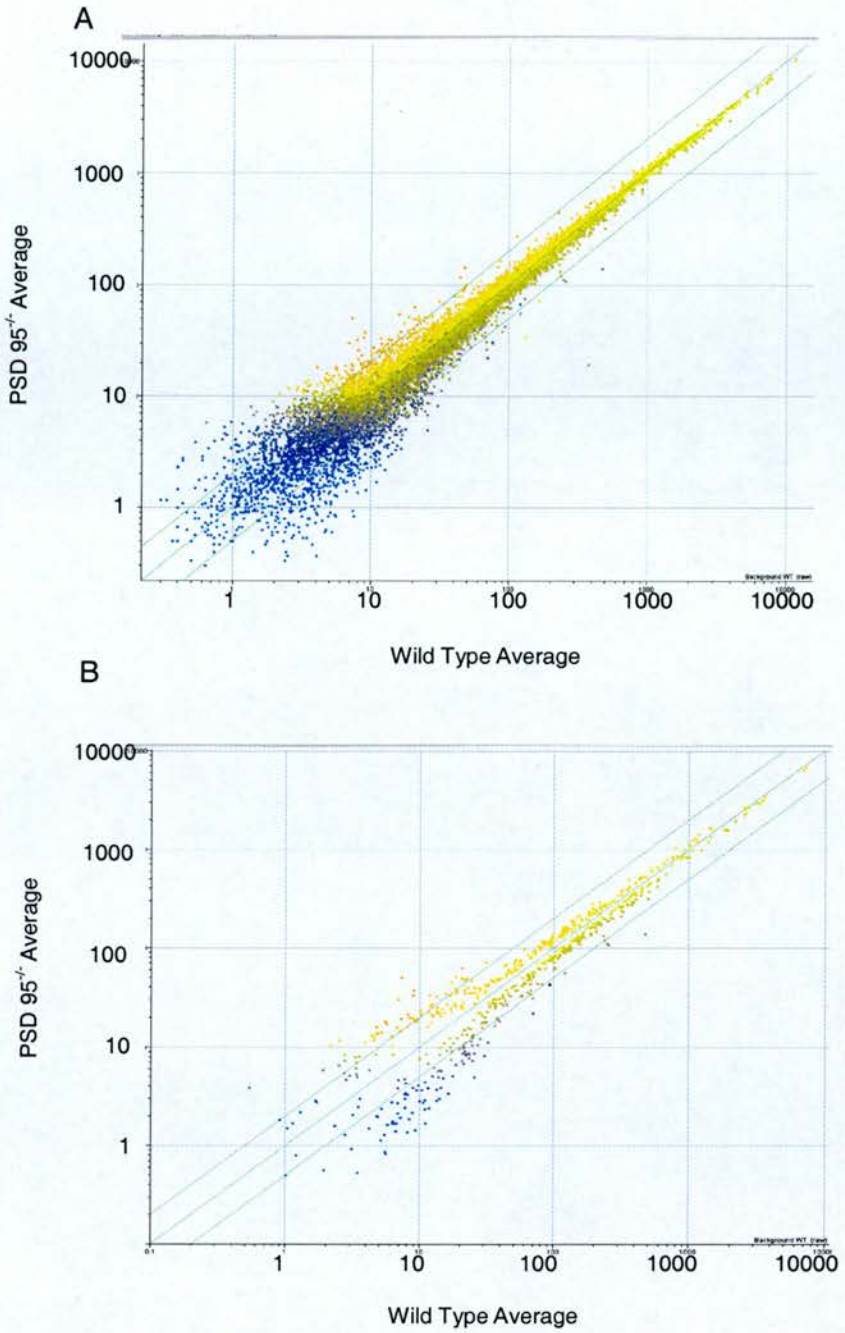

Figure 3.7 - Average Expression Levels On PSD95$^{-/-}$ and Wild Type Arrays. Scatter plots show, on a log scale, the average expression levels of transcripts on PSD95$^{-/-}$ and wild type arrays. **A** shows all transcripts and **B** shows transcripts expressed at significantly different levels on PSD95$^{-/-}$ and wild type arrays with a p value <0.05, as measured by Welch t test.

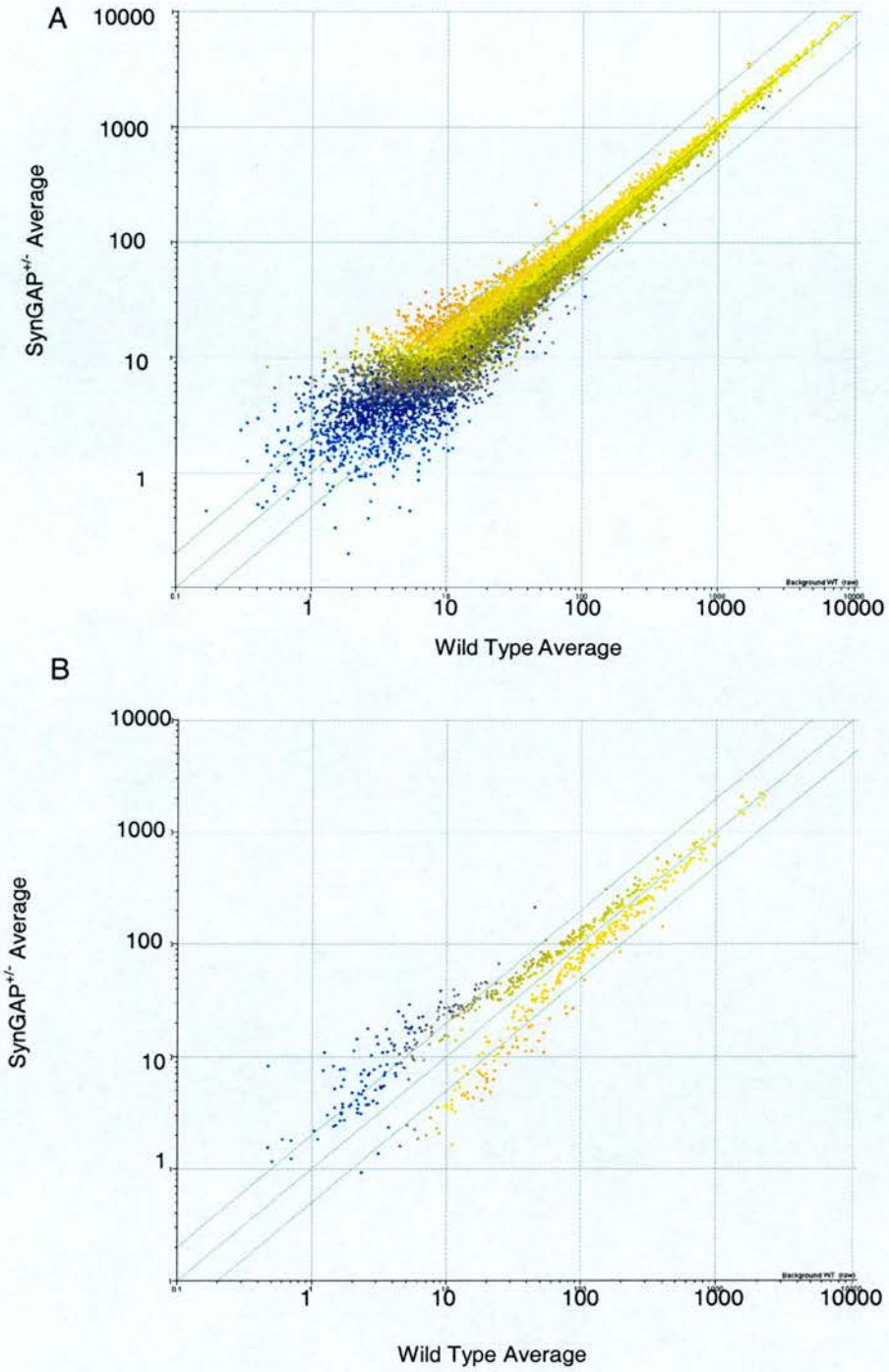

Figure 3.8 - Average Expression Levels On SynGAP$^{+/-}$ and Wild Type Arrays. Scatter plots show, on a log scale, the average expression levels of transcripts on SynGAP$^{+/-}$ and wild type arrays. **A** shows all transcripts and **B** shows transcripts expressed at significantly different levels on SynGAP$^{+/-}$ and wild type arrays with a p value <0.05, as measured by Welch t test.

To identify, from this data, differentially expressed transcripts that may be of biological significance, particular criteria were set. Transcripts that were altered greater than 1.5 fold, with a p value less than 0.05, were considered to be significantly altered. Also, probes that were called absent by Affymetrix MAS 5.1 in both wild type and mutant tissue were discarded. To be considered expressed in tissue from a particular genotype, the transcript had to be called present on all 3 relevant chips.

3.2.2 Genes Significantly Altered in PSD95$^{-/-}$ Forebrain

3.2.2.1 Genes Significantly Altered in PSD95$^{-/-}$ Forebrain

Using the set criteria, the PSD95$^{-/-}$ versus wild type data was analysed. Table 3.4 details genes that showed significant change ($p<0.05$), greater than 1.5 fold, between wild type and PSD95$^{-/-}$ RNA. This analysis revealed changes in a limited number of transcripts. 11 transcripts (0.19% of transcripts detected present) were down regulated in mutant tissue. 3 transcripts (0.05% of those present) were found at a higher level in PSD95$^{-/-}$ forebrain.

Of the downregulated transcripts in PSD95$^{-/-}$ forebrain, 4 are genes regulated by NMDA receptor activity (*nur77*, *cfos*, *egr2* and *junB*; highlighted in table 3.4). The other genes found at a lower expression in the mutant tissue were *Per1*, *GADD45B*, *cyln2* and *PSD95* itself. The probes used by Affymetrix to detect the *PSD95* transcript are designed to the 3' end of the gene, sequence that is left intact following the targetted mutation of PSD95. As such, it is not alarming that PSD95 transcript is detected by these probes in the PSD95$^{-/-}$ samples. 3 unknown ESTs were found down regulated in the mutant tissue.

3 transcripts were found at higher levels in PSD95$^{-/-}$ forebrain. The gene showing the greatest level of up regulation is *Atp7a*, encoding a Cu^{++} transporting ATPase. The other altered transcripts were *syntenin* and *serine palmitoyltransferase, subunit 2*.

AFFYMETRIX ID	GENE	GENBANK NO.	FOLD CHANGE
Lower in Mutant			
104175_at	PSD 95	D50621	3.4
102371_at	**nur 77**	**X16995**	**2.39**
160901_at	**cfos**	**V00727**	**2.22**
102661_at	**egr2**	**M24377**	**2.19**
93619_at	per1	AF022992	2.16
102362_i_at	**junB**	**U20765**	**1.97**
99432_at	CYLN2	AJ228865	1.97
161666_f_at	GADD45B (EST)	AV138783	1.75
94555_at	EST	AI845579	1.57
96242_at	EST	AW125751	1.55
96756_at	EST	AA693236	1.52
Higher in Mutant			
102854_s_at	Atp7a	U03434	1.74
100893_at	serine palmitoyltransferase, subunit 2	U27455	1.57
93017_at	syntenin	AF077527	1.56

Table 3.4 – Genes with Altered Expression in PSD95$^{-/-}$ Forebrain. Table shows Affymetrix IDs of transcripts significantly altered, >1.5 fold, p value <0.05, in mutant tissue. Gene names, Genbank accession numbers and fold change are all shown. EST following gene name indicates Affymetrix probes were designed to an EST that has subsequently been annotated. Transcripts shown in bold are activity regulated genes.

3.2.2.2 Expression Levels of Genes Significantly Altered in PSD95$^{-/-}$Forebrain

Table 3.5 shows the expression levels of significantly altered transcripts in PSD95$^{-/-}$ tissue. The table also indicates whether the transcripts were called as present (P) or absent (A). All, but one, transcripts were present in both wild type and PSD95$^{-/-}$ samples. The Cu^{++} transporting ATPase was found to be absent in wild type samples, but was expressed, at low level, in PSD95$^{-/-}$ forebrain. Figure 3.9 is a bar graph showing the expression levels of significantly altered transcripts.

3.2.3 Genes Significantly Altered in SynGAP $^{+/-}$ Hippocampi

3.2.3.1 Genes Significantly Altered in SynGAP$^{+/-}$ Hippocampi

Table 3.6 shows genes expressed at significantly different levels in wild type and SynGAP$^{+/-}$ hippocampi with a fold change greater than 1.5. As with the PSD95 data, changes were seen in a limited number of genes. 16 transcripts (0.30% of those present) were expressed at lower levels in SynGAP$^{+/-}$ hippocampi. 4 (0.07% of those present) transcripts were up regulated in mutant tissue.

Of the genes down regulated, 3 (*egr2*, *cfos* and *nur77*) are regulated by NMDA receptor activity (highlighted in table 3.6). The other genes down regulated include two potassium channels, one belonging to subfamily K (*TWIK1)* and one to subfamily H (*m-eag).* The other genes with reduced expression in mutant tissue are *sox11, DUSP6, erythroid differentiation factor, glucoses-6-phosphate dehydrogenase, Nrd1, UDP-glucuronosyltransferase 8, N–glycan alpha 2,8-siayltransferase* and *Elovl6*. 3 ESTs were found at a lower level in the SynGAP$^{+/-}$ hippocampi. It should be noted that there were no probes representing SynGAP present on the arrays used.

Of the transcripts up regulated in SynGAP$^{+/-}$ hippocampi, one was an EST. The others encode NADH dehydrogenase, glyoxalase 1 and ribosomal protein L44.

GENE	WILD TYPE			PSD 95$^{-/-}$			P VALUE
	Ave.	St. Dev	Call	Ave.	St. Dev	Call	
Lower in Mutant							
PSD 95	472.57	37.23	P	138.9	4.51	P	0.004
nur 77	256.9	21.81	P	107.2	22.78	P	0.001
cfos	247.8	38.4	P	111.4	9.69	P	0.002
egr2	92.73	9.94	P	42.43	15.67	P	0.014
per1	120.3	23.23	P	55.6	11.85	P	0.024
junB	238.7	30.88	P	121.0	6.12	P	0.019
CYLN2	66.93	10.85	P	34.13	6.94	P	0.017
GADD45B	57.43	7.56	P	32.8	6.89	P	0
EST (94555_at)	497.53	60.58	P	317.17	50.16	P	0.014
EST (96242_at)	31.07	3.36	P	18.07	4.01	A	0.013
EST (96756_at)	65.8	9.61	P	43.27	7.44	P	0.036
Higher in Mutant							
Atp7a	21.47	1.89	A	37.33	5.05	P	0.021
serine palmitoyltransferase	42.6	5.5	P	66.7	7.65	P	0.014
syntenin	25.37	3.57	P	39.6	2.45	P	0.007

Table 3.5 – Levels of Genes with Altered Expression in PSD 95$^{-/-}$ Forebrain. Table shows the average expression levels and standard deviations for significantly altered genes in wildtype and mutant tissue. The 'call' column shows whether the transcript was judged present (P) or absent (A) by Affymetrix MAS 5.1. P values were calculated by comparing wild type and mutant expression levels by Welch t Test.

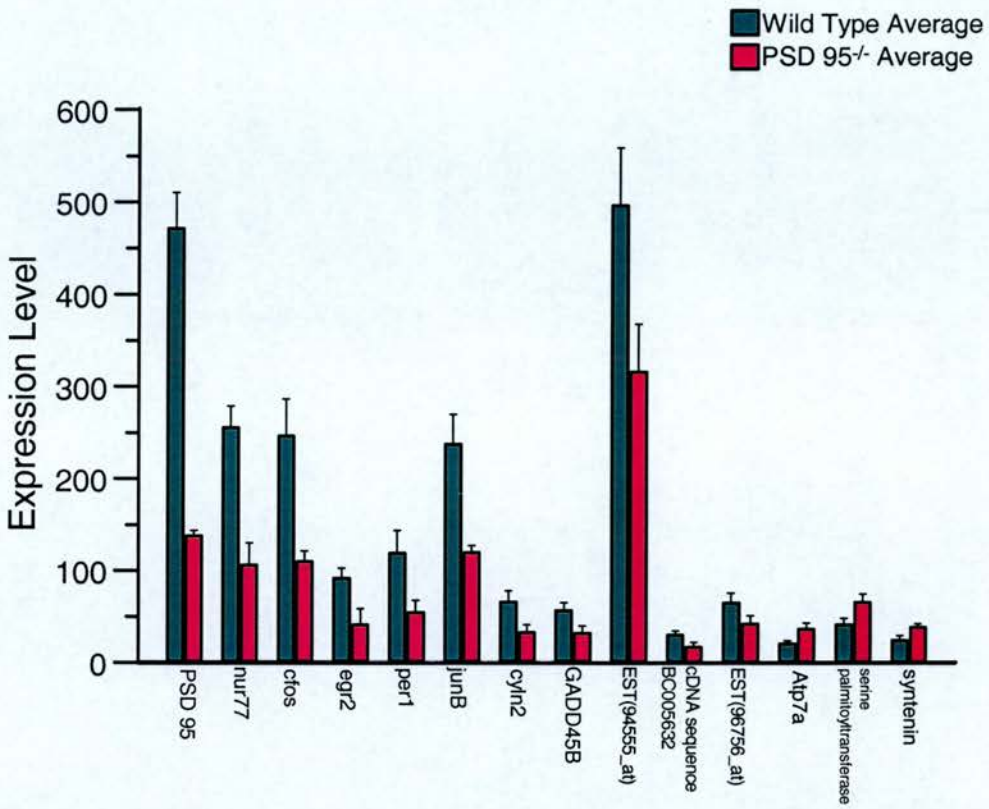

Figure 3.9 – Graphed Expression Levels of Transcripts Significantly Altered in PSD95$^{-/-}$ Forebrain. Graph shows the average expression levels, with standard deviations indicated, of significantly altered transcripts in wild type and mutant forebrain.

AFFYMETRIX ID	GENE	GENBANK NO.	FOLD CHANGE
Lower in Mutant			
102661_at	**egr2**	**M24377**	**3.19**
96215_f_at	EST	AI153421	2.79
93669_f_at	SOX 11 (EST)	AW107922	2.71
98525_f_at	erythroid differentiation factor	AJ007909	2.25
160901_at	**cfos**	**V00727**	**2.17**
93285_at	DUSP6 (EST)	AI845584	1.92
96833_at	EST	AW048468	1.67
94966_at	glucose-6-phosphate dehydrogenase	Z11911	1.61
102371_at	**nur 77**	**X16995**	**1.61**
102335_at	K^+ channel, subfamily K, 1	AF033017	1.59
96661_at	Nrd1 (EST)	AA734806	1.59
98380_at	voltage gated K+ channel, subfamily H, 1	U04294	1.58
98872_at	UDP-glucuronosyltransferase 8	U48896	1.58
102318_at	N-glycan alpha 2, 8-sialyltransferase	NM_008430	1.53
95451_at	EST	AA855382	1.53
103665_at	Evovl6 (EST)	AW122523	1.51
Higher in Mutant			
100775_at	EST	C81070	1.67
93562_at	NADH dehydrogenase (EST)	AI854366	1.60
93269_at	Glyoxalase 1	AI848952	1.57
160081_at	ribosomal protein L44 (EST)	AW045418	1.57

Table 3.6 – Genes with Altered Expression in SynGAP$^{+/-}$ Hippocampi. Table shows Affymetrix IDs of transcripts significantly altered, >1.5 fold, p value <0.05, in mutant tissue. Gene names, Genbank accession numbers and fold change are all shown. EST following gene name, indicates Affymetrix probes were designed to an EST that has subsequently been annotated. Transcripts shown in bold are activity regulated genes.

3.2.3.2 Expression Levels of Genes Significantly Altered in SynGAP$^{+/-}$ Hippocampi

Table 3.7 details the expression level of all transcripts significantly altered in SynGAP$^{+/-}$ hippocampi and indicates whether they were present (P) or absent (A). Apart from 2, all transcripts were called present in both wild type and mutant samples. *Egr2* and an EST (96833_at) were only present in wild type tissue. Figure 3.10 is a bar chart showing the levels of the significantly altered genes.

GENE	WILD TYPE			SynGAP$^{+/-}$			P VALUE
	Ave.	St. Dev	Call	Ave.	St. Dev	Call	
Lower in Mutant							
Egr 2	77.77	19.25	P	24.37	12.4	A	0.021
EST (96215_f_at)	398.87	76.17	P	142.87	82.16	P	0.017
Sox11	75.73	5.35	P	27.93	7.72	P	0.002
Erythroid Differentiation Factor	192.9	14.03	P	85.8	31.72	P	0.016
cfos	105.67	18.3	P	48.6	2.9	P	0.03
DUSP6	281.27	4.68	P	146.7	26.34	P	0.011
EST (96833_at)	88.13	12.16	P	52.67	15.18	A	0.037
Glucose 6 phosphate dehydrogenase	53.23	1.97	P	33.03	7.36	P	0.034
nur77	179.9	17.2	P	111.43	8.96	P	0.009
K^+ channel, subfamily K, 1	332.2	42.55	P	208.87	28.54	P	0.019
Nrd1	221.97	23.99	P	139.33	26.46	P	0.016
voltage gated K channel, subfamily H1	94.07	5.57	P	59.63	11.29	P	0.019
UDP-glucuronosyltransferase 8	31.6	4.69	P	18	6.04	A	0.04
N-glycan alpha 2, 8-sialyltransferase	69.37	6.87	P	45.37	7.11	P	0.014
EST (95451_at)	209.57	17	P	136.53	12.71	P	0.005
Evovl6	121	14.09	P	80.03	9.44	P	0.018
Higher in Mutant							
EST (100775_at)	29.1	2.77	P	48.73	5.6	P	0.013
NADH dehydrogenase	362.83	52.02	P	580.5	89.36	P	0.032
Glyoxalase 1	249.27	9.05	P	390.7	20.98	P	0.003
Ribosomal Protein L44	52.5	14.12	P	82.43	10.12	P	0.046

Table 3.7 – Levels of Genes with Altered Expression in SynGAP$^{+/-}$ Hippocampi. Table shows the average expression levels and standard deviations of significantly altered genes in wildtype and mutant tissue. The 'call' column shows whether the transcript was judged present (P) or absent (A). P values were calculated by t test, comparing wild type with mutant expression levels.

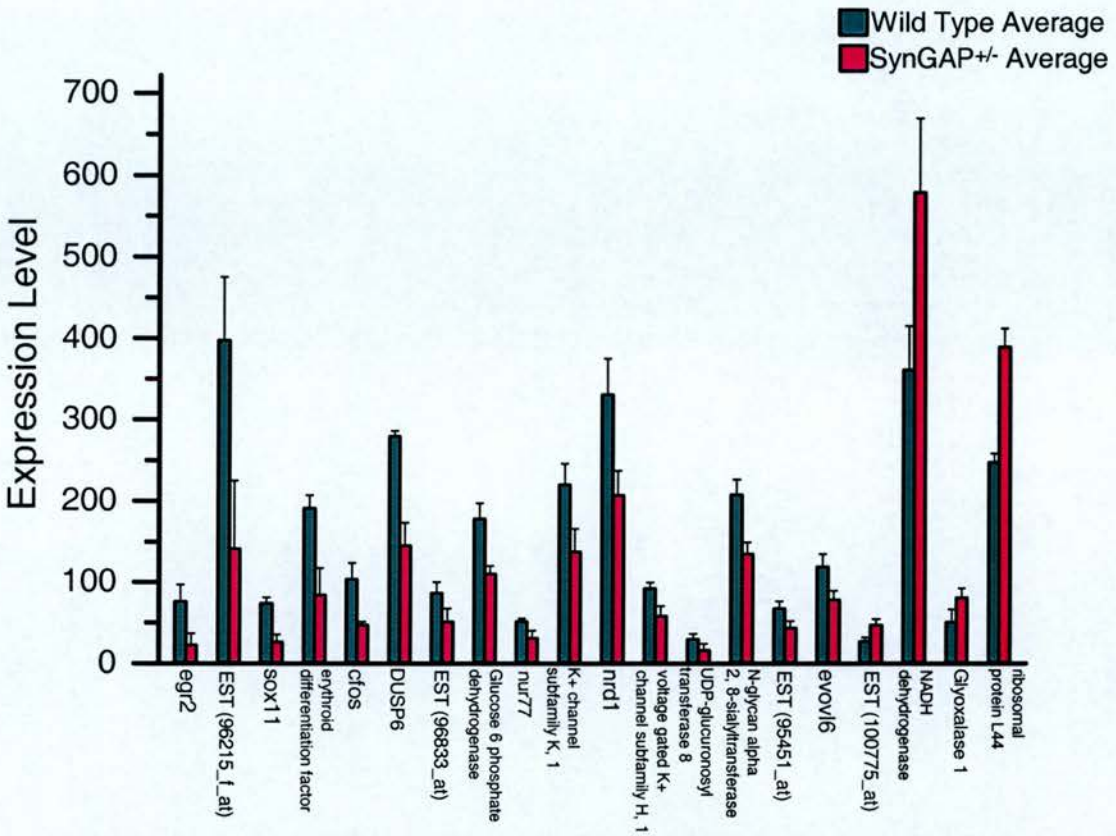

Figure 3.10 – Graphed Expression Levels of Transcripts Significantly Altered in SynGAP$^{+/-}$ Forebrain. Graph shows the average expression levels, with standard deviations indicated, of significantly altered transcripts in wild type and mutant hippocampi.

3.3 MICROARRAY DATA CONFIRMATION USING RT-PCR

To be confident microarray results are accurate, confirmation by an alternative method of RNA analysis method is required. This has been done using RT-PCR.

3.3.1 Primers Used for RT-PCR

Intron spanning primers were designed to genes of interest using Primer 3.0. Figure 3.11 details the primers used for RT-PCR and shows their products were of expected size when used in an RT-PCR reaction with cDNA from wild type forebrain.

3.3.2 Confirmation of Microarray Data by RT-PCR

Using conventional RT-PCR, RNA samples from PSD95$^{-/-}$ and wild type forebrain were amplified with PSD95, cfos and nur77 primers, using GAPDH primers as a control. Figure 3.12 shows the resulting products, run out on a 4% agarose gel. GAPDH was used as a loading control. It should be noted that the PSD95 primers used for the RT-PCR reactions were designed to the 3' region of the gene to which the Affymetrix probes were designed. As such the results from these primers should be comparable to the data from the Affymetrix analysis. For the reactions with PSD95 and cfos primers, the bands in the PSD95$^{-/-}$ lanes (samples 1, 2 and 5) appear less intense than wild type. For the nur77 reaction, the PSD95$^{-/-}$ samples in lanes 1 and 2 appear less intense than wild type samples. However, there is little difference between the mutant sample in lane 5 and wild type lanes.

The PSD95 and cfos data confirms the differential expression levels seen by microarrays in PSD95$^{-/-}$ and wild type forebrain. In the nur77 reaction, the band intensity in only two of the three PSD95$^{-/-}$ sample lanes appear consistent with lower *nur77* expression levels in mutant tissue. It may be that, in the given conditions, the reactions are reaching saturation. If this were the case differential expression of *nur77* in mutant samples may only be clearly detectable at an earlier stage of reaction.

A

GENE	FORWARD PRIMER	REVERSE PRIMER	EXPECTED PRODUCT (BP)
Primers used for RT-PCR			
GAPDH	GTGTTCCTACCCCCAATGTG	ATGTAGGCCATGAGGTCCAC	292
cfos	CTTTATCCCCACGGTGACAG	CTGCAGCCATCTTATTCCGT	298
nur77	TTCTGCTCAGGCCTGGTACT	GATTCTGCAGCTCTTCCACC	199
PSD 95	TAAGACTCCTACCCCTGCCC	AGGTGGGAGGTGTGTGAAAG	312
Additional primers used for QRT-PCR			
egr2	AAGGCCGTAGACAAAATCCC	CTAGGTGCAGAGATGGGAGC	344
Syntenin	AGGTGAACGGACAGAACGTC	AGGTGTCTGGAATGGAGTGG	177
MAP2	TGGCTCACTTGACAATGCTC	TGACATCCTCAGCCAAAGTG	236
RL44	GAACATGGTGAACGTGCCTA	CATCCTCTTAGATCTGCAGTTGG	250

Figure 3.11 – Primers Used for RT-PCR. A shows the details of the primers used for RT-PCR and QRT-PCR and their expected product size. **B** shows gels from RT-PCR reactions. The primers used are detailed above each lane, cDNA from wild type forebrain was used as a template for the reaction. The 1st lanes are 1kb ladder with the relevant band sizes noted on the left.

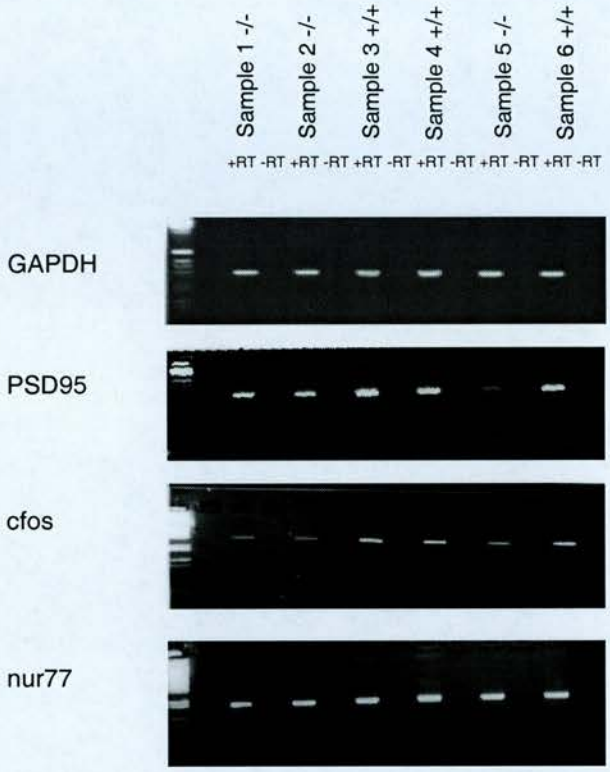

Figure 3.12 – RT-PCR of PSD95$^{-/-}$ and Wild Type RNA. Gels show the products of RT-PCR reactions performed with GAPDH, PSD95, cfos and nur77 primers and PSD95$^{-/-}$ and wild type forebrain RNA samples. The first lane is a water control, the rest are samples 1 – 6 ± reverse transcriptase. Samples 1, 2 and 5 are from PSD95$^{-/-}$ forebrain. 3, 4 and 6 are wild type samples.

3.3.3 Confirmation By Microarray Data by QRT-PCR

To overcome the concerns of RT-PCR reaction saturation, and to quantify the level of RNAs in the samples, quantitative RT-PCR (QRT-PCR), using a lightcycler was employed. SYBR green, which fluoresces in the presence of double stranded nucleic acids, is used to measure the accumulation of double stranded product over the course of a PCR reaction. This is advantageous, compared to regular RT-PCR, as enzyme saturation is not an issue since measurements are taken throughout the reaction. Also, the level of a particular RNA in a sample can be calculated relative to a standard curve of RNA concentrations enabling quantification.

The primers used for QRT-PCR reactions were those detailed in figure 3.11, as used for conventional RT-PCR. Primer products were melted at the end of reactions to confirm the presence of one double stranded product.

3.13A shows a graph of standards, for a particular gene, marked in black. The plot, generated using dilutions of cDNA, is of cDNA quantity against cycle number. 3.13B shows an amplification plot, where the various sigmoidal curves represent the reactions of different samples, with the cycle threshold line marked C_T. Where the sample plots cross the C_T line, the cycle number is taken. The cycle number is then used to calculate the amount of template present using the standard curves. The C_T threshold line is set using the plot of the standards. Adjusting the position of the C_T line alters the regression line through the standard curve, such as figure 3.13A. The C_T is set to where the r^2 value of the line through the standard values is closest to 1.

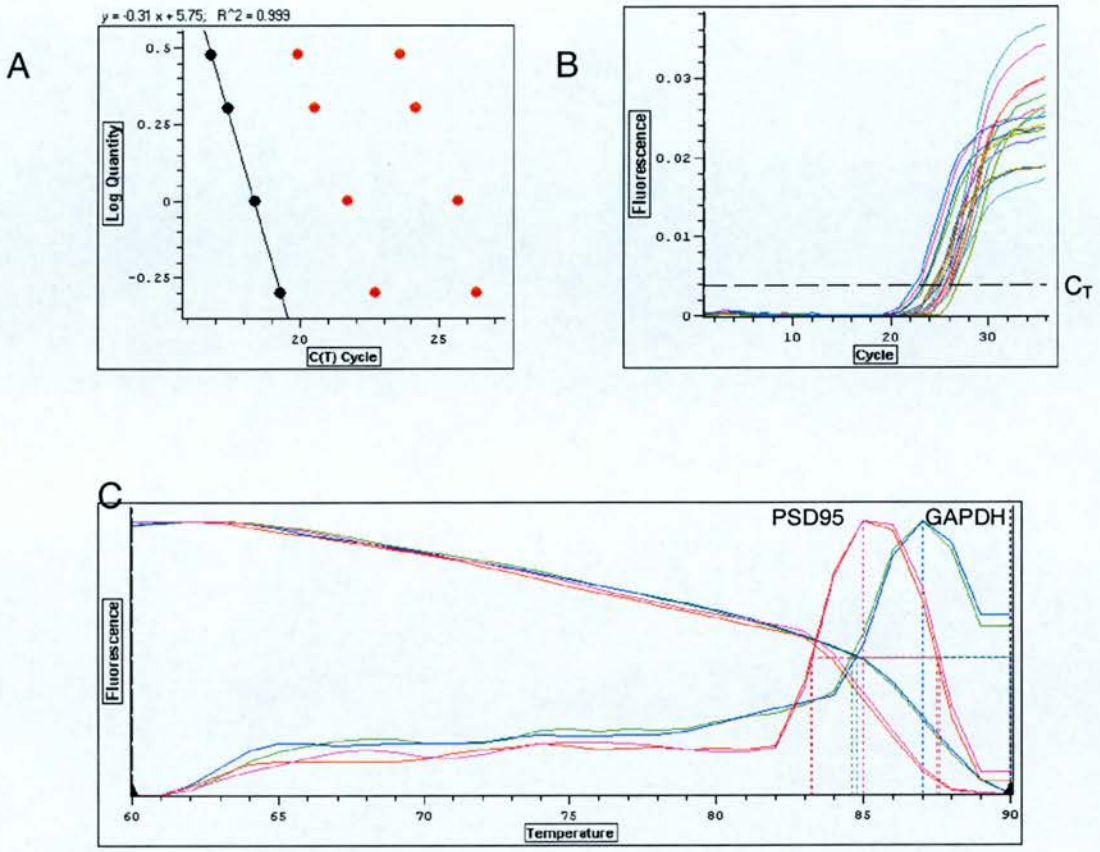

Figure 3.13 – Graphs from QRT-PCR. Figures show examples of graphs generated by QRT-PCR. **A** shows log quantity vs. cycle number for standards of diluted cDNAs run with 3 different primers. The points in black represent the data from one set of primers and the r^2 value of the line through the points is 0.999. **B** shows an amplification plot of reactions plotted as fluorescence vs. cycle number. **C** shows the melting plots (fluorescence vs. temperature) of 4 reaction products, 2 using GAPDH primers and 2 using PSD95 primers.

The melting curves calculated at the end of QRT-PCR reactions graph the loss of fluorescence at different temperatures while the reaction products are heated. The peaks of the graph are at the product melting point. Graph 3.14C shows plots of melting curves for 4 samples, 2 amplified with PSD95 and 2 with GAPDH primers. The melting profiles are individual, and reproducible, for each primer pair and can be used to verify that the reactions have produced only one double stranded product.

3.3.3.1 Confirmation of PSD95$^{-/-}$ Data

For confirmation experiments, RNA from 3 PSD95$^{-/-}$ forebrains and matched wild type tissue was extracted as detailed before. 2µl RNA was used for reverse transcription reactions using Ambion RT protocol. Each cDNA sample was run in triplicate with each primer pair (GAPDH, PSD95, cfos, nur77, egr2, syntenin and MAP2) using the QIAGEN Quantitect SYBR Green PCR kit and DNA Engine Opticon LightCycler (MJ Research). The expression level of every gene in each sample was calculated relevant to a standard curve.

The expression levels of the genes were obtained in triplicate for each sample. The average level of the genes in each sample was then calculated and divided by the average GAPDH level for that sample. Fold changes between wild type and mutant samples were calculated and a t test used to identify the significance of any differences. Table 3.8 details these results for PSD95. The level of PSD95 is 3.94 times higher in wild type forebrain as compared to PSD95$^{-/-}$ tissue ($p=0.028$).

Table 3.9 shows the summary of the data for the rest of the genes compared to the results from the microarray analysis. All genes analysed that were found significantly altered by microarray were found similarly changed by QRT-PCR. The expression of MAP2, which was found unchanged by microarray analysis, was not significantly different in wild type and PSD95$^{-/-}$ samples.

SAMPLE	AVE. PSD95 LEVEL (STDEV)	AVE. GAPDH LEVEL (STDEV)	PSD95/GAPDH
1. +/+	2423 (70)	2944(360)	0.823
2. +/+	10947(1114)	7418(475)	1.476
3. +/+	3951(454)	5076(219)	0.778
		Ave	1.026
4. -/-	2790(70)	8642(129)	0.323
5. -/-	508(133)	2441(53)	0.208
6. -/-	1371(294)	5492(438)	0.250
		Ave	0.260
		Wildtype Ave-PSD95$^{-/-}$ Ave Ratio	**3.94**
		P value	**0.028**

Table 3.8 – QRT-PCR Of PSD95 Levels in Wildtype and PSD95$^{-/-}$ Forebrain. Table shows the average GAPDH and PSD95 levels in 3 wild type and 3 PSD95$^{-/-}$ samples (levels averaged from 3 replicates). The average PSD95:GAPDH ratios are shown for each sample and calculated from each geneotype. The average wildtype:PSD95$^{-/-}$ is shown, along with the p value of the differences between wild type and mutant samples as calculated by t test.

	AVE. WT	AVE. PSD95$^{-/-}$	QRT-PCR DATA		AFFYMETRIX DATA
			FOLD CHANGE	P VALUE	FOLD CHANGE
Down Regulated					
PSD95	1.026	0.260	3.94	0.028	3.40
cfos	2.06	0.282	7.30	0.033	2.22
egr2	0.090	0.022	4.09	0.047	2.19
nur 77	0.022	0.0068	3.24	0.046	2.39
Up Regulated					
syntenin	0.0005	0.0019	3.80	0.047	1.56
Unchanged					
MAP2B	0.655	0.557	1.18	0.67	1.08

Table 3.9 – QRT-PCR Of Gene Levels in Wildtype and PSD95$^{-/-}$ Forebrain. Table shows the average levels of *PSD95*, *cfos*, *egr2*, *nur77*, *syntenin* and *MAP2B* in wildtype and PSD95$^{-/-}$ forebrain (calculated from triplicate values from 3 wild type and 3 mutant samples, normalised by *GAPDH* levels). The fold change and p value for each gene is shown, along with the fold change measured by Affymetrix analysis.

3.3.3.2 Confirmation of SynGAP$^{+/-}$ Data

Confirmation of the SynGAP$^{+/-}$ data was performed in the same way as for PSD95$^{-/-}$. RNA was extracted from 3 SynGAP$^{+/-}$ and 3 matched wild type hippocampi. 2µl RNA from each sample was reverse transcribed to cDNA. Each cDNA was run in triplicate with each primer pair (GAPDH, cfos, nur77, egr2, ribosomal protein L44 and MAP2). The expression levels were normalised using GAPDH levels and the differences between wild type and mutant samples assessed by t test.

Table 3.10 is a summary of QRT-PCR data from SynGAP$^{+/-}$ samples compared to the results from the microarray analysis. All genes analysed were found altered in a similar way to that found by microarray.

	AVE. WT	AVE. SynGAP$^{+/-}$	QRT-PCR DATA		AFFYMETRIX DATA FOLD CHANGE
			FOLD CHANGE	P VALUE	
Down Regulated					
cfos	165.06	57.85	2.85	0.001	2.17
egr2	248.21	42.53	5.84	0.031	3.19
nur 77	32.65	7.03	4.64	0.007	1.61
Up Regulated					
Ribosomal Protein L44	1.48	3.41	2.30	0.049	1.57
Unchanged					
MAP2B	2.50	2.90	1.16	0.55	1.23

Table 3.10 – QRT-PCR Of Gene Levels in Wildtype and SynGAP$^{+/-}$ Hippocampi. Table shows the average levels of *cfos*, *egr2*, *nur77*, *ribosomal protein L44* and *MAP2B* in wildtype and PSD95$^{-/-}$ forebrain (calculated from triplicate values from 3 wild type and 3 mutant samples, normalised by *GAPDH* levels). The fold change and p value for each gene is shown, along with the fold change measured by Affymetrix analysis.

3.4 BIOINFORMATIC ANALYSIS OF MICROARRAY DATA

The results from the microarray analysis of PSD95$^{-/-}$ forebrain and SynGAP$^{+/-}$ hippocampus were confirmed by RT-PCR methods. This means that the data can be considered reliable and analysed further.

3.4.1 Comparison of Genes Altered in PSD95 $^{-/-}$ and SynGAP $^{+/-}$ Tissue

PSD95 and SynGAP are both found in the NRC and there are parts of the brain where the expression of the two genes overlap. The phenotypes of animals carrying mutations in PSD95 and SynGAP suggest that, in some instances, the proteins function in same phenomena, such as spatial learning. PSD95 and SynGAP could, therefore, act in pathways that regulate common genes. The analysis of PSD95$^{-/-}$ and SynGAP$^{+/-}$ mutant tissue was carried out using different brain regions (forebrain in PSD95, hippocampus in SynGAP). As a result, the data from both experiments cannot be directly compared. Nevertheless, studying the two data sets in parallel is useful to reveal any genes with common misregulation in both genotypes.

Figure 3.14 is a comparison of the genes significantly altered, greater than 1.5 fold, in PSD95$^{-/-}$ and SynGAP$^{+/-}$ tissue. The diagram shows the names and number of genes up and down regulated in both genotypes and any crossover between. An overlap of 3 genes, commonly down regulated in mutant tissue, is found between the two data sets. All three genes, *cfos*, *nur77* and *erg2*, are regulated by NMDA receptor activity. Other than these genes, the remaining significantly altered genes were changed uniquely in either PSD95$^{-/-}$ and SynGAP$^{+/-}$ tissue.

Higher in PSD 95$^{-/-}$
syntenin
serine palmitoyltransferase
ATPase, Cu^{++} transporting

Higher in SynGAP$^{+/-}$
EST
NADH dehydrogenase
ribosomal protein L44
Glyoxalase 1

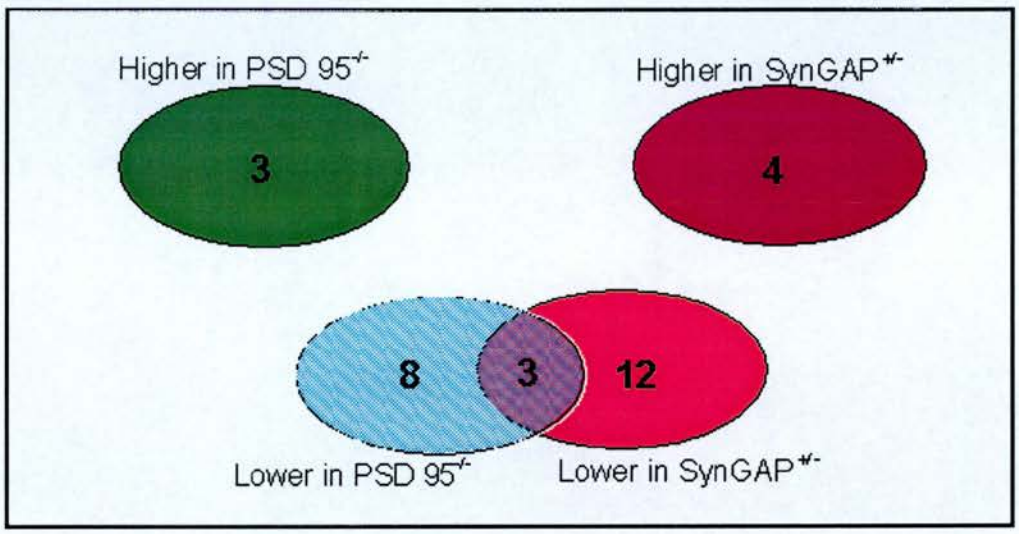

Lower in PSD 95$^{-/-}$
PSD 95
Per1
junB
cyln2
GADD45B
3 x EST

Lower in PSD 95$^{-/-}$ AND SynGAP$^{+/-}$
Cfos
nur77
egr2

Lower in SynGAP$^{+/-}$
SOX 11
DUSP6
Nrd1
Elovl6
K^+ channel, subfamily K , 1
3 x EST
voltage gated K+ channel, subfamily H, 1
N-glycan alpha 2, 8-sialyltransferase
erythroid differentiation factor
glucose-6-phosphate dehydrogenase
UDP-glucuronosyltransferase 8

Figure 3.14 – Comparison of Genes Significantly Altered in PSD95$^{-/-}$ and SynGAP$^{+/-}$ Tissue. Venn diagram shows the comparison of data from PSD95 and SynGAP experiments. 3 genes are found commonly downregulated in both genotypes. Tables show the names of the significantly altered genes and how they are changed.

3.4.2 Expression Levels of Activity Dependent Genes

In both genotypes examined a limited number of genes were found significantly changed, greater than 1.5 fold, in mutant tissue as compared to wild type (0.24% in PSD95$^{-/-}$ tissue, 0.37% in SynGAP$^{+/-}$ tissue). The genes with altered expression in PSD95$^{-/-}$ and SynGAP$^{+/-}$ tissue included several activity dependent genes, three of which were similarly down regulated in both genotypes. Furthermore, the activity regulated genes altered in PSD95$^{-/-}$ and SynGAP$^{+/-}$ tissues were all immediate early genes.

It has previously been estimated that there are between 30 and 40 immediate early transcripts (Lanahan and Worley, 1998) which is consistent with the numbers of transcripts with temporal profiles of immediate early genes found regulated by seizure induction in rats, contextual fear conditioning in mice and NMDA treatment of cultured cortical neurons (Newton *et al.*, 2003; Hong *et al.*, 2004; Levenson *et al.*, 2004). Ensembl predicts there to be 26762 genes in NCBI Mousebuild 32 of the mouse genome (www.ensembl.org), therefore immediate early genes could be estimated to make up approximately 0.149% (40/26762 x 100) of the genes in the mouse genome. Of the 27 different transcripts found altered in PSD95$^{-/-}$ and SynGAP$^{+/-}$ tissue, 4 (14.8%) encode immediate early genes. Thus, the frequency of immediate early genes in this data set is, approximately, 100 times greater than that found in the genome.

There appears to be a significant enrichment of immediate early genes in the transcripts significantly altered, greater than 1.5 fold, in PSD95$^{-/-}$ and SynGAP$^{+/-}$ tissue. To establish whether there were additional significant changes in activity regulated genes, which had previously been unidentified due to being lower than 1.5 fold, the microarray data was re-examined. The levels of known activity regulated transcripts, represented on the array, were compared in wild type and mutant tissues. Table 3.11 details the ratios of expression of these genes in wild type

tissue compared to mutant and the p values indicating the significance of the change. Positive ratios indicate higher expression levels in mutant tissue, negative values indicate a down regulation of the transcript in the mutant sample. Changes of expression, in wild type and mutant tissue, with p values smaller than 0.05 are considered significant.

In PSD95$^{-/-}$ forebrain, in addition to those significantly altered with a greater than 1.5 fold change (*nur77*, *cfos*, *egr2* and *junB*), *fosB* was found to be 1.32 fold down regulated (p value 0.04) as compared to wild type tissue. No other activity regulated genes were found significantly changed.

In SynGAP$^{+/-}$ hippocampi, *cfos*, *nur77* and *egr2* were found significantly changed greater than 1.5 fold. In addition to these transcripts, *BDNF* (ratio –1.49, p=0.019) and *somatostatin* (ratio 1.07, p=0.034) were found significantly altered, though it should be noted that the fold change of *somatostatin* is subtle. It is interesting to note that *junB*, significantly down regulated 1.97 fold in PSD95$^{-/-}$ forebrain, is found 1.66 fold lower in SynGAP$^{+/-}$ hippocampi with a p value of 0.073. This is close to being statistically significant and, as such, *junB* could represent a fourth immediate early gene that is similarly down regulated in PSD95$^{-/-}$ and SynGAP$^{+/-}$ tissue.

Further analysis of the microarray data found few additional activity regulated genes to be significantly altered. Thus, the immediate early genes misregulated in PSD95$^{-/-}$ and SynGAP$^{+/-}$ tissues appear to represent a specific subset of activity regulated genes.

GENE	AFFYMETRIX ID	PSD 95 (-/-) DATA		SynGAP (+/-) DATA	
		WT:MUT ratio	P value	WT:MUT ratio	P value
BDNF	102727_at	-1.04	0.609	**-1.49**	**0.019**
cfos	160901_at	**-2.22**	**0.02**	**-2.17**	**0.03**
Chop10	101429_at	-1.09	0.269	1.05	0.867
c-jun	100130_at	1.16	0.479	1.18	0.396
CNS1	99891_at	-1.24	0.121	-1.07	0.785
Cox2	104647_at	-1.11	0.389	-1.42	0.190
Egr1	98579_at	-1.32	0.106	-1.53	0.108
Egr2	102661_at	**-2.19**	**0.014**	**-3.19**	**0.021**
Fos B	103990_at	**-1.32**	**0.040**	-1.29	0.100
GAP45	102389_s_at	1.12	0.156	1.14	0.305
GR33	101629_at	1.12	0.306	1.2	0.167
IER5	92773_at	-1	0.995	-1.06	0.699
Jun B	102362_l_at	**-1.97**	**0.019**	-1.66	0.073
Narp 2	94099_at	1.18	0.111	1.45	0.270
NMDAR 2α	100726_at	1.08	0.766	1.11	0.808
NT3	92420_at	1.23	0.664	-1.11	0.766
nur77	102371_at	-2.39	0.001	**-1.61**	**0.009**
Pim1	104533_at	-1.06	0.479	1.13	0.319
Pim2	101926_at	1.09	0.536	1.36	0.250
Pip92	99109_at	-1.34	0.120	-1.13	0.589
Presenilin	102201_s_at	-1.01	0.789	-1.05	0.460
Somatostatin	95436_at	1.03	0.580	**1.07**	**0.034**
tPA	170031_f_at	-1.21	0.102	-1.46	0.137
Trk B	99069_at	-1.13	0.495	1.28	0.676

Table 3.11 – Levels of Activity Dependent Gene Expression in PSD95$^{-/-}$ Forebrain and SynGAP$^{+/-}$ Hippocampus. Table shows the wildtype to mutant ratio of the average expression levels of activity dependent genes in PSD 95$^{-/-}$ forebrain and SynGAP$^{+/-}$ hippocampus. A positive ratio indicates expression levels in the wildtype tissue was higher, a negative value that expression was higher in mutant samples. Changes, significant with $p< 0.05$ are in bold.

3.4.3 Chromosomal Location of Significantly Altered Genes

Analysis of gene expression in human and *Drosophila* studies has found groups of genes, clustered together on the same chromosomes, that are similarly expressed in given conditions (Caron *et al.*, 2001; Spellmen and Rubin, 2002; Versteeg *et al.*, 2003). The chromosomal location of transcripts significantly altered in PSD95 and SynGAP mutant tissue was therefore analysed to see if there was any evidence of these genes being clustered to particular chromosomes.

Tables 3.12 and 3.13 show the chromosomal positions of genes significantly altered in PSD95$^{-/-}$ and SynGAP$^{+/-}$ tissues, those on the same chromosome are highlighted in the same colours. Table 3.14 shows this data for the PSD95 and SynGAP data sorted by chromosome. In this table the targeted genes are highlighted in blue and genes with hypothesised roles in learning or plasticity are highlighted in yellow (see discussion 3.5.3 for details). Figure 3.15 shows graphs showing the number of significantly altered on each chromosome for PSD95 and SynGAP data.

Of the genes significantly altered in PSD95 mutant forebrain, several appear to be clustered to the same particular mouse chromosomes. *Syntenin* and EST 96756_at are both on chromosome 4. *Egr2*, *GADD45B* and EST 96242_at are found on chromosome 10. *PSD95*, *Per1* and an EST 94555_at are all found on chromosome 11, whilst *cfos* and *serine palmitolytransferase* both lie on chromosome 12. In the SynGAP$^{+/-}$ data there is also evidence of clustering. *Voltage gated K^{+} channel H1*, *N-glycan alpha 2,8-sialtransferase*, *NADH dehydrogenase* and an EST 96833_at are all on chromosome 1. *UDP-glucuronosyltransferase 8*, *Elovl6* and *ribosomal protein L44* lie on chromosome 3. *Egr2* and *DUSP6* are both on chromosome10. *Sox11* and *cfos* are both present on chromosome 12, while EST 95451_at and glyoxalase 1 both lie on chromosome 17.

Using the chi square test, the data was analysed to see if there was statistically significant evidence of clustering of significantly altered genes to particular chromosomes. Analysis gave a p value of 0.101 for the PSD95 data and a p value of 0.031 for the SynGAP data. Thus, the grouping of significantly altered genes to particular chromosomes is statistically significant for the SynGAP data. The PSD95 data shows no significant clustering, nevertheless, there appears to be a trend of clustering. The lower n number of significantly altered genes in the PSD95$^{-/-}$ data may contribute to the non-significant p value from the chi square test.

AFFYMETRIX ID	GENE	CHROMOSOMAL LOCATION	
Lower in Mutant			
104175_at	PSD 95	chr11: 70631458-70632003 (+)	11 B4
102371_at	nur77	chr15: 102231569-102231972 (+)	15 F
160901_at	cfos	chr12: 80178549-80178747 (+)	12 D1
102661_at	egr2	chr10: 67591056-67591375 (+)	10 B5
93619_at	per1	chr11: 69690481-69690978 (+)	11 B
102362_i_at	junB	chr8: 84678118-84678624 (-)	8 C2-D1
99432_at	CYLN2	chr5: 133094769-133098935 (-)	5 G
161666_f_at	GADD45B	chr10: 80760805-80760949 (+)	10 C1
94555_at	EST	chr11: 71238585-71238877 (+)	11 B4
96242_at	EST	chr10: 6610076 -6610297 (+)	10 C1
96756_at	EST	chr4: 24509746-24510137 (+)	4 A3
Higher in Mutant			
102854_s_at	Atp7a	chrX: 91052240-91052484 (+)	X D
100893_at	serine palmitoyltransferase	chr12: 82023718-82028034 (-)	12 E
93017_at	syntenin	chr4: 5872494-5872730 (+)	4 A1

Table 3.12 – Chromosomal Location of Genes Significantly Altered in PSD 95$^{-/-}$ Forebrain Table shows the mouse chromosomal locations known for transcripts significantly altered in PSD 95$^{-/-}$ forebrain. Genes which appear clustered a region of the same chromosome are highlighted (green= chromosome 4, blue = chromosome 10, yellow = chromosome 11, pink = chromosome 12)

AFFYMETRIX ID	GENE	CHROMOSOMAL LOCATION	
Lower in Mutant			
102661_at	egr2	chr10: 67591056-67591375 (+)	10 B5
96215_f_at	EST	NOT KNOWN	
93669_f_at	SOX 11	chr12: 21410456-21410933 (-)	12
98525_f_at	Erythroid Differentiation Factor	NOT KNOWN	
160901_at	cfos	chr12: 80178549-80178747 (+)	12 D1
93285_at	DUSP6	chr10: 99499994-99500239 (+)	10 C3
96833_at	EST	chr1: 132229216-132230887 (+)	1 E4
94966_at	glucose-6-phosphate dehydrogenase	chrX: 57622845-57623443 (-)	X A2-A3
102371_at	nur77	chr15: 102231569-102231972 (+)	15 F
102335_at	K^+ channel, subfamily K, 1	chr8: 126037677-126037972 (+)	8 E2
96661_at	Nrd1	chr4: 106807384-106808579 (+)	4 C7
98380_at	voltage gated K+ channel, subfamily H, 1	chr1: 194039168-194039746 (+)	1 H6
98872_at	UDP-glucuronosyltransferase 8	chr3: 126497683-126498201 (-)	3 E3-F1
102318_at	N-glycan alpha 2, 8-sialyltransferase	chr1: 96120517-96121080 (-)	1 D
95451_at	EST	chr17: 74732236-74732544 (-)	17 E2
103665_at	Evovl6	chr3: 130137795-130138309 (+)	3 G3
Higher in Mutant			
100775_at	EST	NOT KNOWN	
93562_at	NADH dehydrogenase	chr1: 59181202-59190525 (+)	1 C1.3
93269_at	Glyoxalase 1	chr17: 7198000 7197741(-)	17 A3.3
160081_at	ribosomal protein L44	chr3: 84873383-84873770 (+)	

Table 3.13 – Chromosomal Location of Genes Significantly Altered in SynGAP$^{+/-}$ Hippocampus Table shows the mouse chromosomal locations of genes significantly altered in SynGAP$^{+/-}$ Hippocampus. Genes which appear clustered a region of the same chromosome are highlighted (yellow = chromosome 1, green= chromosome 3, blue = chromosome 10, pink = chromosome 12, red = chromosome 17)

A PSD95 Data

CHROMOSOME	GENES PRESENT		
4	*syntenin*	EST (96756_at)	
5	*cyln2*		
8	*jun B*		
10	*egr2*	*GADD45B*	EST (96242_at)
11	*PSD 95*	*per1*	EST (94555_at)
12	*cfos*	*serine palmitolytransferase*	
15	*nur 77*		
X	*Atp7a*		

B SynGAP Data

CHROMOSOME	GENES PRESENT			
1	*N-glycan α 2, 8-sialyltransferase*	EST (96833_at)	*NADH dehydrogenase*	*voltage gated K+ channel, subfamily H, 1*
3	*UDP-glucuronosyltransferase 8*	*Evovl6*	*ribosomal protein L44*	
4	*Nrd1*			
8	*K+ channel, subfamily K, 1*			
10	*egr2*	*DUSP6*		
12	*cfos*	*Sox11*		
15	*nur77*			
17	EST (95451_at)	*Glyoxalase 1*	*SynGAP*	
X	*glucose-6-phosphate dehydrogenase*			
Unknown	*Erythroid Differentiation Factor*	EST (100775_at)	EST (96215_f_at)	

Table 3.14 – Significantly Altered Genes Sorted by Chromosome. **A** shows the genes, significantly altered in PSD95$^{-/-}$ forebrain, sorted by the murine chromosomes they are present on. **B** shows the same for the genes significantly altered in SynGAP$^{+/-}$ hippocampi. The targeted genes are highlighted in blue, genes with hypothesised roles in plasticity are highlighted in yellow.

A

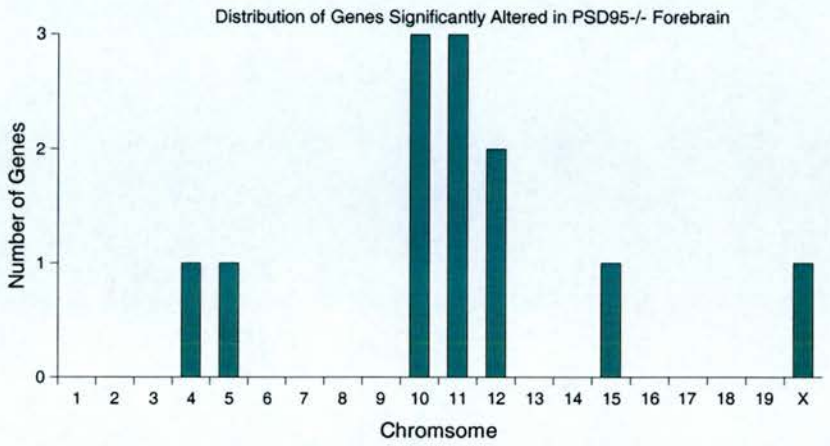

B

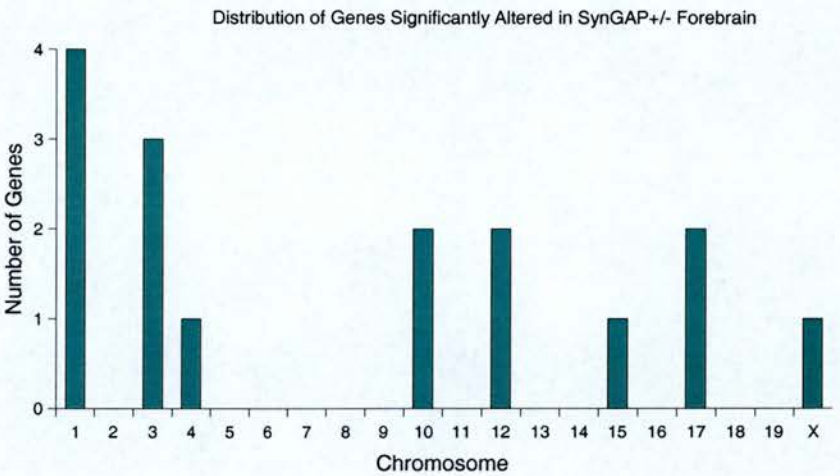

Figure 3.15 – Chromosomal Distribution of Significantly Altered Genes. Graphs show the number of significantly altered genes on each chromosome for PSD95$^{-/-}$ (**A**) and SynGAP$^{+/-}$ (**B**) tissue.

3.4.4 Gene Expression in Wild Type Forebrain and Hippocampus

The only difference in experimental design and analysis between PSD95 and SynGAP experiments, other than the genotypes used, was the tissue source of RNA. As a result the wild type data from the two experiments can be used to compare gene expression in forebrain to that of the hippocampus alone. Identification of transcripts highly expressed in, or with expression restricted to, particular brain areas could be valuable in determining the roles of these genes in the associated brain region function. It also furthers understanding of global gene expression across the brain.

Some genes are widely and evenly expressed in all/most brain regions, e.g. *GAPDH, βActin* and *PSD95.* The levels of these genes should, therefore, be unchanged in wild type forebrain and hippocampal samples. Table 3.15 details the levels of these genes in the wild type tissues, as measured by Affymetrix analysis, and shows there is no significant difference in their expression in forebrain and hippocampal samples as measured by t test. This verifies that the hybridisation and normalisation of data in the PSD95 and SynGAP experiments are equivalent and, thus, comparison of wild type samples from the two experiments is valid.

GENE	FOREBRAIN AVE	HIPPOCAMPUS AVE	FOREBRAIN ST DEV	HIPPOCAMPUS ST DEV	FB/HC RATIO	P VALUE
GAPDH	472.57	553.23	37.23	47.88	0.85	0.09
βActin	7274.03	7049.8	67.17	919.13	1.03	0.71
PSD95	6151.7	6267.5	20.97	624.94	0.98	0.78

Table 3.15 - Expression of Control Genes in Forebrain and Hippocampus. Table details the average levels, with standard deviations (st. dev.) of GAPDH, βActin and PSD95 in wild type forebrain and hippocampus. The forebrain to hippocampus (FB/HC) ratio is given, with p value as calculated by t test.

A diverse range of genes is represented on the microarrays that will include transcripts with specialised neuronal function and, thus, restricted expression to particular brain regions. Analysis of the wild type microarray data found 250 transcripts (4.3% of total detected present) that were expressed at a significantly higher level ($p<0.05$, greater than 1.5 fold) in wild type forebrain as compared to hippocampus. 232 transcripts (4.3% of the total detected present) were expressed at significantly higher levels in the hippocampus as compared to forebrain. Thus, the majority of detected transcripts were uniformly expressed in the hippocampus and the forebrain as a whole.

Table 3.16 shows the 20 transcripts with the highest expression in the forebrain compared to hippocampus ($p<0.05$, fold difference>1.5). Many of these have specialised gene products that function outwith the hippocampus. For example, preproenkephalin encodes the precursor for the endogenous opiod enkephalin and is most highly expressed in the amygdala, striatum and cortex (Su *et al.*, 2002). Also, hypocretin and arginine vasopressin have endocrine function and are expressed, specifically, in the hypothalamus (Su *et al.*, 2002).

Table 3.17 details the transcripts expressed more highly in the hippocampus, compared to forebrain, and also shows some selected transcripts that are more highly expressed in the hippocampus ($p<0.05$, fold difference>1.5). Identification of highly expressed hippocampal genes is of particular interest as these transcripts may be involved in spatial learning or other hippocampal phenomena such as LTP. 3 of the 20 genes showing the greatest expression in the hippocampus compared to forebrain (neurogenic differentiation 6, RIKEN gene 1200008D14, zinc finger protein 288) have previously been found enriched in the hippocampus compared to other brain areas (Zirlinger *et al.*, 2001). The transcript that is most highly expressed in the hippocampus compared to the rest of the forebrain is *klotho*, a gene hypothesised to be a regulator of aging. It has been found that the expression of *klotho* is restricted to the hippocampus in the CNS (Su *et al.*, 2002) and it has recently been shown that the

transcript is particularly enriched to the hippocampal CA1 region (Lein *et al.*, 2004). Mice carrying mutations in *klotho* have early onset of cognitive impairment in novel object recognition and fear conditioning (Nagai *et al.*, 2003). The selected genes, shown in table 3.17, that are enriched in the hippocampus include NRC proteins and other molecules involved in synaptic plasticity, for instance AMPA receptor subunits, signalling proteins such as CaMKIIα and SAP102, a MAGUK protein.

Comparison of wild type gene expression in the forebrain and hippocampus has revealed that the vast majority of genes are expressed at similar levels in these two neuronal samples. Identification of genes more highly expressed in the forebrain as a whole than in the hippocampus has picked out many transcripts with particular function outwith the hippocampus. The transcripts more highly expressed in the hippocampus, compared to forebrain, include several genes that are involved in hippocampal-based function.

RANK	FB/HC RATIO	GENE	FOREBRAIN		HIPPOCAMPUS		P VALUE
			AVE	ST. DEV.	AVE	ST. DEV	
1	7.07	preproenkephalin 1	2245	68.83	317.8	124.5	0.00013
2	6.57	hypocretin	131.3	8.3	19.07	13.35	0.00066
3	4.64	tachykinin 1	136.6	12.97	29.47	7.9	0.00073
4	4.12	arginine vasopressin	82.43	4.35	7.27	2.06	0.00016
5	4.11	RIKEN gene 2810052M02	103.9	25.51	25.27	18.39	0.01518
6	4.1	troponin T1	81.93	13.39	11.93	8.34	0.00307
7	4.08	short stature homeobox 2	81.67	2.05	13.23	8.66	0.00364
8	3.91	cAMP phosphoprotein	404.9	47.13	103.7	11.13	0.00582
9	3.88	rgs 4	163.9	12.08	42.23	10.2	0.00022
10	3.78	keratin complex 1	137.0	16.44	36.23	11.81	0.00152
11	3.63	myocyte factor 2C	426.9	26.06	117.5	7.15	0.00128
12	3.57	RIKEN gene 5430401D19	103.4	12.13	28.93	2.4	0.00697
13	3.47	oxytocin	291.8	18.6	84.03	11.26	0.00028
14	3.39	formin-family protein	93.07	3.23	27.43	9.3	0.00325
15	3.39	myocyte factor 2C	768.6	34.67	226.7	21.53	0.00008
16	3.37	GEF1	153.9	7.0	45.67	7.24	0.00005
17	3.29	secreted phosphoprotein1	128.5	20.14	39.03	18.16	0.00478
18	3.25	GABA A3	65.03	13.51	13.6	9.56	0.00773
19	3.18	cadherin 4	74.43	21.62	23.37	19.87	0.03984
29	3.14	angiotensinogen	318.1	25.08	101.5	3.04	0.00399

Table 3.16 – Genes Expressed More Highly In Wild Type Forebrain As Compared To Hippocampus. Table shows the 20 transcripts with the highest expression in the wild type forebrain, as compared to hippocampus, ranked in order by forebrain to hippocampus ratio. The Affymetrix IDs and transcript names are detailed along with their average expression levels, along with standard deviation, in each tissue. The P values of the differential expression were calculated by Welch t test.

RANK	HC/FB RATIO	GENE	FOREBRAIN		HIPPOCAMPUS		P VALUE
			AVE	ST. DEV.	AVE	ST. DEV	
1	5.4	klotho	27.97	3.35	151.1	33.06	0.022
2	5.31	EST	25	4.56	132.9	21.9	0.011
3	5.18	RIKEN gene 1200008D14	37.4	5.86	193.8	18.95	0.003
4	5.13	RIKEN gene 5730453H04	20.83	2.34	106.8	22.55	0.021
5	4.88	Cytokine factor 1	31.2	0.75	152.1	18.17	0.007
6	4.22	RIKEN gene 1200008D14	16.13	2.73	84.4	11.45	0.007
7	4.21	Neuropeptide receptor Y2	78.2	20.94	328.9	46.98	0.005
8	4.1	zinc finger protein 288	62.23	10.69	255.1	54.9	0.023
9	3.76	neurogenic differentiation 6	58.43	8.46	219.9	22.56	0.003
10	3.66	Transthyretin	572.7	64.86	2099	492.9	0.031
11	3.56	Neuropilin	78.87	14.99	280.8	17.89	0
12	3.51	EST	113.6	55.25	398.9	76.17	0.008
13	3.39	folate receptor 1 (adult)	42.6	9.78	144.6	40.62	0.043
14	3.39	myosin Vb	98.23	14.01	333.2	44.79	0.007
15	3.34	DEXRAS1	39.97	3.83	133.3	8.74	0.001
16	3.16	potential cation channel	42.7	5.99	134.9	21.85	0.013
17	3.11	RIKEN gene 1200003E16	20.8	15.52	64.7	13.04	0.021
18	2.92	EST	11.77	7.63	58.47	19.03	0.037
19	2.88	homer homolog 3	27.77	7.62	79.87	10.33	0.003
20	2.84	procollagen	20.7	10.12	58.7	8.09	0.008
Selected Altered Genes							
	2.42	AMPA1	168	407.13	13.23	17.26	0
	2.38	C/EBP	48.5	115.6	14.48	6.77	0.007
	2.35	Eph receptor A6	45.3	106.5	5.03	9.83	0.002
	2.34	c-Jun	90.03	210.5	28.85	6.42	0.015
	2.04	protein kinase C gamma	522.9	1065	27.98	100.3	0.008
	2	protein kinase C epsilon	127.6	255.7	16.46	27.08	0.004
	1.86	Sox11	40.63	75.73	6.64	5.35	0.002
	1.83	CaMKIIα	94.6	173.4	7.81	29.64	0.037
	1.69	SAP102	111.5	188.9	10.44	17.38	0.005
	1.66	Nurr1	121.3	201.27	26.33	15.58	0.017
	1.58	AMPA2	1830	2892	115.5	100.6	0
	1.53	BDNF	545.9	833.9	12.5	42.41	0.004
	1.5	GABA a2	77.17	116.1	8.15	2.23	0.010

Table 3.17 – Genes Expressed More Highly In Wild Type Hippocampus As Compared To Forebrain. Table shows the 20 transcripts with the highest expression in the wild type hippocampus, as compared to forebrain, ranked in order by hippocampus to forebrain ratio. In addition the details of several selected genes that are expressed at significantly higher levels in the hippocampus are shown. The Affymetrix IDs and transcript names are detailed along with their average expression levels, along with standard deviation, in each tissue. The P values of the differential expression were calculated by Welch t test.

3.5 DISCUSSION

The data presented in this chapter has shown the application of microarray technology to analyse transcription in brain tissue carrying mutated NRC proteins. The resulting data met quality control standards and subsequent analysis revealed results that were verified by RT-PCR methods.

Experimental design was kept as simple as possible with variability, other than the biological condition being analysed, maintained at a minimum. This was key to enable straightforward analysis and interpretation of the results. The experiments produced data on a vast number of genes that was studied in different ways to extract useful information. The following discussion considers several of the main points apparent from the data.

3.5.1 Limited Numbers of Genes are Altered in Mutant Tissue

Analysis revealed that mutation of proteins in the NRC disrupts gene expression in neuronal tissue, thus establishing a role for PSD95 and SynGAP dependent pathways in the regulation of transcription. A striking feature of the data was that very few transcripts had altered expression levels in mutant samples, as compared to wild type. Only 0.24% of the transcripts detected in PSD95$^{-/-}$ samples and 0.37% of those in the SynGAP$^{+/-}$ samples were significantly altered. Thus, it appears that PSD95 and SynGAP play a role in regulating the expression of a restricted group of transcripts.

Since PSD95 and SynGAP are known to act in pathways downstream of the NMDA receptor it is likely that altered gene expression in mutant samples is due to misregulation of NMDA receptor dependent gene expression. Indeed, several of the significantly altered transcripts are known NMDA receptor regulated genes. It may be that, as well as regulating the expression of these genes following intense stimulation, the NMDA receptor and associated proteins control the basal levels of

these genes. As such, the altered transcripts may represent a subset of the total genes regulated by the receptor. Examination of the array data revealed the majority of known activity regulated genes are not significantly altered in the mutant tissues, even at fold change levels less than 1.5. This supports the idea that PSD95 and SynGAP play critical roles in the regulation of basal expression of a particular subset of NMDA regulated genes.

The RNA used for the experiments presented in this chapter came from acutely dissected tissue, thus analysis reveals the basal levels of transcription in the cells. To analyse the contribution of NRC proteins to activity dependent gene expression it would be interesting to study the RNA levels in PSD95$^{-/-}$ and SynGAP$^{+/-}$ tissue following stimulation of the NMDA receptor. This analysis may reveal many more differences between wild type and mutant tissues, particularly since the Affymetrix analysis identified downregulated levels of NMDA receptor regulated transcription factors such as *cfos, nur77* and *egr2*. It may be that, as well as having reduced basal levels, the induction of these genes is impaired which could impact on the expression of late response genes.

3.5.2 PSD95 and SynGAP in the Regulation of Gene Expression

PSD95 and SynGAP are both components of the NRC (Husi *et al.*, 2000). As members of a complex of signalling molecules, capable of interacting with each other (Kim *et al.*, 1998), the proteins potentially act in common pathways as well as functioning independently from each other. Animals carrying mutations in PSD95 and SynGAP have different phenotypes in hippocampal LTP, but both have deficits in spatial learning. Also, the expression patterns of PSD95 and SynGAP do not completely overlap in the brain (K. Porter, personal communication) suggesting the proteins could act in diverse, as well as common, phenomena. Consistent with the idea that PSD95 and SynGAP can function in separate and integrated pathways, microarray analysis identified alterations in diverse groups of genes in the two

genotypes, with a degree of overlap seen in the common misregulation of *cfos, nur77* and *egr2*.

The analysis of tissue of the two genotypes, PSD95$^{-/-}$ and SynGAP$^{+/-}$, found changes in what can be classed as two sets of genes; those that are commonly misregulated in the two genotypes and distinct misregulated transcripts. This raises two scenarios in which PSD95 and SynGAP contribute to the regulation of these genes. It could be that a pathway involving PSD95 and SynGAP regulates the transcription of genes downregulated in both genotypes (*cfos, nur77* and *egr2)* and that pathways in which PSD95 and SynGAP act independently from each other to regulate the expression of genes exclusively misregulated in each genotype. Alternatively, PSD95 and SynGAP may contribute to the regulation of transcription entirely in independent pathways that happen to both regulate the expression of *cfos, nur77* and *egr2*.

3.5.2.1 PSD95 and SynGAP Act in Independent Pathways

It is apparent that PSD95 and SynGAP can regulate the expression of distinct transcripts suggesting they act in independent pathways. Both proteins are members of the NRC, which contains molecules that could orchestrate the response of a variety of transduction pathways, following NMDA receptor activation, to regulate gene expression. As such PSD95 and SynGAP could, potentially, contribute to several different signalling pathways.

PSD95 has many potential binding proteins meaning it could act in multiple pathways that regulate gene expression. As a major adaptor protein in the NRC, disruption of PSD95 function could alter the composition of the receptor complex. As such, the organisation of postsynaptic signalling in response NMDA receptor activity could be altered in PSD95$^{-/-}$ animals.

SynGAP has been shown to have RasGAP function (Kim *et al.*, 1998) and it is likely that SynGAP contributes to signalling via the ras-ERK pathway. SynGAP can directly interact with PSD95, which is hypothesised to anchor SynGAP at an advantaged position for signal transduction following NMDA receptor stimulation. If such an interaction is required for SynGAP to respond to NMDA receptor activity, it may be that it can be mediated through an interaction with a PDZ domain containing protein other than PSD95. For example, SynGAP can associate with SAP102 (Kim *et al.*, 1998), which the microarray data found to be highly expressed in the hippocampus relative to the rest of the forebrain. As such, SynGAP could act to regulate gene expression, via the ras-ERK pathway, independent of PSD95 by interaction with other proteins.

3.5.2.2 PSD95 and SynGAP and the Regulation *cfos*, *nur77* and *egr2* Expression

The downregulation of *cfos*, *nur77* and *egr2* in PSD95 and SynGAP mutant tissues suggests the proteins potentially act in a common pathway that regulates the basal levels of this subset of activity dependent genes. NMDA receptor stimulation can lead to the increased expression of *cfos*, *nur77* and *egr2* (Bading *et al.*, 1995; Inokuchi *et al.*, 1996; French *et al.*, 2001). This is consistent with the signalling pathway regulating these genes, involving both PSD95 and SynGAP, being downstream of NMDA receptor activity.

SynGAP can directly interact with, and is hypothesised to function downstream of, PSD95 (Komiyama *et al.*, 2002) and, given the rasGAP function of SynGAP (Kim *et al.*, 1998), it is possible that PSD95 and SynGAP both act in the Ras-ERK pathway. This pathway can regulate SRE and CRE mediated gene expression in response to NMDA receptor activity (Xia *et al.*, 1996; Impey *et al.*, 1998; Wu *et al.*, 2001). Both of these elements are found in the 5′ regions of the *cfos*, *nur77* and *egr2* genes (Treisman, 1986; Sassone-Corsi *et al.*, 1988; Chavrier *et al.*, 1989; Uemura *et al.*, 1994). A model could, therefore, be proposed whereby PSD95 and SynGAP, downstream

of the NMDA receptor, contribute to the ras-ERK pathway that plays a role in the regulation of basal expression of *cfos*, *nur77* and *egr2* via SRE and CRE promoter elements.

3.5.3 Genes Significantly Altered in Mutant Tissue

PSD95$^{-/-}$ and SynGAP$^{+/-}$ animals demonstrate deficiencies in spatial learning and plasticity (Migaud *et al.*, 1998; Komiyama *et al.*, 2002). Neuronal changes, at a transcriptional level, may be an underlying cause of these phenotypes. Therefore, proteins encoded by genes significantly altered in mutant tissue may play key roles in learning and synaptic plasticity. The following sections details the transcripts found altered in PSD95$^{-/-}$ and SynGAP$^{+/-}$ mutant tissue.

3.5.3.1 Genes Significantly Altered in PSD95 $^{-/-}$ Forebrain

11 transcripts were found down regulated in PSD95$^{-/-}$ forebrain. 7 of these transcripts are known genes (*PSD95*, *nur77*, *cfos*, *egr2*, *Per1*, *junB*, *cyln2* and *GADD45B*) and 3 are ESTs. 3 genes, *Atp7a*, *syntenin* and *serine palmitoyltransferase subunit 2*, are up regulated in the PSD95$^{-/-}$ forebrain.

3.5.3.1.1 PSD95

The *PSD95* transcript is found at a 3.4 fold level lower in PSD95$^{-/-}$ forebrain than wild type. The PSD95 mutant allele was generated by a stop codon insertion to the third PDZ domain. However, the 3' UTR, to which the Affymetrix probes are targeted, is still intact. As such, a transcript containing this sequence could be expressed due to the action of promoters downstream of the stop codon insertion. The translation of any such transcript would give a protein product lacking the third PDZ domain of PSD95 and, as such, unable to bind NMDA receptor subunits.

3.5.3.1.2 Nur77, cfos, egr2 and junB

As previously mentioned, several genes found down regulated in PSD95 and SynGAP mutant tissue are regulated by NMDA receptor activity and 3 of these, *cfos, nur77* and *egr2*, are found similarly altered in both genotypes. In addition, *junB* is found significantly down regulated in PSD95$^{-/-}$ forebrain. These genes are all transcription factors induced by NMDA receptor activity and are thought to regulate the expression of late response genes (reviewed by Platenik *et al.*, 2000). It is hypothesised that late response genes encode proteins critical for the long lasting neuronal changes that occur in synaptic plasticity. If it were that the induction of *cfos, nur77, egr2* and *junB* following synaptic activity is impaired, then this could have many downstream consequences.

The critical role of *cfos* in learning and plasticity been further demonstrated by use of mice carrying mutations in the gene. Mice constitutively lacking *cfos* suffer motor impairments that hinder analysis in behavioural paradigms (Johnston *et al.*, 1992; Paylor *et al.*, 1994). However, a recently published study has shown the effects of mutating *cfos* specifically in the CNS (Fleischmann *et al.*, 2003). These animals show no abnormalities in gross brain architecture and motor function is not affected. They do, however, show impaired spatial learning in the Morris water maze and have deficits in contextual, but not cued, fear conditioning. This suggests that *cfos* is critical in hippocampal dependent learning behaviour. Hippocampal slices from the same animals have reduced LTP, compared to wild type, following a single 100Hz tetanus (Fleischmann *et al.*, 2003).

Egr2 deficient mice have severe deficits in peripheral myelination (Topilko *et al.*, 1994). Mutations of the gene are found in patients with hereditary demyelination neuropathies, including Charcot-Marie Tooth disease type1 (Warner *et al.*, 1998). As yet, no studies have been published looking at hippocampal based phenomena in these animals. Interestingly, a potential egr2 binding site has been identified in the promoter region of SynGAP (N. Komiyama, personal communication). This raises

the interesting possibility that the expression of SynGAP can be regulated by egr2 via this site. This could represent a feedback loop whereby the expression of *egr2*, controlled downstream of SynGAP activity, can act to regulate the expression of *SynGAP* RNA.

3.5.3.1.3 Per1

Per1 (period1) belongs to a family of proteins (period 1-3) that, along with Clock, bmal and cry, are key components of the molecular machinery in the suprachiasmatic nucleus (SCN) that regulates the body's circadian rhythms (reviewed by Ding *et al.*, 1997). It has been demonstrated that, in the SCN, the action of glutamate via NMDA receptors, in response to light, regulates the expression of *Per1* (Tischkau *et al.*, 2000). Furthermore, it has been shown that CREB mediated expression of *Per1*, hypothesised to be initiated via nitric oxide (NO) signalling, is required for this light regulated response (Tischkau *et al.*, 2003). Given that the NMDA receptor is known to regulate the expression of *Per1* in the SCN, it is possible that, in the forebrain, the expression of the gene is regulated by a PSD95 dependent pathway, potentially via NO, downstream of the NMDA receptor. As such *Per1* could represent another activity regulated gene that is misregulated in $PSD95^{-/-}$ tissue.

In the forebrain, a molecule called NPAS2 can act as a Clock analogue and heterodimerise with bmal to regulate the expression of *Per1* (Reick *et al.*, 2001). In turn, Per1 can act to inhibit the action of the NPAS2-bmal dimer. Animals that are homozygote for a mutant form of NPAS2 have impaired long term contextual and cued fear conditioning, suggesting a role for this molecule in the consolidation of memories (Garcia *et al.*, 2000). It is therefore possible that the molecules involved in circadian rhythm that regulate each other, including Per1, have an, as yet, unknown function in the consolidation of long term memory.

3.5.3.1.4 *cyln2*

Cyln2 (cytoplasmic linker-2) encodes a protein, CLIP-115, which belongs to a protein family involved in the attachment of microtubules with organelles (Rickard and Kreis, 1996). It has been found highly enriched in the brain where it facilitates the localisation of a membranous organelle called the dendritic lamellar body (DLB) (De Zeeuw *et al.*, 1995; De Zeeuw *et al.*, 1997), an organelle which is found only in dendritic appendages and is particularly prominent at dendrodentritic junctions (De Zeeuw *et al.*, 1995).

Cyln2 is found in a 1.6Mb region of human chromosome 7, containing at least 17 genes, which is heterozygously deleted in Williams-Beuren Syndrome (Francke, 1999). This developmental disorder has symptoms that include growth deficits in infancy, motor disabilities and mental retardation (Francke, 1999). Mice with targeted mutations of *cyln2*, encoding CLIP-115, have mild growth retardation and significantly larger brain ventricle volumes than wild type, however analysis of brain sections shows no abnormalities in brain morphology (Hoogenraad *et al.*, 2002). *Cyln*$^{-/-}$ animals have deficits in contextual, but not cued fear conditioning (Hoogenraad *et al.*, 2002), suggesting a role for CLIP-115 in hippocampal dependent learning. These animals also have reduced LTP in the CA1 region of the hippocampus (Hoogenraad *et al.*, 2002).

3.5.3.1.5 *GADD45β*

GADD45β (growth arrest and DNA damage inducible gene β) encodes a protein that belongs to the GADD45-like group of proteins. GADD45β can associate with MEKK4 and is thought, via this interaction, to act in the p38/JNK pathway (Takekawa and Saito, 1998; De Smaele *et al.*, 2001). GADD45 proteins are induced by environmental stresses (Takekawa and Saito, 1998) and related protein GADD45α expression is expressed in the hippocampus in response to kainate injection (Zhu *et al.*, 1997). It may be that this, and other GADD45 family proteins, can be induced by glutamate activity at the NMDA receptor.

3.5.3.1.6 *Atp7a*

Atp7a encodes a copper transporting ATPase that was first isolated in humans as a candidate causative gene for Menkes disease (Vulpe *et al.*, 1993). In Menkes disease, loss of Atp7a function results in a failure in copper transport across the blood brain barrier, gastrointestinal tract and liver. This leads to copper accumulation in the cells surrounding these tissues and results in low copper levels in the organs. Low copper levels in the brain lead to severe neurological symptoms including seizures and mental retardation. Elsewhere in the body, the mistransport of copper due to functional loss of Atp7a results in bone abnormalities, particularly of the skull (reviewed by Strausak *et al.*, 2001).

It is unclear what functional effect the upregulation of *Atp7a* in the forebrain would have, but it could result in altered levels of copper in this part of the brain. Abnormal levels of copper in the brain have been found in various disorders with neurological symptoms such as Alzheimer's and Wilson's disease (Basun *et al.*, 1991; Strausak *et al.*, 2001). Therefore, altered copper levels in the forebrain of PSD95$^{-/-}$ animals, due to abnormal Atp7a expression, could result in neuronal phenotype.

3.5.3.1.7 *Syntenin*

Syntenin is upregulated in the PSD95$^{-/-}$ forebrain and encodes a PDZ containing protein that was first identified as a binding partner for transmembrane proteoglycans (Grootjans *et al.*, 1997). Syntenin co-localises and co-immunoprecipitates with syndecan, E-cadherin, β catenin and α catenin and, thus, is suggested to have a role regulating membrane dynamics (Zimmermann *et al.*, 2001). More recently, syntenin, along with PSD95, has been shown, by yeast two hybrid and GST pulldowns, to bind the GluR5-2b, Glur5-2c and GluR6 kainate receptor subunits (Hirbec *et al.*, 2002). In addition, syntenin was detected, along with GluR6/7 subunits, in synaptosomal and postsynaptic density fractions from rat brains (Hirbec *et al.*, 2002). The upregulation of syntenin, a PDZ containing protein,

in PSD95$^{-/-}$ forebrain may be a compensatory mechanism due to the loss of function of another PDZ domain protein.

3.5.3.1.8 Serine Palmitoyltransferase Subunit 2

The third gene upregulated in PSD95$^{-/-}$ forebrain is *serine palmitoyltransferase subunit 2*. Serine palmitoyltransferase is a key enzyme in the biosynthesis of sphingolipids, ubiquitous components of membrane lipids in mammalian cells (Hanada *et al.*, 2000). In humans, *serine palmitoyltransferase subunit 2* has been mapped to an area of chromosome 9 that is the locus of hereditary sensory neuropathy 1 (HSN1). Furthermore, HSN1 affected families have been found to have mutations in this gene (Dawkins *et al.*, 2001). It is not apparent what the functional consequence of the upregulation of this gene would be in PSD95$^{-/-}$ forebrain in terms of synaptic plasticity and learning.

3.5.3.1.9 ESTs

The ESTs that are found expressed at significantly different levels are yet to be annotated and are, as such, of unknown function. At the time of writing (Spring 2004) BLAST analysis of the ESTs failed to identify any significant matches to the sequences of known genes. However, annotations of the mouse genome continue to be updated, so it is likely that, in the future, the genes that the ESTs correspond to will be identified.

3.5.3.2 Genes Altered in SynGAP $^{+/-}$ Hippocampi

In the SynGAP$^{+/-}$ hippocampus the expression of *cfos, egr2* and *nur77* (see 3.5.3.1.2) are significantly altered, along with 6 ESTs (see 3.5.3.1.9). In addition 8 known genes (*erythroid differentiation factor, sox11, DUSP6, glucose 6 phosphate* dehydrogenase, *UDP-glucuronosyltransferase 8, K$^+$ channel, subfamily K 1 [TWIK1], Nrd1, voltage gated K$^+$ channel [m-eag], N-glycan alpha 2,8-sialtransferase* and *Elovl6)*

were found down regulated in SynGAP$^{+/-}$ hippocampi and 3 known genes, encoding ribosomal protein L44, glyoxalase 1 and NADH dehydrogenase were found upregulated.

3.5.3.2.1 Sox11

Sox11 encodes a gene belonging to the SRY like box (SOX) family of developmentally regulated transcription factors. It has been found expressed in developing neurons in various species (Uwanogho *et al.*, 1995; Azuma *et al.*, 1999; Rimini *et al.*, 1999). If required for neuronal differentiation and development, *sox11* may also be induced during changes in neuronal morphology in plasticity.

3.5.3.2.2 DUSP6

DUSP6 encodes MKP3, a dual specificity MAP kinase phosphatase, belonging to a family of molecules that can reverse the activation of MAP kinases by dephosphorylating key sites. MKP3 has been shown to block the phosphorylation of ERK2 in EGF stimulated COS cells (Muda *et al.*, 1996). If this inhibition of ERK phosphorylation also occurred in neurons, then the down regulation of *DUSP6* may contribute to the enhanced levels of pERK found after NMDA receptor stimulation of SynGAP$^{+/-}$ hippocampal tissue.

In the rat brain, *DUSP6* is most highly expressed in the hippocampus and expression is induced in surrounding cortex following seizure (Muda *et al.*, 1996). Thus, *DUSP6* can be induced by neuronal stimulation and could potentially lie downstream of NMDA receptor activity. If it were that *DUSP6* expression was regulated by NMDA receptor stimulation, via SynGAP, then this could directly result in the misregulation of the gene in SynGAP$^{+/-}$ tissue. The regulation of *DUSP6* downstream of the NMDA receptor and SynGAP could represent a feedback loop whereby ras-ERK signalling directly regulates the transcription of a phosphatase that acts as a negative control of the pathway.

3.5.3.2.3 M-eag and TWIK1

Genes encoding two different K^+ channels are downregulated in SynGAP$^{+/-}$ tissue. M-eag is the murine form of eag voltage gated outwardly rectifying K^+ channels (reviewed by Ganetzky *et al.*, 1999). There is data to suggest that Eag, the *Drosophila* homologue of *m-eag*, is modulated by CaMKII and may be involved in neuronal plasticity in *Drosophila* (Griffith *et al.*, 1994). Potentially, *m-eag* has similar function and, as such, could play a role in neuronal plasticity in mice.

In addition to *m-eag*, another gene encoding a K^+ channel is downregulated. TWIK 1 is a weak inward rectifier highly expressed in the hippocampus, cortex and cerebellum of the adult mouse brain. It is hypothesised to maintain membrane resting potential (Lesage *et al.*, 1997).

3.5.3.2.4 N-glycan alpha 2,8-sialtransferase

N-glycan alpha 2,8 -sialtransferase (ST8SiaIV) is an enzyme that is required for sialic acid polymeriasation, which modulates the properties of neural cell adhesion molecule (NCAM) (reviewed by Rutishauser, 1996). The polysialation of NCAM is required for LTP in the hippocampus (Muller *et al.*, 1996) and this polysialated NCAM can be transported to the cell surface (Kiss *et al.*, 1994). It is hypothesised that the presence of NCAM at the cell membrane could be required for altering the 'adhesive' properties of the synapses, which could contribute to plasticity changes in synaptic structure. Therefore, the function of N-glycan alpha 2,8 -sialtransferase in modulating NCAM could be required for plasticity. Indeed, adult mice lacking N-glycan alpha 2,8-sialtransferase have impaired LTP and LTD in the CA1 region of the hippocampus, although LTP is intact in CA3 regions (Eckhardt *et al.*, 2000).

3.5.3.2.5 Glyoxalase 1

The glycation (binding of sugar) of proteins and nucleotides can affect the function of molecules causing cell and tissue damage. *Glyoxalase 1*, upregulated in SynGAP$^{+/-}$ hippocampi, is a key protein in the prevention of glycation, catalysing the conversion of reactive sugars to inert forms (reviewed by Thornalley, 2003).

The upregulation of glyoxalase 1 has also been found, by microarray, in the cerebrum of a mouse model of Alzheimer's disease caused by mutant form of the microtubule-associated protein tau (Chen *et al.*, 2004). It is hypothesised that the aggregation of tau into neurofibrillary tangles, as seen in Alzheimer's causes cell stress and leads to an increase in the expression of *glyoxalase 1*. It is thought that the induction of *glyoxalase 1* in response to stress is the cell's attempt to reduce a damaging accumulation of glycated proteins. It is not clear why *glyoxalase 1* should be upregulated in SynGAP$^{+/-}$ brain tissue, but the hypothesised role of the protein in Alzheimer's disease suggests it could be a neuronal response to cell stress.

3.5.3.2.6 Other Altered Genes

There are several other genes that are significantly altered in SynGAP$^{+/-}$ hippocampal sample (*erythroid differentiation factor, glucose 6 phosphate* dehydrogenase, *UDP-glucuronosyltransferase 8, Nrd1, Elovl6, ribosomal protein L44* and *NADH dehydrogenase*). In some cases (*Nrd1, Elovl6, ribosomal protein L44)* little is known about the encoded proteins. The other genes (*erythroid differentiation factor, glucose 6 phosphate dehydrogenase, UDP-glucuronosyltransferase 8* and *NADH dehydrogenase)* encode molecules that are involved in processes that have no apparent role in NMDA mediated phenomena.

3.5.4 Functional Significance of Genes Significantly Altered in Mutant Tissue

As has been discussed, it is apparent that many of the genes significantly altered in PSD95 and SynGAP mutant tissue have known function in spatial learning, LTP and other plasticity phenomena. Table 3.18 summarises this data and it is striking that of the 21 different known genes misregulated in PSD95 and SynGAP mutant tissue, 13 (62%) have known, or implied, functions in cognitive disorders, synaptic plasticity or learning. This suggests that there is alteration of expression of key genes involved in synaptic mechanisms and plasticity in PSD95$^{-/-}$ and SynGAP$^{+/-}$ and this could be an underlying cause of the animal phenotypes.

GENE	Regulated by the NMDA Receptor	Encodes Synaptic Protein	Role in Neurological Disorder	Function in Memory	Function in Plasticity
Altered in PSD95$^{-/-}$ and SynGAP$^{+/-}$ Tissue					
Cfos	✓			✓	✓
nur77	✓				
egr2	✓		✓		
Altered in PSD95$^{-/-}$ Tissue					
Per1	✓			?	
JunB	✓				
cyln2			✓	✓	✓
GADD45B	?				
Atp7a			✓		
Syntenin		✓			
Altered in SynGAP$^{+/-}$ Tissue					
DUSP6	?				
M-eag					?
N-glycan alpha 2, 8-sialyltransferase					✓
Glyoxalase 1			✓		

Table 3.18 – Summary of Functions of Significantly Altered Genes. Table details genes significantly altered in PSD95 and SynGAP mutant tissue that are regulated by the NMDA receptor, encode synaptic proteins, have a role in a neurological disorder/disease or function in memory or plasticity. Ticks indicate there is evidence for involvement of the gene in the particular category, a question mark means there is data that suggests the possibility that the gene could be involved.

3.5.4.1 Misregulation of Inducible Transcriptions Factors

The downregulation of activity regulated transcription factors (*cfos, nur77, egr2* and *junB*) in PSD95$^{-/-}$ forebrain and SynGAP$^{+/-}$ hippocampus indicates that these genes may not be correctly induced following NMDA receptor activity in mutant tissue. These genes could regulate the transcription of key proteins for neuronal response to stimulation and thus, if they are not correctly induced, there may be resultant phenotypes in NMDA receptor mediated effects.

As yet, the late response genes that inducible transcription factors regulate are largely unknown. However, a recent study showed, in rat Schwann cells, genes responsive to egr2 included *Sap102, Homer-1b, CaMKIV, egr1, cfos, NMDAR2D* subunit and *GluRB* (Nagarajan *et al.*, 2001). Thus, these are potential targets of egr2 downstream of NMDA receptor activity and include proteins with known synaptic roles. This would be consistent with the hypothesis that activity dependent transcription factors can regulate the expression of RNAs that encode proteins critical to long term neuronal responses to synaptic activity.

3.5.4.2 Misregulated Genes and Spatial Learning

PSD95$^{-/-}$ and SynGAP$^{+/-}$ mice have similar deficits in the Morris water maze, a test of hippocampal based spatial learning (Migaud *et al.*, 1998; Komiyama *et al.*, 2002). The misregulation of genes in PSD95$^{-/-}$ forebrain and SynGAP$^{+/-}$ hippocampus could, potentially, be an underlying cause of this phenotype. Indeed, *cyln2*, down regulated in PSD95$^{-/-}$ forebrain and *cfos*, down regulated in PSD95 and SynGAP mutant tissue, have previously been shown to play a role in hippocampal based learning.

Given that animals lacking *cfos* in the central nervous system are impaired in the Morris water maze and contextual fear conditioning, the common downregulation of *cfos* in PSD95$^{-/-}$ and SynGAP$^{+/-}$ brain tissue may be a basis for the animals' similar

deficits in spatial learning. As a transcription factor, the action of *cfos*, downstream of the NMDA receptor activation, has many potential target genes that could include genes required in spatial learning. The genes found similarly down regulated in PSD95$^{-/-}$ and SynGAP$^{+/-}$ tissue are all activity regulated transcription factors and the downregulation of *nur77* and *egr2*, as well as that of *cfos*, could potentially contribute to the behavioural phenotype of the animals. It may be that alterations in this specific group of activity dependent genes impacts on spatial learning, resulting in the common behavioural deficits of PSD95$^{-/-}$ and SynGAP$^{+/-}$ animals.

A recent study, using microarrays to analyse amyloid precursor protein and presenilin-1 mice, has also proposed that misregulation of specific activity regulated genes may contribute to memory phenotypes (Dickey *et al.*, 2003). The animals, models of amyloid deposition in Alzheimer's disease, develop age-related deficits in memory (Arendash *et al.*, 2001). Gene expression was compared in amyloid containing brain areas (hippocampus, cortex) and amyloid free areas (cerebellum, striatum and brainstem). Several 'plasticity related genes' were found at lower levels in amyloid containing brain regions, including the immediate early genes *arc*, *egr1* and *nur77* (Dickey *et al.*, 2003). It was hypothesised that the misregulation of these activity regulated genes may underlie the memory loss in this model of Alzheimer's disease.

3.5.4.3 Misregulated Genes and Synaptic Plasticity

Hippocampal slices from PSD95$^{-/-}$ and SynGAP$^{+/-}$ animals both have abnormal LTP induction, however, unlike spatial learning, the phenotypes are dissimilar. PSD95$^{-/-}$ slices show enhanced LTP, where as the plasticity is diminished in SynGAP$^{+/-}$ slices. Given these different phenotypes, it may be that genes that are differentially altered in PSD95$^{-/-}$ and SynGAP$^{+/-}$ tissue are the ones that underlie the plasticity phenotypes of the animals.

Several of the genes significantly altered in PSD95$^{-/-}$ and SynGAP$^{+/-}$ tissue have been shown necessary for LTP. Mutation of *cyln* and *N-glycan alpha 2,8-sialtransferase,* down regulated in PSD95$^{-/-}$ and SynGAP$^{+/-}$ tissue respectively, results in impaired LTP in the CA1 region of the hippocampus. Also, animals expression mutant *cfos* in the CNS have impaired hippocampal LTP following 100Hz tetanus stimulation. In addition to information from transgenic studies, there is data to suggest that m-eag could have a role in neuronal plasticity.

In the SynGAP$^{+/-}$ hippocampi, the phenotypes of *cfos* and *N-glycan alpha 2,8-sialtransferase* mutants and potential function of m-eag, are all consistent with the reduction of LTP seen in SynGAP$^{+/-}$ slices. However, in the case of PSD95$^{-/-}$ data, the hippocampal LTP phenotypes of *cfos*$^{CNS-/-}$ and *cyln2*$^{-/-}$ animals are not consistent with the increased LTP induction of PSD95 mutants.

The inconsistency of *cfos*$^{CNS-/-}$ and *cyln2*$^{-/-}$ hippocampal LTP phenotypes with that of PSD95$^{-/-}$ slices could have several explanations. It may be due to the tissue source of material for the PSD95$^{-/-}$ experiment and lower levels of *cyln2* and *cfos* in the forebrain might not contribute to the hippocampal LTP phenotype of PSD95$^{-/-}$ animals. In order to identify genes that are more likely to be relevant to the hippocampal LTP phenotype of the animals, RNA from PSD95$^{-/-}$ hippocampi should be examined. However, it may be that the enhanced LTP measured in hippocampal slices from PSD95$^{-/-}$ animals is not a consequence of altered gene expression, but a result of the abnormal PSD95 protein.

3.5.5 Relevance of Chromosomal Clustered Genes

Analysis of the chromosomal location of significantly altered genes found several of the genes to be on the same chromosomes. This clustering effect was statistically significant for the SynGAP data. Table 3.14 shows significantly altered transcripts organised by chromosome. The genes highlighted in the table have known function

in NMDA mediated phenomena or function postsynaptically. The other genes that are altered may have roles in synaptic plasticity that are, as yet, unknown.

The clustering effect may represent loci of genes that function in synaptic plasticity. It has been shown that genes of related function can be found together on the regions of chromosomes. A recent microarray study, identifying genes regulated in the hippocampus during long term memory consolidation also identified significant grouping of altered genes to particular chromosomes (Levenson *et al.*, 2004). In particular, significant numbers of altered genes were found on chromosomes 10, 12, 16, 18 and 19. Comparing this to the data presented in this chapter, although no significantly altered genes were found on chromosomes 16, 18 and 19, multiple significantly altered genes were found on chromosomes 10 and 12 in both PSD95 and SynGAP data.

However, alterations in genes grouped on the same chromosomes could also represent functionally diverse genes that display similar expression patterns due to their proximity on the chromosome. There is evidence of domains, termed as ridges, in human chromosomes where clusters of functionally unrelated genes show comparable levels of expression (Caron *et al.*, 2001; Versteeg *et al.*, 2003). It has been hypothesised that transcription of the human chromosomes could have two levels of control (Versteeg *et al.*, 2003). As well as activity at the specific promoter regions of individual genes, there appears to be factors that act to control transcription of groups of genes within a particular ridge.

Analysis of microarray studies have also found domains of similarly expressed, but functionally diverse, genes in the *Drosophila* genome (Spellmen and Rubin, 2002). It was found that often there appeared to be one or two genes in each domain that showed high levels of differential expression in a given condition, and other genes within the domain were altered but not the same extent. It is proposed that when the chromatin is 'opened' in order for a key gene to be expressed, this may increase

the accessibility of transcriptional machinery to the promoter regions of genes in the surrounding area (Spellmen and Rubin, 2002). Thus, alterations in the expression of multiple genes in a cluster could be seen due to targeted changes in the level of a key gene.

Some of the chromosomal clustering of the PSD95$^{-/-}$ and SynGAP$^{+/-}$ array data could be due to similar reasons. It is probable that domains of similarly expressed genes exist in mouse genome as found in the human and *Drosophila* genomes. As such, it may be that regulation of basal expression of genes such as *cfos* via PSD95 and SynGAP dependent signalling also exerts a degree of control on the levels of genes in the surrounding chromosomal domain. Subsequently, if the regulation of *cfos* is disrupted in mutant tissue, then the expression of neighbouring genes (e.g. *serine palmitoyltransferase*) could also be altered. If this were the case then it could be expected that some of the significantly altered genes are not changed due to a direct functional response to PSD95 or SynGAP mutation, but because of chromosomal proximity to a functionally relevant gene.

3.5 CONCLUSION

This data discussed in this chapter has demonstrated the successful application of microarray technology in the analysis of tissue carrying mutations in NRC proteins. Mutations of PSD95 and SynGAP result in transcriptional changes of a limited number of genes, including several activity regulated genes, genes involved in learning and others with roles in plasticity. The misregulation of these genes may contribute to the phenotypes of PSD95$^{-/-}$ and SynGAP$^{+/-}$ animals. Additionally, evidence of changes in chromosomally clustered genes was found.

Transcriptional alterations in PSD95 and SynGAP mutant tissue imply a role for these proteins in signalling pathways regulating gene expression. The functions of these proteins downstream of the NMDA receptor suggest that the transcripts altered in the mutant tissue could be a subset of the total genes regulated by the

receptor. Given that the material used in the experiments was isolated from acutely dissected brain tissue, this implies that the NMDA receptor and associated proteins regulate basal transcription levels of particular transcripts. Also, analysis of the data suggests that PSD95 and SynGAP act in independent and common pathways that contribute to the control of gene expression.

The data discussed in this chapter has demonstrated the potential of using microarrays in experiments to study brain tissue from transgenic animals. As has been shown, the amount of information generated by a single experiment is immense and can be studied if various ways to extract meaningful data. As such, microarrays could be a useful employed, along with other standard behavioural and electrophysiological tests, to analyse mice carrying mutations in other NRC proteins.

CHAPTER 4

IN VITRO STIMULATION OF THE NMDA RECEPTOR

4. *IN VITRO* STIMULATION OF THE NMDA RECEPTOR

As discussed in chapter 3, mutations in NRC proteins, PSD95 and SynGAP, alter the expression of genes in acutely dissected brain tissue. The transcripts found significantly altered included several activity dependent genes. It may be that the misregulated transcripts in PSD95$^{-/-}$ and SynGAP$^{+/-}$ tissues represent a subset of the genes regulated by NMDA receptor dependent signalling. It would therefore be interesting to identify the total set of genes modulated by NMDA receptor activity and analyse the contribution of NRC proteins to their regulation.

To study activity dependent gene expression a reliable protocol for NMDA receptor stimulation is required. *In vivo* stimulation methods, analysing RNA from relevant brain regions after seizure induction, LTP or learning, are advantageous as they are likely to reveal physiologically relevant activity regulated genes. However, *in vivo* stimulation can be problematic. *In vivo* stimulation assays, particularly seizure models, can activate a variety of receptors and pharmacological isolation would be required to identify the NMDA regulated genes.

In vitro methods of stimulation are widely applied to analyse the genes regulated by NMDA receptor activity. *In vitro* protocols, using chemical or electrical stimulation of primary cultured neurons, cell lines or brain slices, are advantageous in that they can be performed with high throughput. As a result they can, more readily, be exposed to a wide variety of conditions (e.g. different pharmacological treatments). In addition, the stimulated cells can easily be subject to different types of analysis e.g. biochemical, immunohistochemical, electrophysiological. Another benefit of *in vitro* techniques is that primary cultures from embryonic tissues can be used to analyse targeted mutations that are lethal postnatal.

Once a reliable stimulation method has been developed then activity induced gene expression in wild type cells could be analysed. If this were done using microarrays it would reveal the global alterations in gene expression regulated by synaptic

activity and could identify novel genes modulated by NMDA receptor activity. By subsequently analysing mutant cells, such as PSD95$^{-/-}$ neurons, the contribution of NRC proteins to activity regulated gene expression could be examined.

4.1 *IN VITRO* STIMULATION OF NMDA RECEPTORS

For all stimulation experiments, primary cultured cortical neurons from E17.5 mouse embryos were used. The cultures were grown for 10-12 days in 6 x 35mm well dishes at a surface density of 1 x 10^5 cells/cm^2. Figures 4.1A and 4.1B are images of such a culture, A shows the phase image and B shows the same field with DAPI staining. The nuclei stain reveals there are many cells present in the culture. The majority of these are likely to be neurons, with glia also present. Figures 4.1C and 4.1D are images of another culture, C in phase and D with cy3-MAP2B staining. This neuronal marker shows the culture is a dense network of neuronal processes.

It is thought that the maturation of primary cultured neurons follows the same temporal profile as cells *in vivo*. It has previously been shown that developmental changes in NMDA receptor subunit expression in cultured cortical neurons mimics the temporal changes of that *in vivo* (Zhong *et al.*, 1994). Also, the expression of PSD95 protein in cultures, as used in this chapter, increases from DIV11 to DIV26 as it does between postnatal days 7 to 21 (K. Dickson, personal communication). It can therefore be assumed that the cells used in stimulation assays from cultures DIV10-12 would be of equivelent maturity as cells, *in vivo*, postnatal day 6-8.

4.1.1 Activity Dependent Gene Expression Following NMDA Treatment

NMDA application to the cultures was chosen as the initial *in vitro* method of stimulation. This protocol should directly stimulate the receptor of interest and published studies have used glutamate or NMDA treatment successfully to study activity regulated gene expression in cultured neurons (Bading *et al.*, 1995; Szekely *et al.*, 1990; Bulleit *et al.*, 1994; Rage *et al.*, 1993).

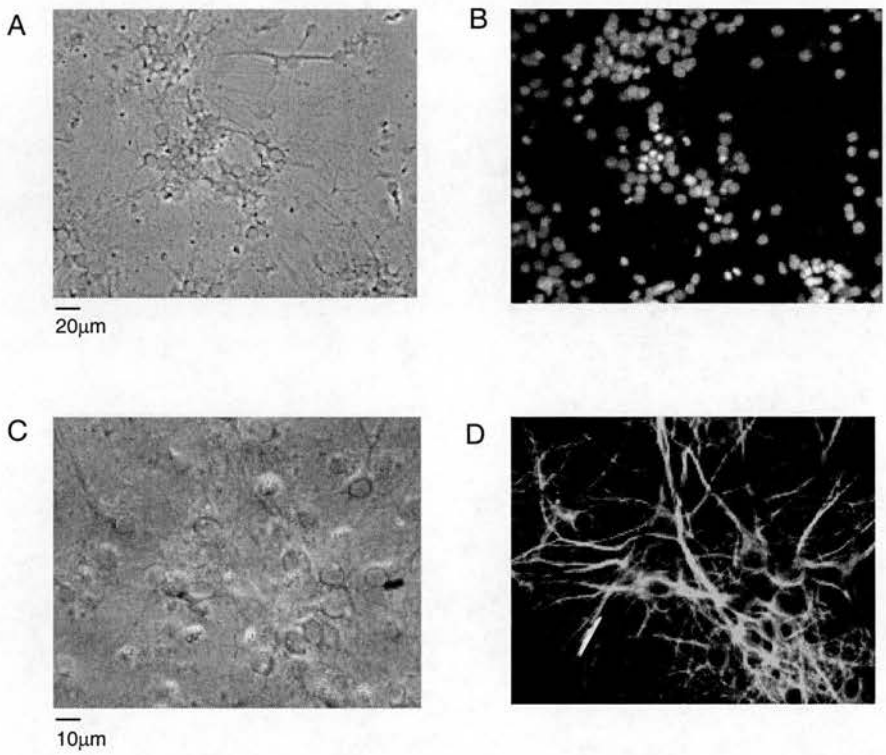

Figure 4.1 – Images of Cultured Neurons. Pictures show images of E17.5 primary cultured cortical neurons, as those used for stimulation assays. **A** and **B** are pictures of the same culture. A is the phase and B is DAPI staining of the nuclei present. **C** and **D** are pictures of a culture, C is the phase and D shows cy3-MAP2B neuronal staining.

4.1.1.1 Treatment of Primary Cortical Cultures with NMDA

For stimulation by NMDA cells were treated as detailed in figure 4.2. To reduce basal cell activity media in wells for stimulation was treated with 1μM TTX 2hrs before agonist treatment. Stimulation was induced by media change to Mg^{2+} free solution containing 100μM NMDA and 10μM glycine, a co-agonist of the NMDA receptor. A Mg^{2+} free solution was used to ensure relief of the NMDA receptor voltage dependent Mg^{2+} block. RNA was extracted from the cells 30mins after NMDA treatment. An unstimulated condition, with 2hr TTX treatment and then media change to Mg^{2+} free solution without NMDA, was included to test whether the media change alone could alter activity dependent gene expression. RNA was extracted from cells, using QIAGEN RNeasy minikits, in 3 different conditions; untreated, unstimulated and stimulated.

4.1.1.2 Analysis of Activity Dependent Gene Expression

RNA was reverse transcribed to cDNA using Ambion protocols. The expression of activity dependent genes was then measured by RT-PCR and the products run out on a 4% agarose gel (figure 4.3) to visualise any changes in expression. Figure 4.3A shows the products from the primers used in RT-PCR reactions with cDNA from wild type forebrain samples to confirm that they are of expected size. Figure 4.3B shows the effects of stimulation on *cfos, egr1, egr2* and *nur77* levels, with *GAPDH* used as a control. 30mins after NMDA stimulation the levels of immediate early genes *cfos, egr1, egr2,* and *nur77* were increased. However, the unstimulated samples also showed upregulation of the same activity regulated genes. In most cases this increase was not as great as that induced by NMDA, but was still clearly apparent. The increase in gene expression seen in unstimulated samples may be due to chemical or mechanical stress to the cells caused by removal from the incubator and subsequent media change.

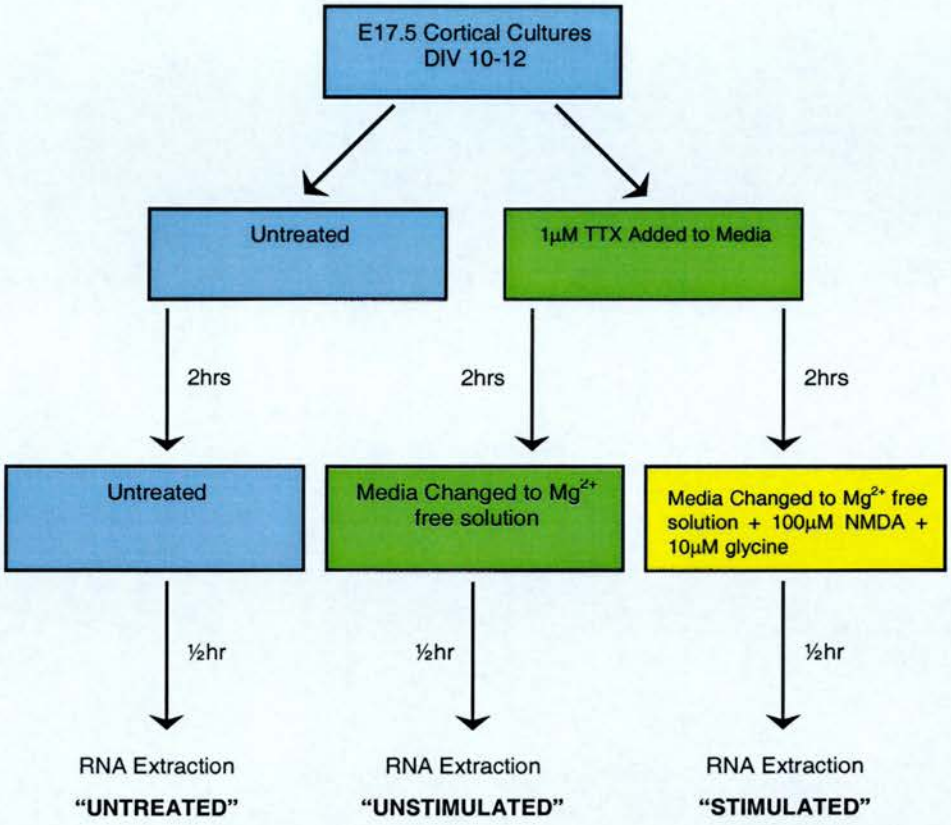

Figure 4.2 – NMDA Stimulation Protocol. Flow chart shows the stimulation protocol for primary cultured cortical neurons using NMDA. There are three conditions from which RNA is extracted. "Untreated" cells have no treatment following culture. "Unstimulated" cells have TTX added to the media for 2hrs and are then changed to a Mg^{2+} free solution for ½hr before RNA extraction. "Stimulated" cells are changed to TTX containing media for 2hrs before ½hr treatment with a Mg^{2+} free solution containing 100μM NMDA and 10μM glycine before RNA extraction.

A

GENE	FORWARD PRIMER	REVERSE PRIMER	EXPECTED PRODUCT (BP)
GAPDH	GTGTTCCTACCCCCAATGTG	ATGTAGGCCATGAGGTCCAC	292
Cfos	CTTTATCCCCACGGTGACAG	CTGCAGCCATCTTATTCCGT	296
Nur77	TTCTGCTCAGGCCTGGTACT	GATTCTGCAGCTCTTCCACC	199
Egr2	AAGGCCGTAGACAAAATCCC	CTAGGTGCAGAGATGGGAGC	344
Egr1	TCCTTTCCTCACTCACCCAC	TGGGATAACTCGTCTCCSCC	295

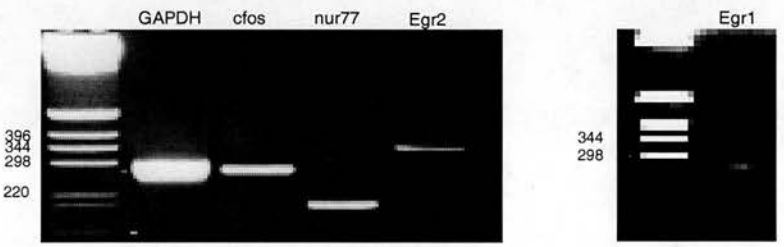

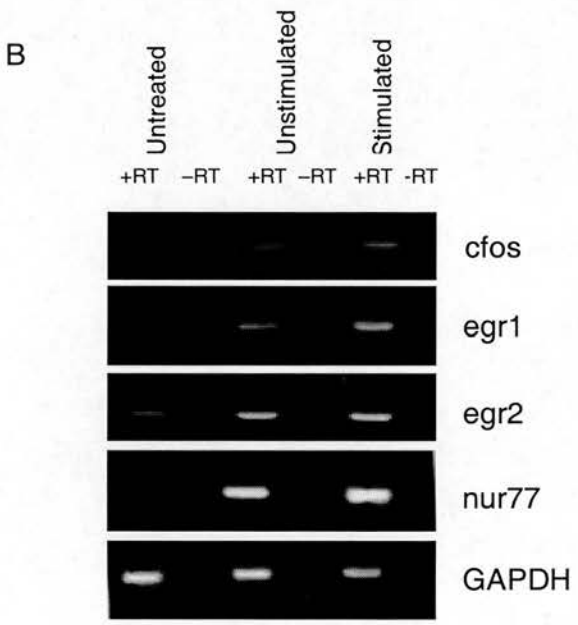

Figure 4.3 – RTPCR of Stimulated Samples. **A** details the primers used in RTPCR reactions and shows that the PCR products of these primers, in a reaction with wild type forebrain cDNA, are of expected size as compared to a 1kB ladder. **B** shows the results of RTPCR reactions using cDNA transcribed from untreated cells, unstimulated cells (2hr TTX treatment of media, change of media to Mg^{2+} free solution 30mins before RNA extraction) and stimulated cells (2hr TTX treatment of media, change of media to Mg^{2+} free solution containing 100μM NMDA + 10μM glycine 30mins before RNA extraction).

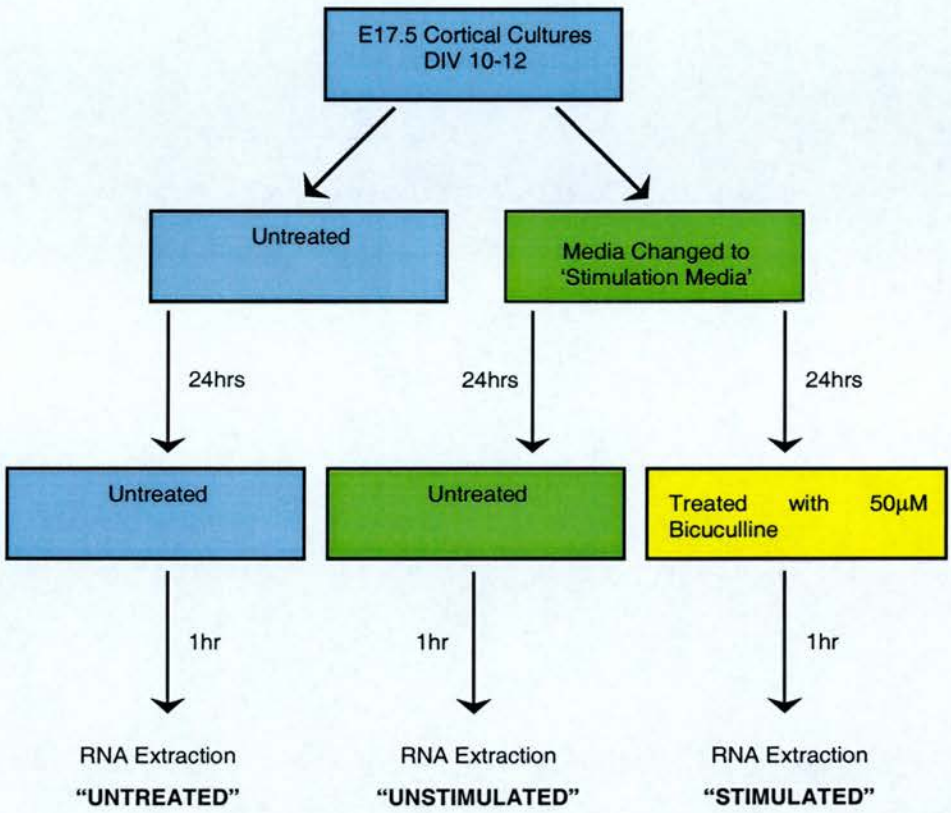

Figure 4.4 – Bicuculline Stimulation Protocol. Flow chart shows the stimulation protocol for primary cultured cortical neurons using bicuculline. There are three conditions from which RNA is extracted. "Untreated" cells have no treatment following culture. "Unstimulated" cells have a media change to stimulation media 25hrs before RNA extraction. "Stimulated" cells are changed to the stimulation media for 24hrs, are then treated for 1hr with 50µM bicuculline before RNA extraction.

The results of the experiment revealed problems using the NMDA stimulation protocol to study activity dependent gene expression. Due to the induction of immediate early genes in unstimulated samples, it's unclear whether transcriptional increases in stimulated cell are due to the media change or to the action of the NMDA.

4.1.2 Activity Dependent Gene Expression Following Bicuculline Treatment

4.1.2.1 Treatment of Primary Cortical Cultures with Bicuculline

Due to the induction of activity dependent genes in unstimulated samples using the NMDA treatment protocol, an alternative stimulation assay was sought. Bicuculline treatment of rat hippocampal neurons has been used to analyse CRE mediated gene expression as it effectively induces NMDA receptor dependent phosphorylation of CREB (Hardingham *et al.*, 2001; Hardingham *et al.*, 2002). Furthermore this method has been demonstrated to increase cfos protein, *BDNF* RNA levels and CRE-dependent gene expression (Hardingham *et al.*, 2001; Hardingham *et al.*, 2002).

Bicuculline is a $GABA_A$ (γ-aminobutyric acid) antagonist and its addition to cultured cells removes inhibitory GABA input to the neurons. This should promote spontaneous firing of stimulatory neurons, increasing synaptic activity. Bicuculline treatment is an appealing stimulation protocol as it only activates synaptic NMDA receptors and is, therefore, more physiologically relevant than pharmacological stimulation of all NMDA receptors. Also, there is no requirement for a media change to a Mg^{2+} free buffer before stimulation as an increase in synaptic activity caused by bicuculline will depolarise the postsynaptic membrane, relieving the voltage dependent Mg^{2+} block of the NMDA receptor.

Cells were treated as detailed in figure 4.4 based on the protocols from (Hardingham *et al.*, 2002). Cells were changed to 'stimulation media', as detailed in (Bading *et al.*, 1993) 24 hrs before drug treatment. Since the media change is 24hr

before stimulation any increases in immediate early gene expression, caused by media change, should have returned to basal levels before bicuculline treatment. The cultures were stimulated by application of 50μM bicuculline. As with the NMDA treatment, RNA was also extracted from unstimulated (media change 24 hours before time of stimulation, no bicuculline treatment) and untreated conditions. The RNA extractions, using QIAGEN RNeasy mini kits, were performed 1hr after bicuculline treatment.

4.1.2.2 Analysis of Activity Dependent Gene Expression

Following bicuculline stimulation RNA was analysed using QRT-PCR. This ensured subtle increases in expression could be identified, without concerns about reaction saturation. For the initial experiment, using the bicuculline protocol, 4 wells of a culture dish were analysed. One well was left untreated, one had a media change but remained unstimulated and 2 wells were treated with bicuculline. Following RNA extraction, 0.5μg of RNA from each sample was reverse transcribed and QRT-PCR performed by lightcycler to measure the levels of *cfos* and *GAPDH*. Each sample was run in duplicate and the average *cfos/GAPDH* ratio calculated for each sample. The ratios of the unstimulated and stimulated samples were compared to that of the untreated samples.

Table 4.1 shows the results of this experiment. The ratio of *cfos* in the unstimulated sample compared to untreated was 0.94. This suggests that the media change, 24hrs prior to extraction, had no effect on the levels of *cfos* in cultured cortical neurons. The ratios of *cfos* expression in the stimulated samples compared to untreated were 0.930 and 13.221. Thus, in one well bicuculline successfully induced the expression of *cfos*.

SAMPLE	cfos	GAPDH	*cfos* AVE.	*GAPDH* AVE.	cfos/GAPDH	RATIO RELATIVE TO UNTREATED
Untreated	1508.4 1033.3	1234.5 1450.7	1270.89	1342.59	0.987	
Unstimulated	920.8 1103.8	1058.7 1216.9	1012.29	1137.82	0.890	0.940
Stimulated 1	1216.4 879.6	1365.4 1016.0	1048.03	1190.72	0.880	0.930
Stimulated 2	21380.2 17247.0	1147.0 1813.7	19313.59	1480.32	13.047	13.221

Table 4.1 – Initial Results Of Bicuculline Treatment. Table shows cfos and GAPDH levels in RNA samples from untreated, unstimulated (media change, no bicuculline treatment) and stimulated (media change, 50μM bicuculline) cultured cortical neurons. A ratio of the expression of cfos and GAPDH was taken from the average of duplicates for each sample. This ratio was then compared to untreated samples to determine induction of cfos.

To determine if bicuculline treatment reproducibly induces *cfos* expression, bicuculline stimulation was repeated several times (see table 4.2). Each experiment was performed on cells from individual neuronal cultures that had been prepared in the same way. The bicuculline treatments were carried out as for the initial experiment, though for control purposes, in some experiments, wells were treated with Actinomycin D (10μg/ml) or 50μM APV 1hr prior to bicuculline application.

As with the initial experiment, RNA was extracted from experimental wells using QIAGEN RNeasy mini kits and analysed by lightcycler. The reactions were run in duplicate and average *cfos* levels normalised by taking their ratio to *GAPDH*. The stimulated *cfos* levels were then compared to untreated *cfos* levels to assess stimulation.

Table 4.2 shows that bicuculline stimulation of 6 cultures produced highly variable results; on average, *cfos* levels were 3.19 fold higher in stimulated samples, with a standard deviation of 4.77. A t test found no significant induction of *cfos* ($p=0.32$) in bicuculline treated samples compared to untreated samples. As such, bicuculline treatment was considered to be ineffective as a reliable method of inducing activity dependent gene expression.

CONDITION	Treated/Untreated	STATISTICS	
Stimulated	0.95		
	12.86	Average	3.19
	1.49	Standard Dev	4.77
	0.61	P value	0.32
	0.99		
	2.24		
Actinomycin D	0.011	Average	0.028
	0.022	Standard Dev	0.020
	0.051	P value	0.00008
APV	0.289	Average	0.46
	0.088	Standard Dev	0.48
	1.001	P value	0.19

Table 4.2 – Results Of Bicuculline Treatment. Table shows the ratio of normalised cfos levels in RNA samples from primary cultured cortical neurons treated with 50μM bicuculline alone, 50μM bicuculline in the presence of 10μg/ml actinomycin D, 50μM Bicuculline in the presence of 500μM APV and those left untreated. The average ratios and standard deviations are shown. The p values were calculated by t test.

Treatment of cultures with transcriptional inhibitor, actinomycin D, prior to bicuculline stimulation resulted in a significant decrease in *cfos* expression. On average the expression was 0.028 of that in untreated samples. From this data the halflife of *cfos* RNA can be calculated to be 23.3mins. This is consistent with published data which has reported the half life to *cfos* RNA to range between 10 and 30 mins (Rahmsdorf *et al.*, 1987, Chagnovich and Cohn, 1997, Blattner *et al.*, 2000). The treatment of cultured neurons with APV prior to bicuculline treatment resulted, in 2 of 3 experiments, in a decrease in the levels of *cfos*. However, overall this was not a significant effect (p=0.19).

4.1.3 Activity Dependent Gene Expression Following APV Treatment

In the previous experiment it was noted that treatment of cells with APV before bicuculline treatment reduced the level of *cfos* in two of three experiments. It was therefore decided to further investigate the effect of APV treatment on *cfos* RNA levels in cultured neurons.

4.1.3.1 Treatment of Primary Cortical Cultures with APV

The media of wells of cultured cortical neurons, as used bicuculline treatments, was replaced with 'stimulation media' 24hrs before 50μM APV treatment. APV was applied to the cells 1hr before extraction of RNA using QIAGEN RNeasy mini kits.

4.1.3.2 Analysis of Activity Dependent Gene Expression

After extraction, 0.5μg of RNA from each sample was reverse transcribed and QRT-PCR performed by lightcycler measuring levels of *cfos*, *nur77*, *egr2* and *GAPDH*. Samples were run in duplicate and the average ratios of *cfos*, *nur77* and *egr2* to *GAPDH* calculated for each sample. The ratios of the APV treated samples were compared to that of the untreated samples.

Table 4.3 shows the results of these experiments. Treatment of the cultured neurons caused a reduction in the levels of *cfos*, *nur77* and *egr2*. On average these reductions were to levels 0.475 (*cfos*), 0.588 (*nur77*) and 0.626 (*egr2*) of that in untreated samples. Although the degree of APV induced reduction showed variation, the levels of expression of *cfos*, *nur77* and *egr2* in untreated samples were significantly different ($p < 0.05$) from APV treated cells as calculated by t test. As such, APV treatment can be effectively used to analyse the expression of NMDA receptor regulated genes in spontaneously active neurons.

GENE	CULTURE	TREATED/UNTREATED	STATISTICS	
cfos	1	0.226		
	2	0.168	Average	0.475
	3	0.539	Standard Dev	0.149
	4	1.006	P value	0.024
	5	0.435		
nur77	1	0.281		
	2	0.616	Average	0.588
	3	0.214	Standard Dev	0.159
	4	1.104	P value	0.032
	5	0.711		
egr2	1	0.252		
	2	0.259	Average	0.601
	3	0.618	Standard Dev	0.269
	4	1.188	P value	0.048
	5	0.687		

Table 4.3 – Results Of APV Treatment. Table shows the ratio of normalised *cfos*, *nur77* and *egr2* levels in RNA samples extracted from primary cultured cortical neurons 1hr after treatment with 50μM APV compared to those that were left untreated. The average ratios standard deviations and p values calculated by t tests, comparing treated and untreated levels, of gene expression are shown.

4.2 ELECTROPHYSIOLOGICAL ANALYSIS OF PRIMARY CULTURES

Bicuculline treatment of cultured neurons did not result in the expected increases in activity regulated gene expression. It was therefore decided to use electrophysiology to analyse the effect of drug treatment on the activity of primary cultured cortical neurons. To do this, multi-electrode arrays (MEA) were employed. The arrays used consisted of a glass well with a grid of 60 recording electrodes on the bottom. By coating the array with poly-D-lysine and laminin, cell cultures could be grown on this substrate and, subsequently, extracellular recording of activity taken across the cultures. The electrodes measured spike activity generated by the firing of action potentials

Primary cultures of mouse E17.5 cortical neurons were prepared as described for stimulation assays. Cells were plated at a surface density of 1 x 10^5 cells/cm^2 in neurobasal supplemented with B27 and glutamine and incubated at 37°C for 10-13 days before use. Figure 4.5 shows an example of the cultures grown on the array.

4.2.1 Primary Culture Activity Following Bicuculline Treatment

4.2.1.1 Treatment of Cultures with Bicuculline

MEA recordings have been used previously to study the effects of bicuculline on cultured neurons (Hardingham *et al.*, 2001, Hardingham *et al.*, 2002). These studies found that bicuculline increased the number of action potential spikes in the burst of firing in primary cultured rat hippocampal neurons (Hardingham *et al.*, 2002). Treating the cultures with bicuculline in the presence K^+ channel blocker 4-aminopyridine (4AP) increased the frequency of burst firing (Hardingham *et al.*, 2001, Hardingham *et al.*, 2002).

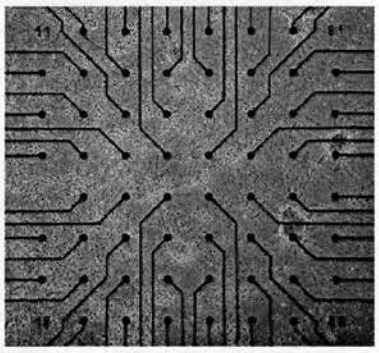

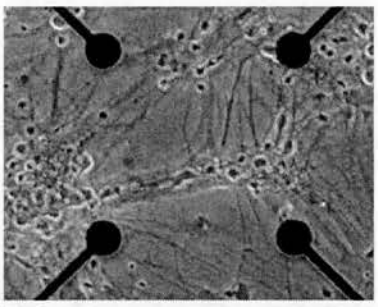

Figure 4.5 – Neuronal Cultures Grown on MEA. Figure shows 2 images of the same neuronal culture grown on MEA at two different magnifications. The cells were primary cultured mouse E17.5 cortical neurons, 12 DIV.

After 10-13 days *in vitro*, cells were removed from the incubator and arrays placed into the recording equipment. Cells were perfused with Locke's solution (containing 1mM $MgCl_2$). This magnesium concentration was used to be consistent with the stimulation media used for bicuculline treatment for the gene expression experiments. After recording a period of control activity from the culture, 50μM bicuculline was added to the Locke's perfusion. Cells were treated with bicuculline for at least 10 minutes, until activity levels appeared stable. In accordance with previous studies of bicuculline action on cell culture activity (Hardingham *et al.*, 2001; Hardingham *et al.*, 2002) the cells were then perfused with Locke's solution containing 50μM bicuculline and 50μM 4AP for approximately 10 minutes. The cells were then washed by perfusion with Locke's solution. Following this wash period, the cells were perfused with Locke's solution containing 1μM TTX to ablate cell activity and establish the level of background noise measured by the electrodes.

4.2.1.2 Culture Activity Following Bicuculline Treatment

The experiment was performed 3 times. For each array recording electrodes measuring low noise levels and detectable activity were selected for analysis. Thresholds for measuring spikes were determined, specific to each array, using the levels of activity during TTX perfusion to ensure all activity was measured, with no interference from noise. The number of spikes per second was recorded from each electrode selected for analysis.

Figure 4.6 is a graph showing the activity measured at several channels from one microelectrode array over the course of an experiment. The graph shows spike frequency over time with drug application indicated. The individual channels, represented by different colours on the graph, behaved in different ways. In basal conditions a high level of spontaneous activity was detected at each channel. In general, the application of bicuculline caused an initial decrease of activity, followed by a slow increase in spike frequency. In the case of the channel shown in yellow,

this increase was to a level above that of the control period. Following 4AP application the channels shown in red and blue show increased spike frequency, but the yellow and black channels show less activity. Activity across the culture was inconsistent, with different channels displaying variable activity patterns.

To study the overall effect of the drugs on each culture, the average spike frequency from each channel was calculated for each given condition. This value was converted to a percentage of the control, pre treatment activity for each channel. Then, for each array, the average spike frequency in each condition, as a percentage of control, was calculated. T tests were performed to establish whether activity during drug exposure was significantly different from control. In addition, the same calculations were performed with data combined from all analysed channels from all 3 arrays.

Figure 4.7A shows this data and figure 4.7B graphs the average spike frequency, as a percentage of control in each condition, for each array (expt1-3) and combined for all experiments. For each array, and with all data combined, the addition of bicuculline had no significant effect on spike frequency. In the case of one array (expt 1) exposure to bicuculline and 4AP caused a significant increase in spike frequency. For all arrays, activity during the wash period was significantly lower than control.

Bicuculline treatment of cultured cortical neurons had no significant effect on the firing rate of the cells. This could explain the lack of induction of activity regulated genes in cells following bicuculline application. As APV was found to reliably decrease the expression of activity regulated genes in spontaneously active cultures, it was decided to study the effect of APV on cultured cell activity.

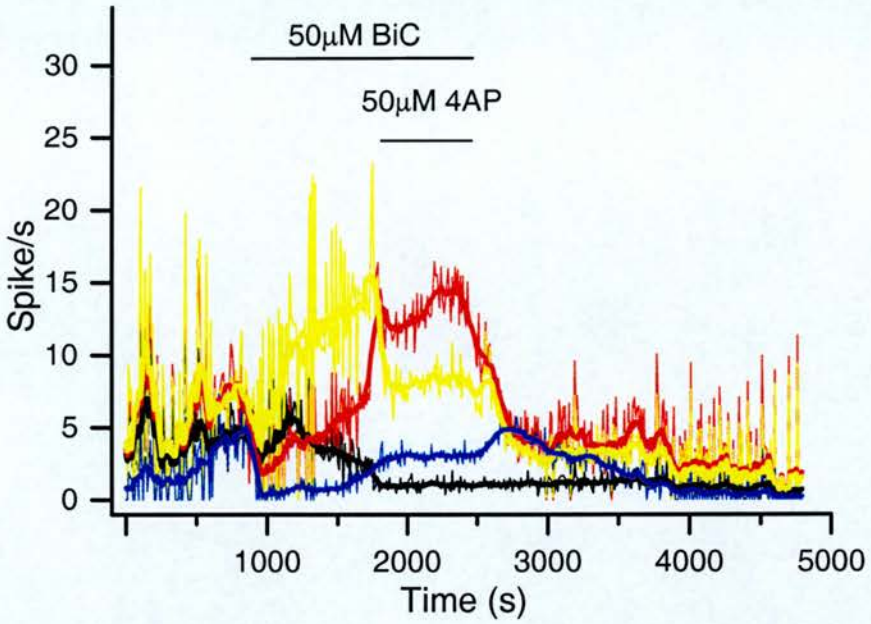

Figure 4.6 – Culture Activity Following Bicuculline and 4AP Treatment. Graph shows the spike frequency over time at four different channels (represented red, yellow, blue and black) of one multi electrode array. Timing of 50μM bicuculline and 50μM 4AP application is indicated.

A

	n	CONTROL	SPIKE FREQUENCY AS % OF CONTROL (AVE ± SE)		
			50μM BIC	50μM Bic + 50μM 4AP	WASH
Expt 1	9	100	87.32 (±17.24)	166.95 (±15.45)*	60.78 (±5.63)*
Expt 2	12	100	166.03 (±31.25)	100.59 (±36.26)	44.33 (±7.64)**
Expt 3	10	100	72.85 (±14.45)	87.65 (±20.66)	41.27 (±7.74)**
All Channels	31	100	113.12 (±15.55)	115.68 (±16.83)	48.12 (±4.33)**

B

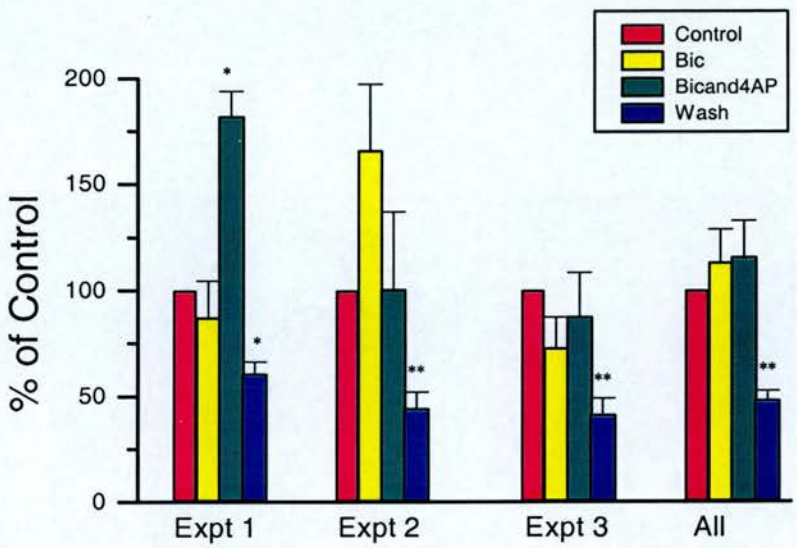

Figure 4.7 Table and Graphs Of Spike Frequency Following Bicuculline Treatment. A. For each experiment (array) n is the number of channels analysed. Table shows average spike frequency, as a percentage of the control, ± standard error in different drug conditions for each array. The data from analysed channels from all arrays is combined to give the data termed 'all'. Stars indicate if frequency is significantly different from control values, as determined by t test. (*p<0.05, **p<0.01). **B.** For each experiment (array), the average spike frequency in the presence of 50μM bicuculline, 50μM bicuculline + 50μM 4AP and during washing is plotted as a percentage of control. 'All' shows the data from combination of all channels. As in A, stars indicate a significant difference from control.

4.2.2 Primary Culture Activity Following APV Treatment

4.2.2.1 Treatment of Cultures with APV

Experiments were performed in a similar way as detailed for bicuculline to measure the effect of APV on cultured cell activity. Briefly, after 10-13 days *in vitro,* cells were perfused with Locke's solution (containing 1M $MgCl_2$). After recording control activity cells were perfused with 50μM APV in Locke's solution and activity measured for approximately 10 minutes. Cells were washed with Locke's solution until activity appeared consistent. The cells were perfused with 1μM TTX to establish baseline noise when neuronal firing is blocked.

4.2.2.2 Culture Activity Following APV Treatment

As with bicuculline, 3 arrays were run and channels chosen from each with low noise levels and measurable activity for analysis. Spikes per second were measured from each channel selected for analysis in the different drug conditions.

Figure 4.8 is a graph showing the spike frequency measured at several channels from one array over the course of an experiment. For all channels shown the application of APV resulted in a decrease in spike frequency that is relieved quickly when the drug was removed. Unlike the bicuculline treatment, APV appears to have a uniform effect at different channels across a culture.

The data was analysed, as described for bicuculline treatment, and figure 4.9 shows this data tabulated and in graph form. APV significantly reduced the spike frequency of the culture on all arrays. Also, for 2 arrays the frequency during the wash period was significantly higher than control. Analysis of data combined from all channels revealed a significant decrease in activity during APV treatment.

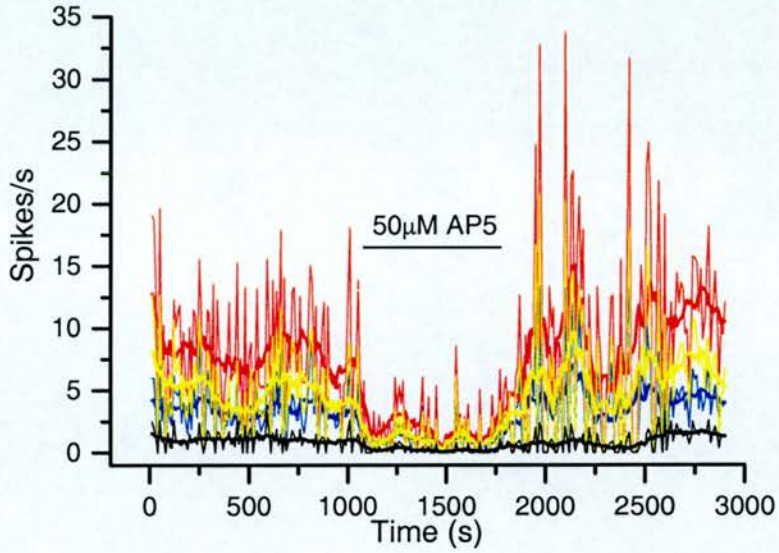

Figure 4.8 - Culture Activity Following Treatment with APV. Graph shows spike frequency over time at four different channels (represented red, yellow, blue and black) of one multi electrode array. Timing of 50μM APV application is indicated.

A

	n	CONTROL	SPIKE FREQUENCY AS % OF CONTROL (AVE ± SE) 50μM APV	WASH
Expt 1	11	100	10.21 (±1.70)**	75.23 (±13.64)
Expt 2	10	100	24.55 (±2.29)**	122.79 (±9.97)*
Expt 3	7	100	64.86(±2.96)**	167.60 (±5.81)*
All Channels	9.3	100	28.99 (±4.34)**	115.31 (±9.50)

B

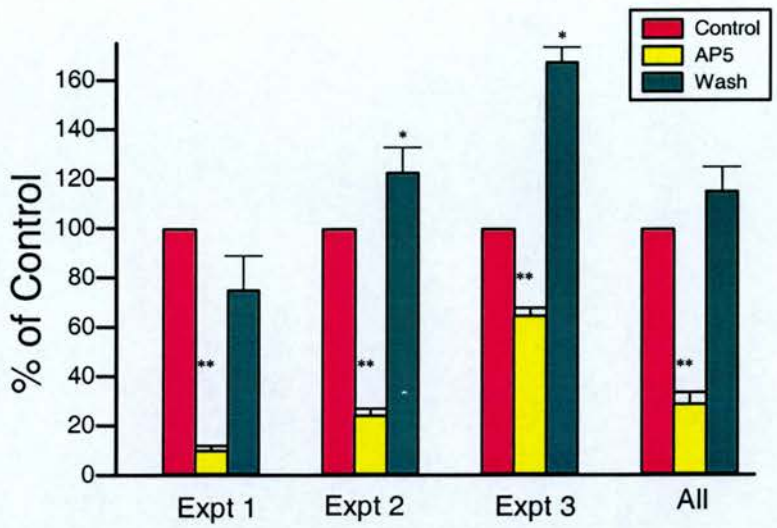

Figure 4.9 Table and Graphs Of Spike Frequency Following APV Treatment. **A**. For each experiment (array) n is the number of channels analysed. Table shows average spike frequency, as a percentage of the control, ± standard error in different drug conditions. The data from analysed channels from all arrays is combined to give the data termed 'all'. Stars indicate if frequency is significantly different from control values, as determined by t test. (*p<0.01, **p<0.01) **B**. For each experiment (array), the average spike frequency in the presence of 50μM APV and during washing is plotted as a percentage of control. 'All' shows the data from combination of all channels. As in A, stars indicate a significant difference from control.

4.3 DISCUSSION

The objective of the experiments detailed in this chapter was to establish a reliable protocol for the *in vitro* stimulation of the NMDA receptor. Gene expression was measured following treatment of primary culture cortical neurons with NMDA, bicuculline and APV. Using MEA recordings, the electrophysiological behaviour of the cultures in basal conditions and in the presence of bicuculline and APV were analysed. This gave insight to the effects of these drugs on cultured neurons and the relationship between neuronal activity and gene expression.

4.3.1 NMDA Treatment of Cultured Neurons

The initial experiment presented in this chapter used NMDA to stimulate cultured neurons. This method involved TTX treatment of the cells, then replacement of the plating media with a Mg^{2+} free solution containing NMDA and glycine. NMDA treatment induced increases in the expression of *cfos, egr1, egr2,* and *nur77.* However, increases in the levels of these genes were also seen in 'unstimulated' cultures in response TTX treatment followed by media change to Mg^{2+} free solution. Due to this the protocol was considered problematic as it was anticipated that there would be difficulty in identifying increases in gene expression caused solely by NMDA receptor activity.

Initially, it was thought that induction of gene expression in 'unstimulated' samples (cells treated with TTX followed by media change to Mg^{2+} free solution with no NMDA and glycine) was a result of the media change in the protocol. Changing the media could cause mechanical or chemical stress to the cells, altering neuronal activity and inducing transcription of immediate early genes. If this were the case it would be unlikely that the induced transcription would be mediated via NMDA receptor activity alone. As such, it would be unsatisfactory to use this protocol to study NMDA dependent gene expression.

The simplest way to alleviate a problem caused by media change would be add NMDA and glycine directly to the cells. However, addition of NMDA and glycine direct to a Mg^{2+} containing plating media does not cause stimulation, as measured by ERK phosphorylation (N. H. Komiyama, personal communication), likely due to the voltage dependent Mg^{2+} block of the receptor. Therefore, a media change was considered essential to the protocol to enable NMDA receptor activation.

However, electrophysiological analysis of cultured cells made apparent another explanation for the gene expression induction in 'unstimulated' cells. MEA analysis revealed a high level of spontaneous firing in cultured cortical neurons, with a large NMDA component in the propagation of activity. By treating cells with TTX, as in the 'unstimulated' cultures, neuronal activity would be abolished. The subsequent replacement of the media with a TTX, and Mg^{2+}, free solution would cause spontaneous activity to resume. Relief of the Mg^{2+} block, combined with the increase of synaptic activity, would result in the rapid induction of NMDA receptor activity and thus mediate receptor regulated gene expression. This could explain the increases in activity dependent gene expression in 'unstimulated' cells. To confirm the induced transcription was NMDA receptor dependent, the experiment could be run in the presence of APV. If it were that gene expression in 'unstimulated' cells was APV sensitive then this protocol could, in fact, be successfully used to study NMDA receptor regulated gene expression.

4.3.2 Bicuculline Treatment of Cultured Neurons

Treating a cortical cell culture with bicuculline, a $GABA_A$ antagonist, should reduce inhibitory neuron activity. As a result, spontaneous activity of glutaminergic neurons will increase, activating synaptic NMDA receptors. It would therefore be expected that treating cultured neuronal cells with bicuculline would rapidly induce *cfos* expression. Published data has shown bicuculline treatment to increase activity of a CRE-mediated expression reporter system based on the *cfos* promoter, effectively induce CREB phosphorylation, sensitive to MK801, and increase cfos

protein levels in rat hippocampal cultures (Hardingham *et al.*, 2001; Hardingham *et al.*, 2002). Furthermore, published MEA analysis has found bicuculline to increase the number of spikes in a given burst of activity in rat hippocampal neurons (Hardingham *et al.*, 2002).

However, the results of bicuculline treatment of cultured cortical neurons, detailed in this chapter, were inconsistent with published data. Bicuculline was found to be ineffective in reliably inducing activity regulated gene expression. On average, no significant increase was observed in *cfos* RNA 1hr after bicuculline treatment. Additionally, MEA analysis found bicuculline caused no significant increase in spike frequency of cultured cortical neurons. The individual MEA channels, from any given array, showed variability in response to the drug, with some channels appearing to have increased activity in the presence of bicuculline. This uneven effect may due to a differential GABAergic input across different areas of a single culture. Overall, bicuculline had no significant effect on the activity of the cultures. This electrophysiology data was consistent with the results of the gene expression analysis. If bicuculline failed to increase spike frequency, it would be unlikely to cause any increase in synaptic NMDA receptor activity that would induce gene expression.

The disparities between published data and the experiments detailed in this chapter may be due to differences in the activity of the cultures used. The published experiments were performed using rat hippocampal cultures, where as the experiments detailed in this chapter used mouse cortical neurons. During the control periods of the MEA recordings, there appeared to be a high level of spontaneous firing. As a result, the effect of bicuculline may be difficult to identify relative to this. It may be that the cultures used in the published experiments had less basal activity than those used for the experiments presented here.

The effectiveness of bicuculline will also depend on the cell content of a culture. If there are few GABAergic cells present, or if few inhibitory neurons synapse with stimulatory ones, then treating cells with a $GABA_A$ inhibitor will have little effect to the overall culture activity. Without increasing synaptic activity, bicuculline will be ineffective at inducting activity regulated gene expression. (Hardingham *et al.*, 2002) estimated GABAergic cells to make up 10% of the total cells in their cultures. It may be that this figure was lower for the cultures stimulated in these experiments. To establish whether this is the case, staining of the cultures, using differential cell markers, could be used. For example, a double immunohistochemical stain of a culture with MAP2B and GAD, would stain all neuronal cells and GABAergic neurons respectively. Counting the stained cells would enable the calculation of the relative levels of inhibitory neurons in the culture.

4.3.3 APV Treatment of Cultured Neurons

Typically NMDA receptor regulation of activity dependent genes has been studied by inducing activity at the receptor. However, NMDA inhibition by APV treatment, included as a control before bicuculline stimulation, revealed a reduction of *cfos* expression in 2 out of 3 experiments. This was further examined

cfos, *egr2* and *nur77* are all activity dependent genes induced by NMDA receptor dependent phenomena (Bading *et al.*, 1995; Inokuchi *et al.*, 1996). Specifically blocking the NMDA receptor with APV resulted in a reduction in the levels of these genes in cultured cortical neurons. This suggests that, in spontaneously active neurons, the NMDA receptor regulates the basal levels of these activity dependent genes. It has been shown that blocking the NMDA receptor in cortical cultures reduces the levels of cfos protein (Murphy *et al.*, 1991). This could be due to reduced levels of *cfos* mRNA, consistent with the data presented in this chapter.

APV application to a culture would directly remove the NMDA receptor component of synaptic transmission. MEA analysis revealed a significant reduction in spike frequency of cultured neurons during APV treatment, indicating a high level of

NMDA receptor activity contributing to neuronal firing in these cultures. It is therefore reasonable to assume that, in spontaneously activity cultures, there is significant activity at the NMDA receptor, and this could regulate the basal levels of particular activity dependent genes.

Due to difficulties in interpreting the data from other stimulation protocols, APV treatment proved the most effective in the analysis of NMDA receptor dependent gene regulation. However, a reliable protocol of stimulating the NMDA receptor would still be highly desirable to study the regulatory pathways downstream of the receptor that contribute to induced transcription. As discussed earlier one method to investigate would be to analyse gene expression following TTX treatment of the cells. Another method, similar in principal to this, would be to study transcription in neuronal cultures in wash periods after APV treatment. If there is a high level of basal activity in the neurons then the expression levels of genes such as *cfos* may be too high to see reproducible induction in response to stimulation. However, by blocking NMDA receptor activity with APV, these levels would be reduced to a new 'basal' level. Removal of the APV would increase spontaneous cell activity, and NMDA receptor stimulation, and thus induce activity dependent gene expression that could then be analysed.

4.4. CONCLUSION

The work in this chapter details analysis of *in vitro* stimulation of the NMDA receptor, by measuring activity dependent gene expression. Due to the time restrictions of this project, the work could not be continued further. However, as discussed, there are several ways in which the protocols could be altered to develop a reliable method of NMDA receptor stimulation in primary cultured neurons. This could then be applied to analyse activity regulated gene expression in wild type and mutant cells.

Bicuculline stimulation caused inconsistent induction of activity dependent genes. MEA analysis revealed that treatment with this drug did not result in the expected increase of spontaneous activity. This could be due to a low level of GABAergic input, combined with the high levels of basal cell activity observed in the cultures by MEA analysis.

Specifically blocking the NMDA receptor, by treatment with APV, reduced the levels of *cfos*, *nur77* and *egr2* in neuronal culture. This suggests that the NMDA receptor plays a critical role in controlling the basal levels of these activity regulated genes. MEA analysis established that APV treatment resulted in a significant reduction in spike frequency.

In the data presented in this chapter, gene expression and MEA analysis were effectively combined to further the understanding of drug effects on primary cultured cortical neurons. Integrating such methods may prove valuable in the development of a reliable *in vitro* stimulation protocol for cultured neurons.

CHAPTER 5

DESIGN AND VALIDATION OF A CUSTOM MICROARRAY

5. DESIGN AND VALIDATION OF A CUSTOM MICROARRAY

As demonstrated in chapter 3, commercial microarrays are a powerful method of analysing gene expression. However, commercial arrays are expensive to use and, once genes of interest have been identified by large scale analysis, there is limited value in screening the levels of tens of thousands of transcripts. An alternative is to use custom designed arrays. Using these many transcripts can be analysed simultaneously, however, the genes of interest represented on the array can be specified. They offer a more cost effective high throughput method of gene expression analysis. However, a disadvantage of using custom arrays is that they have to be thoroughly validated and do not necessarily have the range of controls contained on them that commercial systems offer.

This chapter discusses the design and validation of a custom, oligonucleotide based, microarray. In the context of the work of this project, custom arrays could be used to examine mutant tissue or to study activity regulated gene expression in wildtype, as well as mutant, cells.

5.1 DESIGN AND MANUFACTURE OF A CUSTOM MICROARRAY

5.1.1 Selection of Genes of Interest

The advantage of designing a custom microarray is that the genes of interest can be specified. For our custom array, genes were chosen that have implied involvement in synaptic activity. The genes selected can be organised into different categories; genes encoding proteins of the NRC, genes encoding receptor subunits, activity regulated genes, genes involved in synaptic signalling pathways, genes that may be involved in local translation and genes significantly altered in $PSD95^{-/-}$ and $SynGAP^{+/-}$ mutant tissue (transcripts were chosen from those in the Affymetrix experiments altered greater than 1.3 fold). 240 genes of interest were chosen, 188 of which are represented on the Affymetrix u74Av2 arrays used in chapter 3. Some genes of interest, such as SynGAP isoforms, were not present on the commercial array but were included on the custom chip. Also present on the custom array were oligonucleotides representing positive control genes and negative control genes designed to *Arabodopsis* and mouse cytomegalovirus sequence. Table 5.1 details the 240 genes of interest, 30 positive control and 28 negative control genes represented on the array. All genes of interest appear in the table only once, although some could belong to multiple categories.

5.1.2 Design of Oligonucleotides

Oligonucleotides for all genes of interest were designed in the manner described below. Control probes, positive and negative, were added to the array from stock controls used by the Scottish Centre for Genomic Technology and Informatics (SCGTI), University of Edinburgh. Sequences for the genes to be represented on the custom arrays were obtained from www.ncbi.nlm.nih.gov/nucleotide. For the majority of the genes of interest murine sequence could be obtained however, at the time of design, mouse data was not available for some genes (*cpg1, EphA3, EphA7, Fzd2, gephryn, GiRa2, KA1, mGluR5, neuritin, NT4, SynGAP, trkA* and *yotiao*), in these cases, rat sequence was used.

Genes from NRC Complex		Translation	Genes from Affymetrix Experiment	
Scaffolding	*Modulators*	4E-BP2	5HT3 Receptor 4	Protease28 subunit, beta
AKAP150	H-ras	aCaMKII	Adrenergic receptor, beta 1	PTTG
Homer 1a	NF1	CPEB	AIF	RAB34
Homer 1b + 1c	RalA	CPSF100	APC	Rap1
Homer 2a + 2b	sacrospan	CPSF160	Atonal homolog 2	Rgs2
Homer 3	synGAP-a	CREB	Bag1	RyR3
NSF	synGAP-b	eEF1A	Bcl2	Serine palmitoyltransferase
PSD 93	synGAP all forms	eEF2	Bcl-associated death promoter	signal transducing adaptor 2
PSD 95		eIF4E	CACYBP	SOS2
Sap 97	*Cytoskeletal*	eIF4GII	CD53	Transformation related 53
Sap102	alpha actinin 2	FMR1	Cfos	X-box binding protein 1
Shank	beta Catenin	FMR2	cyln2	
Yotiao	Cortactin	Frap1	DUSP 6	*ESTS*
	Desmoglein	gephyrin	Egr1	AI836641
Signalling	Dynamin	GlyR2	egr 2	AW125272
PKC beta	L1	map-2	eIF4A	AI843358
PKC epsilon	Hsp-70	MNK1	Erythroid Diff Factor	AI852001
PKC gamma	Myosin	MNK2	Est2 repressor factor	AI848952
CaMK II beta	N-Cadherin	NAT1/DAP-5	FosB	
PYK2	spectrin	p38dMAPK	GADD45B	**Glutamate Receptors**
Src	pp120cas	PABp1	glycogenin 1	NR1
c-raf1		PABp2	growth factor-inducible IEG	NR2A
ERK 1	*Others*	PERK	IP3 receptor 3	NR2B
ERK 2	Bassoon	PI3Kp85a	Insulin-like GF2	NR2C
MKK4	ZO-1	PP1	interferon responsive15 kDa	NR2D
MEK 1	Phosphofructokinase	PP2A	IP3 receptor 1	NR3A
MEK 2	APPL Adaptor Protein	Quaking	JunB	NR3B and NR4
Arg 3.1	Alpha Internexin	RC3	K+ channel, subfamily H, 1	GluR1
Calmodulin	Tubulin A4	RL17	K+ channel, subfamily K, 1	GluR2
Citron		S6K	K+ channel Kv4.2	GluR3
cPLA2	*Phosphatases*	Staufen 1	Kinesin family member 3a	GluR4
nNOS	PP1	Stk13	MEKK4b	GluR5
P13 Kinase	PP2A	Tubulin B4	MKK2	GluR6
PLC gamma	PP5	histone deacetylase 3	neoplastic progression 3	GluR7
		GlRa2	N-glycan α 2,8-sialyltransferase	KA1
			Nip3	KA2
			nur 77	mGluR1
			period homolog	mGluR5
			Platelet derived growth factor	

CONTINUED OVER PAGE

Signalling Molecules		ADG	Positive Controls	Negative Controls
APC	PKA C-alpha + beta	CBP	Alpha tubulin	1;4 alpha glucanotransferase
C-src tyrosine kinase	PLC b1	CHOP 10	BDNF	alkaline neutral invertase
EphA1	PLC b2	Cjun	beta-actin	alpha glucosidase like protein
EphA2	PLC b3	CNS1	B-raf	beta amylase
EphA3	PLC b4	COMT	calcium activated neutral protease large subunit	branching enzyme
EphA4	PKA RI-alpha	Cox 2	cell division cycle 42 homolog	fructose bisphosphatase like protein
EphA5	PKA RI-beta	cpg 1	collagen type V alpha 3 chain	Glucose-1-phosphate adenyltransferase
EphA6	PKA RII-beta	CREM	connective tissue growth factor-like protein precursor	glucose-6-phosphate phosphate translocator
EphA7	Wnt 4	DUSP10	cyclin E2	glucosidase alpha subunit
EphA8	Wnt 7(a and b)	GADD45G	Gapdh	phosphoglucomutase (plastidic)
EphB1	Wnt 7b	GAP 43	Histon H2A	soluble starch synthase
EphB2		GnrH receptor	HPRT	sucrose synthase
EphB3	**Neurotrophins**	GR33	integrin alpha6	*vMC003*
EphB4	TrkA	Hsp 27	JNK1	*vMC009*
EphB6	TrkB	Ier5	matrix metalloproteinase 14	*vMC014*
FRP-1	TrkC	Narp	myeloid leukemia factor 1	*vMC015*
FRP-2	BDNF	Pim1	PDHA1	*vMC017*
FRP-3	NGF	Pim2	phospholipaseA2	*vMC057*
FRP-4	NT 3	Pip 92	proalpha1(II) collagen	*vMC059*
Fzd1	NT 4	Presenilin-1	proalpha2(I) collagen	*vMC101*
Fzd2/Fzd10		RheB	procollagen, IV α 3	*vMC109*
Fzd3		Somatostatin	putative lysophosphatidic acid acyltransferase	*vMC118*
Fzd4		Syndecan	Ribosomal L15	*vMC130*
Fzd5		tPA	Ribosomal L32	*vMC145*
Fzd6			Ribosomal L32-3A	*vMC146*
Fzd7			Thioredoxin reductase 1	*vMC152*
Fzd8			Transcriptional activator (E2F3)	*vMC155*
Fzd9			Transforming growth factor, beta 2	*vMC159*
MEK4			tumor necrosis factor	
MKK2			Ubiquitin	

Table 5.1 - Genes Represented on Custom Microarray. Table details the genes included on the custom microarray, arranged into categories. All oligonucleotides for genes of interest were designed using Oligo 6. Positive and negative control probes were taken from stock probes at the SCGTI. Oligonucleotides for genes of interest and positive controls were designed to murine sequence and, if that were not available, rat sequence. Negative controls to named genes were designed to *Arabidopsis* sequence and, those in italics, mouse cytomegalovirus sequence.

55 base pair oligonucleotides were designed using Oligo6 software. The oligonucleotides were designed with 3′ bias, ideally around 500 base pairs from the terminal polyA tail if this sequence information were available. For genes of high homology, or to distinguish splice variants, similar sequences were compared pairwise using BLAST (www.ncbi.nlm.nih.gov/BLAST) to identify areas of diversity and oligonucleotides designed to the most 3′ of these areas.

The Oligo6 software selects several oligonucleotides to a specified area of input sequence, within set melting temperature parameters. From these candidate oligonucleotides the most suitable probe was picked. Oligonucleotides were chosen to have a melting temperature within a 10°C range of each other (approximately 90°C to 100°C) so optimal hybridisation temperatures would be similar. To minimise the secondary structure of selected oligonucleotides, potential hairpins were analysed and only those with Δ loop G scores greater than –3 were considered suitable. Once chosen, the 55mers were checked for specificity to the target genes using nBLAST. Any oligonucleotide with more than 15 contiguous base pairs common to a mouse gene other than the target was discarded and redesigned.

Tables 5.2 - 5.3 and figures 5.1 – 5.2 show the design stages of the oligonucleotide designed for DUSP6. The mRNA sequence (NCBI accession number NM_026260) was put into Oligo6 and suitable 55mers were searched for within 1000 bases of the 3′ end of the sequence. Table 5.2 shows the choice of oligonucleotides returned by Oligo6. The selected oligonucleotide was number 4, which had a melting temperature (94.6°C) that falls within the 10°C range of the other oligonucleotides and started 512 bases from the predicted poly A tail in the sequence. Table 5.3 details the loop ΔG scores for the chosen oligonucleotide. The smallest score is 0.2kcal/mol and thus the secondary structure of the oligonucleotide should not be problematic. Figure 5.1 shows where the selected oligonucleotide is within the DUSP6 mRNA sequence. It shows the DUSP6 sequence with the predicted poly A site and oligonucleotide highlighted.

	POSITION (bp from start of sequence)	T_M (°C)
1	2259	94.2
2	2260	95.0
3	2261	94.5
4	**2262**	**94.6**
5	2263	93.7
6	2265	93.3
7	2266	95.1
8	2267	95.4
9	2268	96.7
10	2269	98.0
11	2270	98.4
12	2271	98.0
13	2273	96.7
14	2273	95.3
15	2274	94.5
16	2275	94.3

Table 5.2 – 55mers Suggested By Oligo6 For DUSP6. Table details the oligonucleotides suggested by Oligo6 for DUSP6 sequence. 16 55mers were suggested and their distance from the start of the sequence and predicted melting temperatures (°C) are detailed. The oligonucleotide that was chosen is highlighted.

	LOOP ΔG (kcal/mol)	DUPLEX LENGTH (nucleotides)	LOOP SIZE (nucleotides)
1	0.2	3	3
2	0.5	3	6
3	0.8	3	9
4	1.1	3	12
5	1.1	3	11
6	1.8	4	26
7	2.3	3	18
8	2.4	3	15
9	2.9	4	26
10	3.3	3	26
11	3.9	3	23
12	4.1	3	33
13	4.2	3	28
14	4.4	3	25
15	4.4	3	26
16	5.2	3	28
17	6.0	3	26

Table 5.3 – Loop ΔG Scores For DUSP6 Oligonucleotide. Table details the loop ΔG scores for hairpin structures in the chosen DUSP6 oligonucleotide. The length of the duplex and size of loop (both measured by nucleotides) are also shown.

NM_026268 Mus musculus dual specificity phosphatase 6 (Dusp6), mRNA
Length 2793, Poly A signal: 2774 – 2779

DUSP Oligonucleotide - GGGTATATTTGCAGCATGCTTGACCTTGATGTACCAATTCTGACGGCATTTTCGT
(2262 – 2316)

GATCCATTGAGGAGCTGCCTCGCACAGGGGGTGTGCTCTCGCGGAGTCCTAGGGACTGTGAGCAAACCCA
GTCTTGAATAATCCGGCGAGAAACACCGGGTTGGATCCGAGGTGCAGCCTCAGAGGGAAGGATTAAGAGC
CGCTAGACTTTTTTTCTTTTCCCTTTTTCTCCTCTCAGTGGCACGGAGTCCGAATTAATTGGATTTCATT
CACTGGGTAGGAACAAAACTGGGCACCTTCATTCAGAGAGAGAGATTCATTGACTCGGAGAGTGATCTGG
TGCAGAGGGACCACCGACTTGACTTCTGTGTCGCTTTCCCTAACCGCTAGCCTCGGCTTGGGAAAGGCGA
GGCGGAATCAAACCCCGCTCCGAGAGCGGGAGCTTCGCGCAGCGTGCTCGGCCTATGCCTGCCTCGAGGG
GCGTCTGCTAGGCACCCCGCCTTCTCCTGCAGCTCGACCCCCATGATAGATACGCTCAGACCCGTGCCCT
TCGCGTCGGAAATGGCGATCTGCAAGACGGTGTCGTGGCTCAACGAGCAGCTGGAGCTGGGCAACGAACG
GCTTCTGCTGATGGACTGCCGACCACAGGAGCTGTACGAGTCGTCACACATCGAATCTGCCATTAATGTG
GCCATCCCCGGCATCATGCTGCGGCGTCTGCAGAAGGGCAACCTGCCCGTGCGTGCGCTCTTCACGCGCT
GCGAGGACCGGGACCGCTTTACCAGGCGCTGCGGCACCGACACCGTGGTGCTGTACGACGAGAATAGCAG
CGACTGGAATGAGAACACTGGTGGAGAGTCGGTCCTCGGGCTGCTGCTCAAGAAACTCAAAGACGAGGGC
TGCCGGGCGTTCTACCTGGAAGGTGGCTTCAGTAAGTTCCAGGCCGAGTTCGCCCTGCACTGCGAGACCA
ATCTAGACGGCTCGTGCAGCAGCAGTTCCCCGCCTTTGCCAGTGCTGGGGCTCGGGGGCCTGCGGATCAG
CTCGGACTCTTCCTCGGACATTGAGTCTGACCTTGACCGAGACCCCAATAGTGCAACGGACTCTGATGGC
AGCCCGCTGTCCAACAGCCAGCCTTCCTTCCCGGTGGAGATTTTGCCCTTCCTTTACCTGGGCTGTGCCA
AGGACTCGACCAACTTGGACGTGTTGGAAGAGTTTGGCATCAAGTACATCTTGAATGTCACCCCCAATTT
GCCCAATCTGTTTGAGAATGCGGGCGAGTTCAAATACAAGCAAATTCCTATCTCGGATCACTGGAGCCAA
AACCTGTCCCAGTTTTTCCCTGAGGCCATTTCTTTCATAGATGAAGCCCGAGGCAAAAACTGTGGTGTCC
TGGTGCATTGCTTGGCAGGTATCAGCCGCTCTGTCACCGTGACAGTGGCGTACCTCATGCAGAAGCTCAA
CCTGTCCATGAACGATGCTTACGACATTGTTAAGATGAAGAAGTCCAACATCTCCCCCAACTTCAACTTC
ATGGGCCAGCTGCTTGACTTCGAAAGGACCCTGGGACTGAGCAGCCCTTGTGACAACCGTGTCCCCACTC
CGCAGCTGTACTTCACCACGCCCTCCAACCAGAACGTCTACCAGGTGGACTCCCTGCAGTCTACGTGAAA
GGCACCCACCTCTCCTAGCCGGGAGTTGTCCCCATTCCTTCAGTTCCTCTTGAGCAGCATCGACCAGGCT
GCTTTCTTTCTGTGTGTGGCCCCGGGTGTCAAAAGTGTCACCAGCTGTCTGTGTTAGACAAGGTTGCCAA
GTGCAAAATTGGTTATTACGGAGGGAGAGATTTGCTCCATTCATTGTTTTTTTGGAAGGACAGGACATGC
TGTCTCTAGATCCAGCAATAGGTTTGCTTCTGTACCCCAGCCTACCCAAGCAGGGACTGGACATCCATCC
AGATAGAGGGTAGCATAGGAATAGGGACAGGAGCATCTGTTCTTTAAGGCCTTGTATGGCTGTTTCCTGT
TGCATCTGGAACTAACTATATATATTGTCTTCAGTGAAGACTGATTCAACTTTGGGTATAGTGGAGCCAA
AGAGATTTTTAGCTCTGTATTTGCGGTATCGGTTTAGAAGACAAAAAAAATTAAAACCTGATACTTTTAT
CTGATTATTGTAAATATTTGATCTTCAATCACTTGACAGTGTTTGTTTGGCTTGTATTTGTTTTTTATCT
TTGGGCTTAAAAGAGATCCAAAGAGAGAAAGAGCAGTATGCCACTTCTTAGAACAAAAGTATAAGGAAAA
AAATGTTCTTTTTAATCCAAAGGGTATATTTGCAGCATGCTTGACCTTGATGTACCAATTCTGACGGCAT
TTTCGTGGATATTATTATCACTAAGACTTTGTTATGATGAGGTCTTCAGTCTCTTTCATATATCTTCCTT
GTAACTTTTTTTTTCCTCTTAATGTAGTTTTGACTCTGCCTTACCTTTGTAAATATTTGGCTTACAGTGT
CTCAAGGGGTATTTTGGAAAGACACCAAAATTGTGGGTTCACTTTTTTTTTTTTTTTAAATAACTTCAGC
TGTGCTAAACAGCATATTACCTCTGTACAAAATTCTTCAGGGAGTGTCACCTCAAATGCAATACTTTGGG
TTGGTTTCTTTCCTTTTAAAAAAAAAATACGAAACTGGAAGTGTGTGTATGTGTGCGAGTATGAGCGCCC
ATTTGGTGGATGCAACAGGTTGAGAGGAAGGGAGAATTAACTTGCTCCATGATGTTCGTGGTGTAAAGTT
TTGAGCTGGAATTTATTATAAGAATGTAAAACCTTAAATTATTAATAAATAACTATTTTGGCT

Figure 5.1 - DUSP6 Gene Sequence and Oligonucleotide. Figure shows the murine sequence for DUSP6 mRNA, accession number NM_026268. The location of the designed 55mer is highlighted in yellow (bases 2262 – 2316) and the predicted polyA signal is highlighted in blue (2774 – 2779).

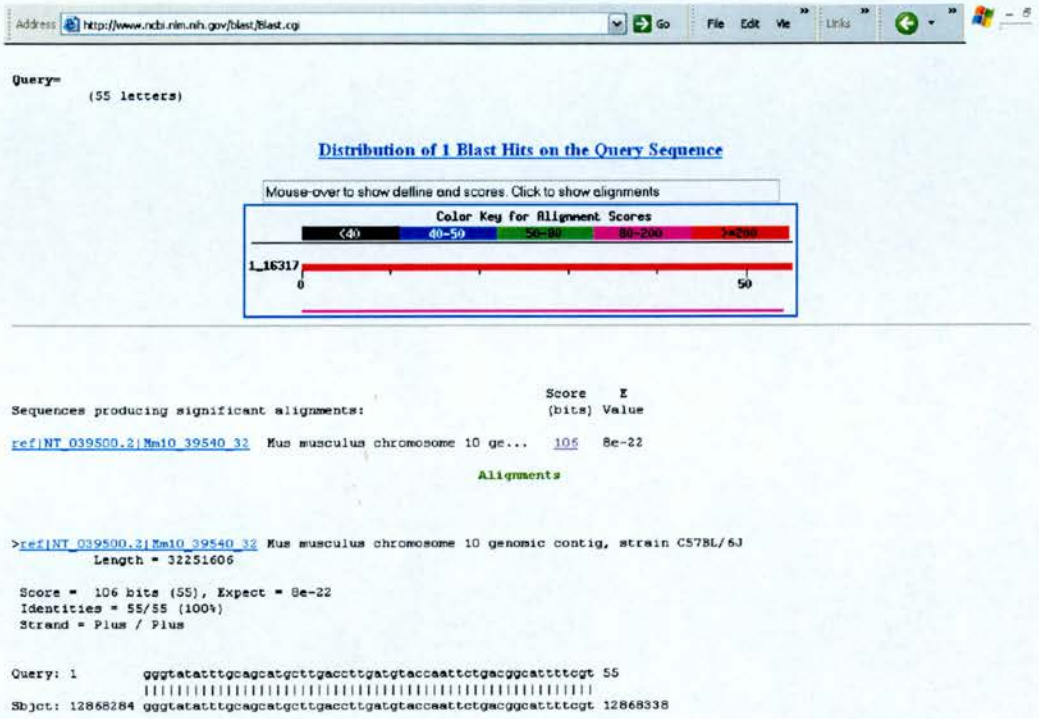

Figure 5.2 – DUSP6 Oligonucleotide mBLAST result. Figure shows the results of mBLAST search of the DUSP6 55mer against the entire mouse genome. Only one match was found, on chromosome 10, where the DUSP6 gene is located.

To ensure the selected oligonucleotide was specific to DUSP6 alone, the 55mer was analysed using mBLAST. This program searches for sequence matches across the entire mouse genome. Analysis of the oligonucleotide found the 55mer matched only one sequence in the mouse genome, on chromosome 10 where the DUSP6 gene is located (see Figure 5.2). It is apparent that the chosen oligonucleotide for DUSP6 should be selective to this gene and not hybridise to other RNAs.

All oligonucleotides for genes of interest were designed in this way. The oligonucleotide sequences, along with melting temperatures and position in input sequence, are detailed in Appendix 3. The oligonucleotides were manufactured, without modification, by Illumina. Liquid handling and array spotting of these oligonucleotides were performed at the SCGTI, University of Edinburgh according to their standard protocols.

5.1.3 Layout and Printing of Microarray

Figure 5.3 shows a simplified diagram of the chip layout design. The printed areas of the arrays were divided into 4, each area containing 3 panels of identical oligonucleotides, thus each gene is represented on the chip in triplicate. The oligonucleotides were placed randomly across the arrays, although housekeeping controls were placed in the top left corners of each panel to act as guide lights to orientate the arrays upon scanning. Also, buffer spots (150mM phosphate buffer + 0.01% SDS) were spotted in the first row of each repeated panel. These can be used to identify any high levels of background, nonspecific binding. Appendix 4 details the layout of the genes of interest, control genes and buffer spots on the array.

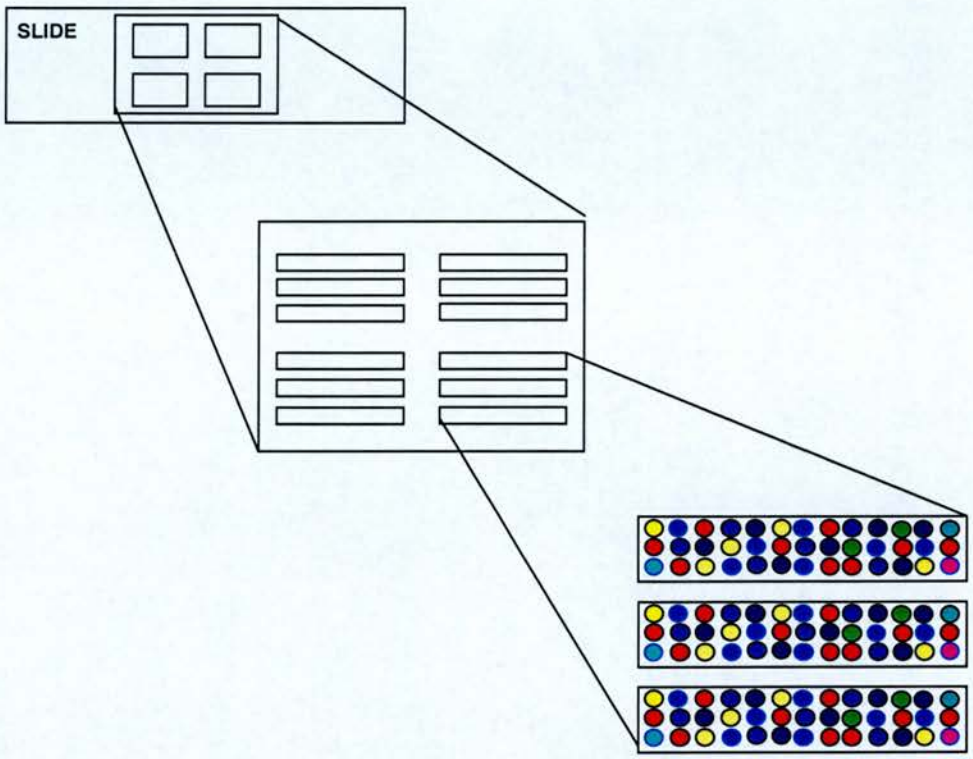

Figure 5.3 – Diagram of Chip Layout. The diagram shows a simplified version of the chip layout. The array is divided into 4 areas, each of 3 identical panels of oligonucleotides, thus each gene is represented on the chip in triplicate. The probes were randomised apart from housekeeping controls (in yellow) which were placed in the corners of the arrays to act as guide lights to orientate the arrays upon scanning.

The oligonucleotides were spotted onto Corning GAPII slides at 50μM using a BioRobotics MG2 machine. Initial quality control of the arrays was done using SpotCheck (Genetix), a kit of random 9mers that checks the presence and quality of spots on the slides. All array printing and SpotCheck quality control of the slides was done by Marie Craigon at the SCGTI, University of Edinburgh.

Figure 5.4 shows the results of hybridising SpotCheck to arrays from two batches of spotted slides. Hybridisation was successful in both cases and the basic layout of the arrays can be clearly seen. However, examination of the slide shown in figure 5.4A shows a lack of several spots where oligonucleotides should be printed, most apparent in the top left quadrant. Also, the intensity of SpotCheck binding at different spots would be expected to be more uniform. These problems were identified to be due to errors with the machine when printing the arrays. Figure 5.4B shows the SpotCheck hybridisation to a slide from a second batch of printed arrays. In this case, there appears to be smaller variation in the intensity of binding and only 1 spot (in the bottom right quadrant) appears to be missing in each panel replicate.

5.2 VALIDATION OF CUSTOM MICROARRAY

To further validate the spotted arrays, a hybridisation experiment was performed using RNA samples with profiles of transcription levels. Wildtype forebrain RNA (as used in the Affymetrix wildtype and PSD95$^{-/-}$ forebrain experiment) and a control murine RNA, extracted from C127 mammary tumour cells, in standard use at the SCGTI, were hybridised to the arrays.

5.2.1 Hybridisation of the Custom Array

The RNAs were reverse transcribed with Cy3 labelled UTP and hybridised overnight at 55°C, then washed and immediately scanned. The slides used for this validation were those from the first run of printing, which had several spots missing.

A

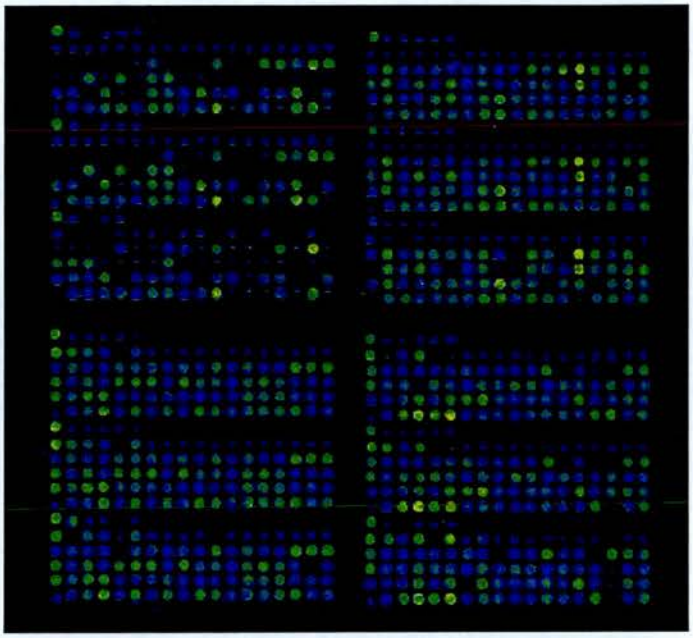

B

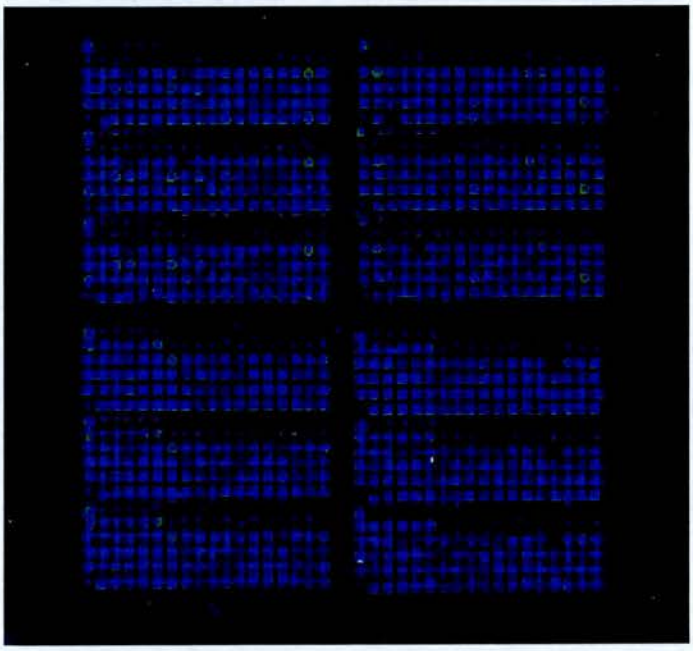

Figure 5.4 – Quality Control Hybridisation of Custom Arrays. A is an image of hybridisation of SpotCheck (random 9mers) to one of the arrays from the first batch of printing, with certain spots seen to be missing. **B** is an image of SpotCheck hybridisation to an array from the second round of printing.

Figure 5.5 shows the scanned images of the arrays with forebrain (Figure 5.5A) and C127 (Figure 5.5B) samples. Hybridisation appears successful, with the distinct spots from each oligonucleotide clearly identifiable. The C127 hybridisation appears to have a smear down the right side of the array. This could be due to areas under the coverslip drying out during the hybridisation.

5.2.2 Analysis of Hybridisation

The hybridisation using wild type forebrain RNA as starting material was more closely examined to identify whether groups of genes represented on the array behaved as expected. Figure 5.6 is a box and whiskers plot of the different spot types on the array (genes of interest, negative controls, positive controls and buffer spots). The plot shows the range of median cy3 intensity at the probes for each of these types of spot.

In general, the RNA hybridised to the arrays as expected. The threshold of expression was calculated to be 1841, using the average expression level at the buffer spots plus 2 standard deviations of the buffer values. The genes of interest showed a wide range of expression, 88% of them greater than this threshold of expression. The negative controls were detected over a narrow range below the threshold of expression. In contrast, the positive controls were all expressed at a range of levels above the threshold of expression. Hybridisation at the buffer spots was similar to that of the negative controls. One outlying buffer spot was found expressed above the threshold of expression, this could be due to contamination at this spot. The data suggests successful hybridisation of labelled cDNA to the chips, with a wide range of expression levels measured.

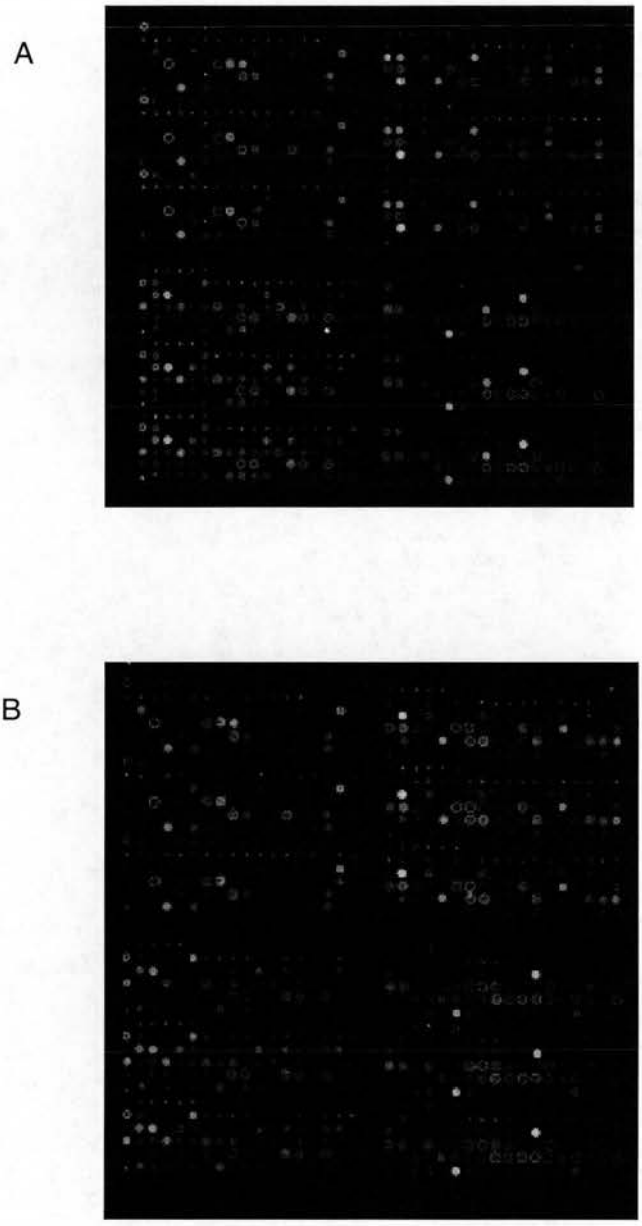

Figure 5.5 – Hybridisation of Control RNAs to Custom Arrays. **A** is an image of hybrisdation of labelled forebrain RNA to custom array. **B** is an image of hybridisation of labelled C127 RNA to custom array.

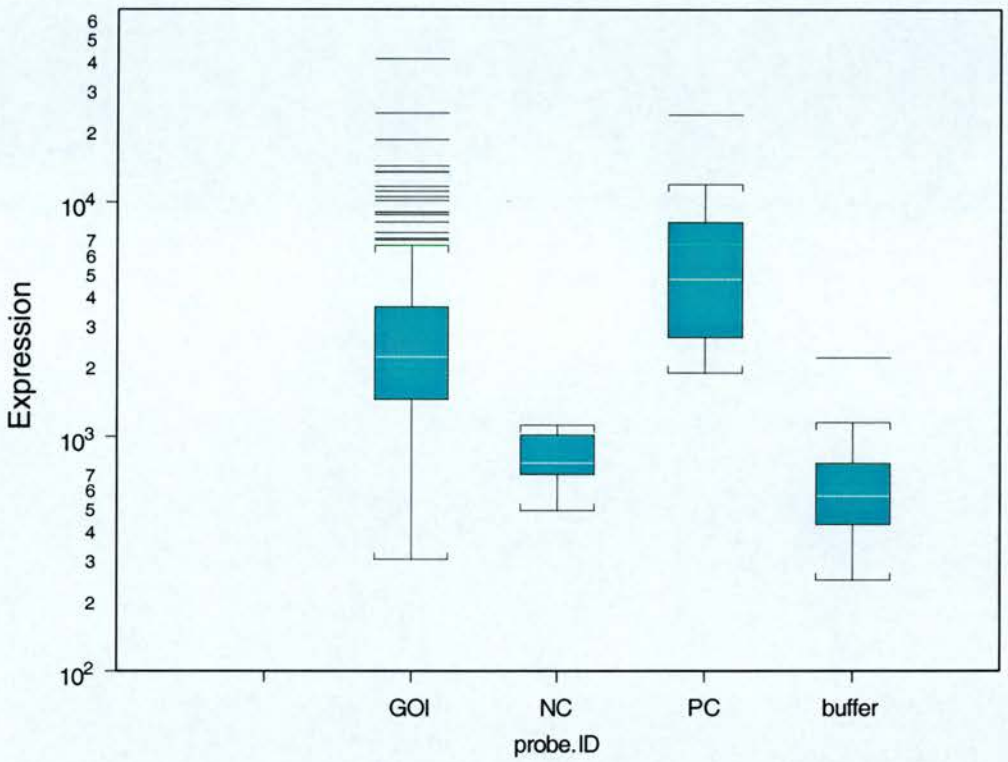

Figure 5.6 – Box and Whiskers Plot of Array Validation Data. The plot illustrates to range of expression, median and 1st and 3rd quartile values for GOI (genes of interest), NC (negative control) and PC (positive control) transcripts. The level of expression detected at the buffer spots is also shown.

5.3 COMPARISON OF CUSTOM AND COMMERCIAL MICROARRAYS

In order to validate their performance, the custom arrays were hybridised with labelled samples from wild type and PSD95$^{-/-}$ forebrain, as used for the Affymetrix experiment. Alan Ross at the SCGTI, University of Edinburgh carried out the hybridisation and initial data analysis for this experiment.

5.3.1 Hybridisation of the Custom Array

The RNA samples used for the hybridisation were aliquots of the PSD95$^{-/-}$ and wildtype forebrain samples detailed in table 3.1 in chapter 3. The RNA samples had been stored at –80°C during the time between conducting the Affymetrix and custom array experiments. It was confirmed that the RNA had not degraded during this time using the Agilent Bioanalyser. The 3 wildtype and 3 PSD95$^{-/-}$ samples were each labelled and hybridised to individual arrays from the second batch of slides that were printed.

The RNA was reverse transcribed to biotin-labelled cDNA using the QIAGEN LabelStar kit. The cDNA, in a hybridisation cocktail, was hybridised to the arrays overnight at 42°C. After washing, QIAGEN RLS (resonance light scattering) particles were bound to the arrays. These nano-sized gold particles are coated in biotin antibodies and, when exposed to a white light source, emit energy, the intensity of which can be measured as the level of particle binding to the labelled cDNAs. This protocol was adopted since it is highly sensitive and requires less starting material (4.54µg RNA) as compared to the standard hybridisation of custom chip (25µg RNA).

Figure 5.7 is an image of a scanned array hybridised with labelled wildtype forebrain sample. The more intense the light at a particular spot is, the more highly expressed the transcript is.

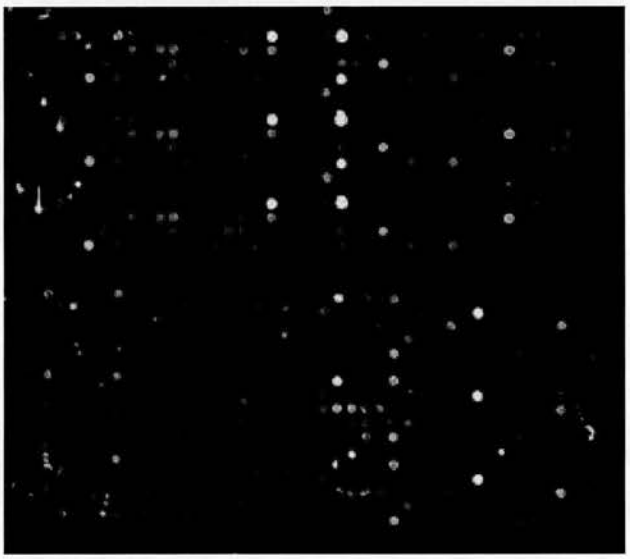

Figure 5.7 – Image of Array Following RLS Hybridisation. Picture shows the scanned image of an array hybridised, using the RLS protocol, with labelled wild type forebrain RNA. The higher the intensity of light, the more highly expressed the transcript represented by that particular probe is.

5.3.2 Analysis of Hybridisation

The data from the arrays was scaled by a factor calculated from the average 75th percentile expression value from all arrays divided by the 75th percentile expression value for each particular array. The mean expression values for each transcript in wild type and mutant samples were calculated from the scaled median value of the transcript on each array. Figure 5.8 shows a box and whisker plots showing the levels of the genes of interest as well as negative and positive controls averaged for wild type (Figure 5.8A) and mutant (Figure 5.8B) arrays. The plots of wild type and PSD95$^{-/-}$ data look similar. However, a notable feature of this data is that the range of expression of the negative controls overlaps with the positive controls and the genes of interest. This suggests that these probes are not performing as expected.

The threshold of expression was determined for each array using the 80th percentile expression level of the negative controls on the array. Table 5.4 shows the number of genes of interest determined to be present and absent on each array and the average across all arrays. On average 32.7% of the genes of interest were found present in the forebrain samples. This is lower than the average percentage of transcripts detected present on the Affymetrix chips (46.75%) and lower than the number of transcripts determined present by the previous hybridisation of wild type forebrain samples to the custom array (88%). Thus the results from the hybridisation are not consistent with previous experiments and may indicate a problem with the hybridisations.

	WILDTYPE ARRAYS			PSD95$^{-/-}$ ARRAYS			ALL ARRAYS
	1	2	3	1	2	3	AVE
ABSENT	172	170	168	129	152	172	160.17
PRESENT	68	66	64	111	90	68	78.50
% Present	28.8	27.9	27.1	46.7	37.9	28.8	32.7

Table 5.4 – Numbers of Detected Transcripts on Custom Arrays by RLS Hybridisation. Table shows the number of genes of interest detected absent and present, along with the percentage of transcripts present out of total on chip, for each custom array. The average values from all arrays are also shown.

5.3.3 Comparison of Affymetrix and Custom Array Results

In order to compare the custom array results with that of the Affymetrix data, genes significantly altered in wild type and mutant samples by custom array were identified. The 3 scaled expression values for each transcript on each array were used to compare expression in wild type and PSD95$^{-/-}$ tissue by t Test.

5.3.3.1 Genes Found Significantly Altered by Custom Array

As with the Affymetrix arrays, to be considered significantly altered in mutant tissue, a gene had to have a differential expression greater than 1.5 fold with a p value less than 0.05. Of the 240 genes of interest on the custom array, 108 transcripts were differentially expressed in wild type and mutant tissue, greater than 1.5 fold. However, of these 108 transcripts only 1, considered present in the samples, was altered with a p value < 0.05. This gene was *fzd6*.

Table 5.5 shows custom and commercial array data for *fzd6* expression in PSD95$^{-/-}$ and wildtype forebrain. *Fzd6* was considered absent by the Affymetrix array, but was classed as present by custom array analysis. Although the expression levels cannot be directly compared across the systems, *fzd6* was found highly expressed by the custom array. Indeed, *fzd6* was the second most highly expressed of all transcripts in the wild type samples according to the custom arrays.

	PROBE ID	WILD TYPE AVE	MUTANT AVE	WT/MUTANT RATIO	WT/MUTANT RATIO	P VALUE
Custom Array Data						
Fzd6	34607	42719.1	27230.4	1.6	0.63	0.001
Affymetrix Array Data						
Fzd6	101142_at	2.43 (absent)	7.13 (absent)	2.93	0.34	0.141

Table 5.5 – Expression of Fzd6 in Wild Type and PSD95$^{-/-}$ Forebrain. Table shows data from custom and Affymetrix arrays. The table details the expression levels of fzd6 in wild type and PSD95$^{-/-}$ tissue, the ratio of these expressions and the p value of these differences as measured by t Test.

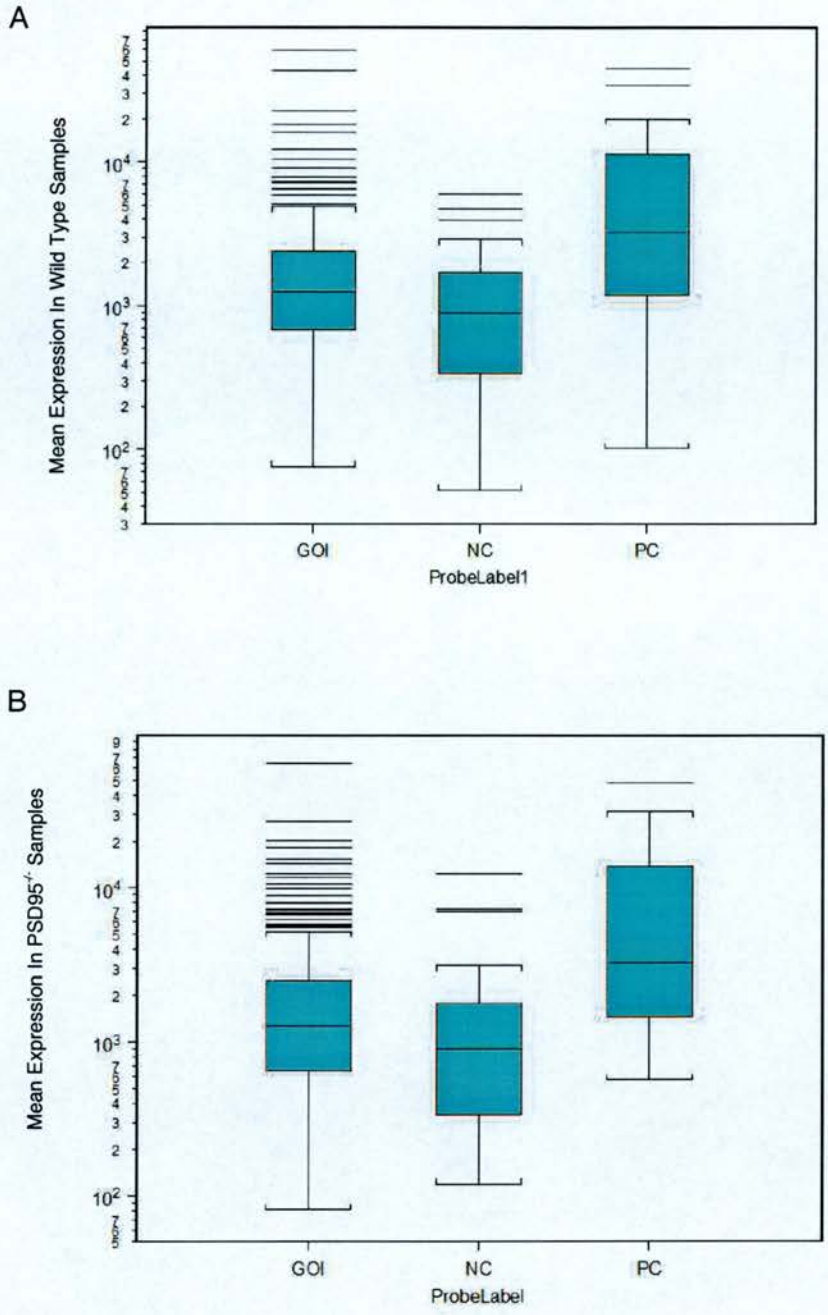

Figure 5.8 – Box and Whiskers Plots of RLS Data. **A** illustrates the range of mean expressions for GOI (genes of interest), NC (negative control) and PC (positive control) transcripts on the arrays hybridised with wild type forebrain RNA. **B** illustrates the same as A, but using data from the arrays hybridised with PSD95$^{-/-}$ forebrain RNA.

5.3.3.2 Genes Found Significantly Altered by Affymetrix Array

Table 5.6 compares the data from custom and commercial arrays for those transcripts, present on the custom array, that were found significantly altered in PSD95$^{-/-}$ forebrain by Affymetrix chips. Of the 9 transcripts present on the custom array that were found significantly altered by Affymetrix arrays, only 3 showed similar changes in expression in mutant tissue. None of these were statistically significant. An obvious difference in the data is that no significant alteration in the level of the *PSD95* transcript is found by the custom array.

5.3.3.3 Comparison of Custom and Affymetrix Array Performance

Table 5.7 compares the overall performance of custom and Affymetrix arrays. The custom and commercial arrays found 1.66% (4 out of 240 transcripts) and 5.15% (644 out of 12496 transcripts), respectively, of the genes of interest differentially expressed in wild type and mutant tissues with a p value less than 0.05. The custom array found 45% of the genes to be altered in mutant tissue greater than 1.5 fold, where as only 1.9% of the genes on the Affymetrix array showed this level of change.

The custom arrays found alterations, greater than 1.5 fold, in the expression of many more genes than the Affymetrix array did. This could be expected since the genes of interest on the custom array were chosen due to their involvement in postsynaptic mechanisms. However, of the 108 genes altered greater than 1.5 fold, only 1 transcript, expressed above threshold, was of statistical significance. The commercial array found 14 significantly altered transcripts that were called as present in either wildtype, mutant or both tissues.

NAME	CUSTOM ARRAY DATA				AFFYMETRIX DATA	
	WILD TYPE MEAN	MUTANT MEAN	WT/MUTANT RATIO	TTEST	RATIO	TTEST
Lower in Mutant						
PSD 95	1858.7	1730.7	1.07	0.20	3.4	0.004
nur77	1410.4	1591.8	0.89	0.27	2.39	0.001
cfos	1100.6	2232.6	0.49	0.99	2.22	0.002
egr2	316.0	1041.5	0.30	0.35	2.19	0.014
Per1	**907.5**	**397.3**	**2.28**	**0.53**	**2.16**	**0.024**
junB	4059.3	5778.7	0.70	0.75	1.97	0.019
cyln2	**3739.4**	**1959.7**	**1.91**	**0.15**	**1.97**	**0.017**
GADD45B	**656.9**	**369.3**	**1.78**	**0.26**	**1.75**	**0**
Higher in Mutant						
Serine palmitoyltransferase	774.6	555.0	0.72	0.37	1.57	0.014

Table 5.6 – Comparison of Affymetrix Results with Custom Array Data. Table shows the levels of genes, found significantly altered in PSD95$^{-/-}$ forebrain by Affymetrix analysis, as measured by custom array. Those that show similar changes in both systems, regardless of p value, are in bold.

	CUSTOM ARRAY	AFFYMETRIX ARRAY
3 of genes of interest on array	240	12496
# of genes with > 1.5 fold change between wild type and PSD95$^{-/-}$ tissue	108	238
- as % of genes of interest on array	45%	1.90%
# of genes of interest significantly different in wild type and PSD95$^{-/-}$ tissue ($p<0.05$)	4	644
- as % of genes of interest on array	1.66%	5.15%
# of genes, called as present, with > 1.5 fold change between wild type and PSD95$^{-/-}$ tissue ($p<0.05$)	1	14
- as % of genes of interest on array	0.42%	0.11%

Table 5.7 – Comparison of Statistics From Custom and Commercial Arrays. Table details the differences in gene expression found in PSD95$^{-/-}$ forebrain compared to wild type as found by custom and Affymetrix arrays.

5.4 DISCUSSION

5.4.1 Designing and Printing a Custom Array

There are several advantages in designing and using a custom microarray. Wide scale analysis can be maintained, while genes of interest can be specified. Therefore all transcripts represented on a chip can be chosen to be relevant to the system being studied. This means genes of interest, that are not present on commercial chips, can be included on a custom array. For example, SynGAP is not present on the Affymetrix u74v2A array, but was included on our custom array. Using a oligonucleotide based array allows for specification of probes to particular regions of a gene, which can be exploited to identify splice variants or to distinguish highly conserved genes.

The limitation of using an oligonucleotide based array is that design depends on the availability of sequence. At the time the oligonucleotides for this array were designed (Autumn 2002), complete murine sequence was not available for all genes of interest, and in some cases no mouse sequence was available from public access databases. If the probes on the array were to be redesigned at the present time, it is likely that more sequence information would be available to aid this process. Another disadvantage of using custom based arrays, which will be discussed, is that they require thorough validation before they can be used reliably.

5.4.2 Comparison of Custom and Commercial Arrays

5.4.2.1 Comparison of Custom and Commercial Array Data

The genes represented on the custom array were selected due to their involvement in synaptic plasticity processes, including several transcripts that were found significantly altered in PSD95 and SynGAP mutant tissue by Affymetrix arrays. RNA aliquots of the same material extracted from the forebrain of wild type and $PSD95^{-/-}$ animals and hybridised to Affymetrix arrays, as detailed in chapter 3, were

used to compare the custom arrays to the commercial systems. The results from the custom arrays were not similar to those from the Affymetrix experiment.

The custom arrays identified alterations greater than 1.5 fold in 45% of the genes represented on the chip, however of these 108 transcripts only 1 gene determined present was significantly changed ($p<0.05$). This suggests that there was a variability in the expression levels measured by hybridisation to the custom arrays, such that many differences greater than 1.5 fold were detected but that high levels of variation meant few of these were of statistical relevance.

The only gene that was detected present in forebrain samples and was significantly altered, greater than 1.5 fold, in the PSD95$^{-/-}$ forebrain was *fzd6*. However this transcript, encoding a receptor acting in Wnt signalling pathways, was not found significantly altered in PSD95$^{-/-}$ tissue using commercial arrays. Indeed, the transcript was not even detected present by Affymetrix analysis. The disparities in the custom and commercial array results could be due to problems with the probes. It may be that the custom oligonucleotide is cross hybridising to another, highly expressed RNA, although it should be noted that mBLAST analysis found the probe to be specific to *fzd6* (data not shown). Alternatively, it may be that the Affymetrix probes for *fzd6* did not effectively hybridise their target.

Of the 9 transcripts represented on the custom array that were found significantly altered in PSD95$^{-/-}$ forebrain by Affymetrix analysis, only 3 showed similar changes on the custom array. None of these alterations were significant. While it could not be expected that the custom array would replicate the results of the Affymetrix experiments, a degree of overlap would have been assumed. A particularly striking difference in the custom and commercial array results is the data from the PSD95 probe. The PSD95 transcript was reliably found expressed at significantly lower levels in the PSD95$^{-/-}$ forebrain by Affymetrix array and RT-PCR protocols. The custom array detected the PSD95 transcript, however the level of the expression was

found to be unchanged in PSD95$^{-/-}$ and wild type samples. These results could be due to poor performance of the custom oligonucleotide. Also, the hybridisation temperature of the custom array could have been inappropriate, resulting in nonspecific binding to the probe.

5.4.2.2 Differences Between Custom and Commercial Systems

There appears to be clear differences in the results obtained by commercial and custom systems, for which there are several possible reasons. While no system can be 100% reliable, the Affymetrix arrays meet the high levels of quality control expected of a commercial system. The process of gene expression analysis by Affymetrix chip involves several stages of control to confirm whether the labelling and hybridisation protocols have been efficient. Thus, if experiments produce unexpected results, the control steps can help pinpoint the specific stages where problems may have occurred. As detailed in chapter 3, the Affymetrix hybridisation reactions met all quality standards and some of the results were validated using RT-PCR methods. Therefore, the Affymetrix data should be considered reliable, particularly since the limited genes identified as significantly altered include several with known roles in synaptic plasticity and neuronal function.

A disadvantage of the custom arrays is that they have fewer built in controls than the commercial system and hybridisation protocols have to be optimised before they can be used reliably. The custom arrays included positive and negative controls. However, in the RLS hybridisation of wild type and PSD95$^{-/-}$ samples some of the negative controls on the custom arrays were expressed at levels above the threshold of expression. This could be due to problems with these oligonucleotides, however, the negative controls were probes in standard use at the SCGTI. This suggests there may be a problem with the hybridisation reaction, with unusual background hybridisation occurring.

The limited numbers of genes classed as present (on average 32.7%) in the forebrain samples also indicates there may be a problem with the RLS hybridisation. The Affymetrix experiments found, on average, 46.75% of the transcripts represented on the array to be expressed in forebrain (wild type and PSD95$^{-/-}$) samples. Since the genes of interest specified on the custom array are known to be involved in postsynaptic mechanisms, it would be likely that the majority would be expressed in resting neuronal tissue. Of the 188 genes present on both the custom array and Affymetrix chip, 72% were detected present in wild type forebrain by Affymetrix analysis. It would therefore be expected that the custom arrays would detect at least this percentage of genes present, if not more to account for the probes on the custom array that are not included in the Affymetrix analysis. Consistent with this, the initial hybridisation of the custom arrays with Cy3 labelled samples found 88% of the genes of interest above the threshold of expression. The subsequent RLS hybridisation would have been expected to detect similar numbers. Since the threshold of detection for the RLS experiment was determined using the data from the negative controls, the unexpected levels of expression at the negative probes will have contributed to the reduced levels of detected transcripts.

The apparent problems with the RLS hybridisation could be due to a lack of optimisation of the reaction conditions. It may be that the hybridisation or washing temperatures used could be unsuitable. Unexpected expression of particular probes could also be due to inappropriate length of time for hybridisation or incubation with the RLS particles. Due to time constraints of this project, the comparison of wild type and PSD95$^{-/-}$ forebrain RNA was carried out before thorough validation of the custom arrays using RLS array hybridisation protocols. The ideal conditions for reaction may not have been used for the experimental hybridisation and, as a consequence, it produced unreliable results.

Another contributing factor to the differing results from custom and commercial arrays could be the number of probes, per transcript, used in each experiment.

Affymetrix arrays use at least 16 different probes to represent every transcript on each array. However, the custom arrays only have 3 identical probes present for each target gene. As such, in order to replicate the number of data points used by Affymetrix on a single array to calculate the expression of a transcript, at least 6 custom arrays would be required. A lack of replication may account, in part, for the results of custom array analysis of PSD95$^{-/-}$ forebrains. By using replicate slides for each sample, the custom array data may have sufficient data points contributing to measures of expression to reduce variation in results.

Another source of differences in results between the custom and commercial arrays could be the performance of particular probes on the arrays. Probes, either on the custom or Affymetrix array, for particular transcripts may not be behaving as expected to detect their intended target. In such cases, the measured level of expression would be inaccurate. Custom arrays oligonucleotides met particular criteria and were specific to target genes. However, some oligonucleotides (approximately 5-10%), even when designed to standard criteria with specificity to their target, do not perform as expected and may require redesigning (K. Veirlinger, personal communication). Thus, some of the unexpected results could be due to poor performance of such oligonucleotides. The probes designed by Affymetrix would be expected to meet strict quality standards, but they too could perform poorly with no obvious reason. However, Affymetrix arrays have multiple different probes, designed to each transcript, present on every chip. As such, individual probes that do not perform as expected would have a smaller impact on the measured expression levels of target genes on the Affymetrix arrays compared to the effect of a poorly performing probe on the commercial chips.

Before drawing firm conclusions from the comparison of wildtype and mutant RNA on custom arrays, the chips should be further validated. Standard RNAs could hybridised to multiple arrays and conditions of reaction optimised to ensure reproducibility of the data. Subsequently, RNA samples with known profile could

be used to ensure particular oligonucleotides are performing in the expected manner.

5.5 CONCLUSION

The data presented in this chapter has shown the development of a custom microarray. The genes of interest were selected and 55mers specific to each transcript were designed.

The arrays were printed and initial validation confirmed that the chips had been effectively printed and control oligonucleotides were behaving as expected. However, comparison PSD95$^{-/-}$ and wild type RNA from the forebrain of adult mice using the custom chip failed to replicate results found with the Affymetrix system. In this experiment, the control probes did not act as predicted with several of the negative control genes being determined to have unexpected high levels of expression. It may be that, due to a lack of thorough validation of the custom array, the reaction conditions for the chip were not optimal and thus the experiment yielded the unanticipated results.

The custom array that was designed would be valuable in studying NRC mutated RNA and NMDA receptor stimulated samples. It would enable the wide scale analysis of relevant genes with high throughput. However, further validation of the array is required to optimise reaction conditions in order for the chip to be used as a reliable tool for measuring gene expression.

CHAPTER 6

DISCUSSION

6. DISCUSSION

The NMDA receptor and it's protein complex is critical for spatial learning, synaptic plasticity and pathological conditions such as neuropathic pain. Therefore, further knowledge of the regulation of transcription by the NMDA receptor and associated molecules could be significant to the understanding of these important phenomena.

The objective of this project was to study the contribution of NRC proteins to NMDA receptor regulated gene expression. To achieve this microarray technology was used and methods of *in vitro* stimulation of the NMDA receptor studied, the results of which have been discussed in the appropriate chapters.

6.1 MICROARRAY ANALYSIS OF BRAIN TISSUE

6.1.1 Mutation of PSD95 and SynGAP Alters Gene Expression

It has been successfully demonstrated, for the first time, that mutations of NMDA receptor complex proteins disrupt gene expression. PSD95$^{-/-}$ and SynGAP$^{+/-}$ animals have significant alterations in a limited number transcripts in acutely dissected brain tissue, which include several genes induced by NMDA receptor activity. Given that PSD95 and SynGAP are known to act in pathways regulated by the receptor, it appears that the basal levels of particular genes are regulated by the NMDA receptor. Consistent with this, *in vitro* studies found that AP5 treatment of primary cultured cortical neurons significantly downregulated the levels of *cfos*, *nur77* and *egr2* RNA. The data suggests spontaneous synaptic activity regulates NMDA receptor dependent expression of particular genes and this is altered in PSD95$^{-/-}$ and SynGAP$^{+/-}$ tissue.

Analysis of NMDA receptor regulated gene expression is typically studied following induced activity of the receptor, for example, following LTP induction or pharmacological stimulation of the receptor. It is with such methods that *cfos*, *nur77* and *egr2* have been found to be activity regulated (Bading *et al.*, 1995; Inokuchi *et al.*,

1996). In contrast, the work presented in this thesis has found evidence of activity dependent gene regulation in acutely dissected brain tissue and spontaneously active neuronal cultures. The data from these experiments suggests that, in addition to any roles following intense stimulation, the NMDA receptor and associated proteins are critical to the regulation of basal transcription of particular genes.

Given that known activity regulated genes are altered in PSD95$^{-/-}$ and SynGAP$^{+/-}$ samples it suggests that the genes significantly altered in the mutant tissues could be a subset of the total genes regulated by the NMDA receptor. This raises the possibility that, although not previously identified as such, some of the significantly altered genes, other than *cfos, nur77, egr2* and *junB,* are also activity regulated transcripts. Indeed, there is already evidence to suggest some of these genes could be regulated via the NMDA receptor. *Per1* expression is regulated by the NMDA receptor in the SCN (Tischkau *et al.*, 2000) and this could also be the case in the hippocampus. *DUSP6* can be induced by seizure (Muda *et al.*, 1996), although it has not been shown whether this is NMDA receptor dependent. Also, *GADD45β* belongs to a family of proteins that are induced by environmental stress (Takekawa and Saito, 1998) and related transcript *GADD45α* is regulated by kainate seizure (Zhu *et al.*, 1997). As such, *GADD45β* may also be a transcript regulated by synaptic activity.

In addition to the activity regulated genes, several other genes that have known or hypothesised role in cognitive disorders, learning and plasticity were significantly altered in the mutant tissues. It appears that mutation of PSD95 and SynGAP results in the misregulation of key genes that are required for NMDA receptor mediated effects. As such, the Affymetrix analysis has identified several interesting candidate genes, such as *Per1,* which could have previously unreported function in learning processes and synaptic plasticity. In addition, significantly altered ESTs may represent novel genes that are involved NMDA receptor mediated effects.

The microarray analysis has also suggested ways in which the regulation of genes via NRC proteins could act as feedback to control signalling pathways downstream of the NMDA receptor. *Egr2* and *DUSP6* are both expressed at significantly lower levels in SynGAP$^{+/-}$ tissue, suggesting they could be regulated by the NMDA receptor via a SynGAP-ERK pathway. An egr2 binding site has been found in the SynGAP promoter. Thus the induction of egr2, via a SynGAP-ERK pathway, could result in a subsequent increase in SynGAP levels. Increases in SynGAP could then act to negatively regulate the ERK pathway. If *DUSP6* was induced by NMDA receptor activity via a SynGAP-ERK pathway, then the phosphotase could act as a negative regulator of ERK activity.

The misregulation of genes in PSD95$^{-/-}$ and SynGAP$^{+/-}$ animals could be the underlying cause of the phenotypes of these mice. In particular, the common alterations of *cfos, nur77* and *egr2* in PSD95$^{-/-}$ and SynGAP$^{+/-}$ tissue appear to correlate with the similar deficits in spatial learning seen in the animals. Also, mutation of several of the significantly altered genes (*cfos, cyln2* and *N-glycan alpha 2,8-sialtransferase)* results in phenotypes in LTP. As such, it appears that the basal expression of particular genes, critical for NMDA mediated effects in learning and plasticity, is regulated via the NMDA receptor and associated protein complex.

6.1.2 Further Application of Microarrays

There are several ways in which microarray analysis could be further employed to study NRC proteins and gene regulation in brain tissue. A key experiment, to follow the analysis of PSD95$^{-/-}$ forebrain and SynGAP$^{+/-}$ hippocampi, would be to analyse PSD95$^{-/-}$ hippocampi by microarray. This experiment may reveal similar changes to those seen in PSD95$^{-/-}$ forebrain, but may detect additional genes that specifically contribute to the hippocampal phenotypes of the animals. This experiment would also enable direct comparison of PSD95$^{-/-}$ and SynGAP$^{+/-}$ hippocampal data, an additional way to identify commonly misregulated genes in

these genotypes. It would also be interesting to carry out such analysis on tissue from animals carrying double mutations in PSD95 and SynGAP.

The successful analysis of PSD95$^{-/-}$ and SynGAP$^{+/-}$ tissue has proved microarrays to be a useful approach in the study of transgenic animals. As such, they could be effectively employed as a standard tool to analyse animals with plasticity phenotypes or carry targeted mutations in other NRC proteins. This analysis could help reveal which NMDA associated proteins are involved in the regulation of neuronal gene expression and could identify key genes that are similarly misregulated in animals sharing plasticity and learning phenotypes.

An important consideration in using the microarrays as a standard analysis tool for transgenic studies is ensuring experimental conditions are consistent. Since microarrays analyse the levels of thousands of transcripts simultaneously they are sensitive to variation between samples. The Affymetrix analysis of PSD95 and SynGAP mutant RNA was performed on material extracted from age, sex and, where possible, litter matched mutant and wild type animals. Dissections were all performed at the same time of day and subsequent RNA extraction and treatment carried out in parallel. The experimental design was deliberately kept simple and treatment of all samples consistent in order to maintain variation at a minimum. Any future analysis of mutant tissue should be carried out in the same way in order to yield reliable experimental results and ensure comparison of data sets from different genotypes is valid.

Commercially available microarrays were successfully used to study transgenic tissue. A custom array was subsequently designed of selected genes of interest that could be used more cost effectively for higher throughput analysis. The validation of the custom array using PSD95$^{-/-}$ RNA did not replicate the Affymetrix results as expected which, due to the time constraints of this project, could not be further analysed. It is likely that the custom array hybridisation protocol requires more

optimisation. Once the custom arrays are validated they could be applied to study mutant tissue and also used in the analysis of activity regulated gene expression following stimulation of the NMDA receptor.

6.2 ANALYSIS OF ACTIVITY REGULATED GENE EXPRESSION

The misregulation of genes in PSD95 and SynGAP mutant tissue is likely due to alterations in signalling downstream of the NMDA receptor. It would therefore be very interesting to study the effects of these mutations in stimulated cells. As has been discussed, there were problems in developing a reliable *in vitro* protocol for stimulating cultured cortical neurons. There are several ways in which the protocols could be modified that could make them more effective. The use of electrophysiology in combination with gene expression analysis could prove valuable in establishing the effects of pharmacological treatment on the behaviour of the cultures, and thus aid the development of stimulation methods.

If a suitable *in vitro* stimulation protocol were established this would enable the profile of wild type activity regulated gene expression to be identified. Also, the analysis of NMDA dependent gene expression in PSD95$^{-/-}$ and SynGAP$^{+/-}$ cells could confirm if the transcriptional alterations detected in mutant tissue were, indeed, a consequence of changes in NMDA mediated signalling. Due to the postnatal lethality of mice homozygote for SynGAP mutation, tissue from heterozygote animals was analysed by microarray. An *in vitro* method of stimulation could enable the study of SynGAP$^{-/-}$ cells as embryonic cultured cells could be used.

In vitro stimulation analysis could be applied to other mutant genotypes and could be conducted in the presence of inhibitors of different signalling pathways (e.g. CaM kinase inhibitors, MEK inhibitors). This would establish key pathways and molecules in the regulation of particular genes downstream of NMDA receptor activity. Furthermore, if the custom arrays were successfully validated, then the

gene expression analysis could be preformed on a relatively large scale with high throughput.

6.3 CONCLUSION

The work detailed in this thesis has demonstrated, conclusively, for the first time that mutation of NRC proteins results in altered gene expression. Transcripts significantly altered in PSD95$^{-/-}$ and SynGAP$^{+/-}$ tissue include activity regulated genes suggesting these changes could be due to disruption of NMDA receptor dependent transcription. The altered gene expression in PSD95$^{-/-}$ and SynGAP$^{+/-}$ mice correlates with phenotypes in spatial learning and could be the basis of the behavioural deficits of these animals. Development of a reliable *in vitro* stimulation protocol and optimisation of custom microarrays could be valuable to further analyse the contribution of NRC proteins to activity dependent gene expression.

INDEX OF FIGURES

INDEX OF TABLES

DETAILS OF APPENDIX 1 - 4

All appendices are contained, in Excel format, on the CD in the back page of the thesis.

Appendix 1 Wild Type and PSD95$^{-/-}$ Forebrain Affymetrix Analysis Data

Appendix 2 Wild Type and SynGAP$^{+/-}$ Hippocampus Affymetrix Analysis Data

Appendix 3 Oligonucloetides Designed for Custom Microarray

Appendix 4 Layout of Custom Microarray

REFERENCES

Abel T, Nguyen PV, Barad M, Deuel TA, Kandel ER, Bourtchouladze R. 1997. Genetic demonstration of a role for PKA in the late phase of LTP and in hippocampus-based long-term memory. *Cell* 88:615-26.

Adams JP, Sweatt JD. 2002. Molecular psychology: roles for the ERK MAP kinase cascade in memory. *Annu Rev Pharmacol Toxicol* 42:135-63.

Andreasson K, Worley PF. 1995. Induction of beta-A activin expression by synaptic activity and during neocortical development. *Neuroscience* 69:781-96.

Arendash GW, King DL, Gordon MN, Morgan D, Hatcher JM, Hope CE, Diamond DM. 2001. Progressive, age-related behavioral impairments in transgenic mice carrying both mutant amyloid precursor protein and presenilin-1 transgenes. *Brain Res* 891:42-53.

Atkins CM, Selcher JC, Petraitis JJ, Trzakis JM, Sweatt JD. 1998. The MAPK cascade is required for mammalian associative learning. *Nat Neurosci* 1:602-09.

Azuma T, Ao S, Saito Y, Yano K, Seki N, Wakao H, Masuho Y, Muramatsu M. 1999. Human SOX11, an upregulated gene during the neural differentiation, has a long 3' untranslated region. *DNA Res* 6:357-60.

Bach ME, Hawkins RD, Osman M, Kandel ER, Mayford M. 1995. Impairment of spatial but not contextual memory in CaMKII mutant mice with a selective loss of hippocampal LTP in the range of the theta frequency. *Cell* 81:905-15.

Bading H, Ginty DD, Greenberg ME. 1993. Regulation of gene expression in hippocampal neurons by distinct calcium signaling pathways. *Science* 260:181-6.

Bading H, Segal MM, Sucher NJ, Dudek H, Lipton SA, Greenberg ME. 1995. N-methyl-D-aspartate receptors are critical for mediating the effects of glutamate on intracellular calcium concentration and immediate early gene expression in cultured hippocampal neurons. *Neuroscience* 64:653-64.

Balschun D, Wolfer DP, Gass P, Mantamodiotis T, Welzl H, Shutz G, Frey JU, Lipp HP. 2003. Does cAMP Response Element-Binding Protein Have a Pivotal Role in Hippocampal Synaptic Plasticity and Hippocampus-Dependent Memory? *J Neurosci* 23:6304-14.

Bartsch D, Ghirardi M, Skehel PA, Karl KA, Herder SP, Chen M, Bailey CH, Kandel ER. 1995. *Aplysia* CREB2 represses long-term facilitation: relief of repression converts transient facilitation into long-term facilitation and structural change. *Cell* 83:979-92.

Basun H, Forsell LG, Wetterberg L, Winblad B. 1991. Metals and trace elements in plasma and cerebrospinal fluid in normal aging and Alzheimer's disease. *J. Neural. Transm. Park. Dis. Demen.*

Berkowitz LA, Riabowol KT, Gilman MZ. 1989. Multiple sequence elements of a single functional class are required for cyclic AMP responsiveness of the mouse c-fos promoter. *Mol Cell Biol* 9:4272-81.

Bessho Y, Nawa H, Nakanishi S. 1994. Selective up-regulation of an NMDA receptor subunit mRNA in cultured cerebellar granule cells by K(+)-induced depolarization and NMDA treatment. *Neuron* 12:87-95.

Bito H, Deisseroth K, Tsien RW. 1996. CREB phosphorylation and dephosphorylation: a Ca(2+)- and stimulus duration-dependent switch for hippocampal gene expression. *Cell* 87:1203-14.

Blalock EM, Chen K-C, Sharrow K, Herman JP, Porter NM, Foster TC, Landfield PW. 2003. Gene Micorarrays in Hippocampal Aging: Statistical Profiling Identifies Novel Processes Correlated with Cognitive Impairment. *J Neurosci* 23:3807-19.

Blattner C, Kannouche P, Litfin M, Bender K, Rahmsdorf HJ, Angulo JF, Herrlich P. 2000. UV-induced stabilisation of *cfos* and other short-leved mRNAs. *Mol Cell Biol* 20:3616-25.

Blum S, Moore AN, Adams F, Dash PK. 1999. A mitogen-activated protein kinase cascade in the CA1/CA2 subfield of the dorsal hippocampus is essentail for long-term spatial memory. *J Neurosci* 19:3535-44.

Bourtchuladze R, Frenguelli B, Blendy J, Cioffi D, Schutz G, Silva AJ. 1994. Deficient long-term memory in mice with a targeted mutation of the cAMP-responsive element-binding protein. *Cell* 79:59-68.

Brenman JE, Chao DS, Gee SH, McGee AW, Craven SE, Santillano DR, Wu Z, Huang F, Xia H, Peters MF, Froehner SC, Bredt DS. 1996. Interaction of nitric oxide synthase with the postsynaptic density protein (PSD95) and alpha1-syntrophin mediated by PDZ domains. *Cell* 84:757-67.

Brown V, Jin P, Ceman S, Darnell JC, O'Donnell WT, Tenenbaum SA, Jin X, Feng Y, Wilkinson KD, Keene JD, Darnell RB, Warren ST. 2001. Microarray identification of FMRP-associated brain mRNAs and altered mRNA translational profiles in fragile X syndrome. *Cell* 107:477-87.

Bulleit RF, Cui H, Wang J, Lin X. 1994. NMDA receptor activation in differentiating cerebellar cell cultures regulates the expression of a new POU gene, Cns-1. *J Neurosci* 14:1584-95.

Caron H, van Schaik B, van der Mee M, Baas F, Riggins G, van Sluis P, Hermus M-C, van Asperen R, Boon K, Voute PA, Heisterkamp S, van Kampen A, Versteeg R. 2001. The Human Transcriptome Map: Clustering of highly expressed genes in chromosomal domains. *Science* 291:1289-93.

Cavallaro S, D'Agata V, Manickam P, Dufour F, Alkon DL. 2002. Memory-specific temporal profiles of gene expression in the hippocampus. *PNAS* 99:16279-84.

Cavallaro S, Meiri N, Yi C, Musco S, Ma W, Goldberg J. 1997. Late memory-related genes in the hippocampus revealed by RNA fingerprinting. *Proc Natl Acad Sci U S A* 94:9669-73.

Chagnovich D, Cohn SL. 1997. Activity of a 40 kDa RNA-binding protein correlates with MYCN and c-fos mRNA stability in human neuroblastoma. *Eur J Cancer* 33:2064-7.

Chavrier P, Janssen-Timmen U, Mattei MG, Zerial M, Bravo R, Charnay P. 1989. Structure, chromosome location, and expression of the mouse zinc finger

gene Krox-20: multiple gene products and coregulation with the proto-oncogene c-fos. *Mol Cell Biol* 9:787-97.

Chawla S, Hardingham GE, Quinn DR, Bading H. 1998. CBP: A signal-regulated transcriptional coactivator controlled by nuclear calcium and CaM Kinase IV. *Science* 281:1505-09.

Chen F, Wollmer MA, Hoerndli F, Munch G, Kuhla B, Rogaev EI, Tsolaki M, Papassotiropoulos A, Gotz J. 2004. Role for glyoxalase I in Alzheimer's disease. *PNAS*:0402338101.

Chen HJ, Rojas-Soto M, Oguni A, Kennedy MB. 1998. A synaptic Ras-GTPase activating protein (p135 SynGAP) inhibited by CaM kinase II. *Neuron* 20:895-904.

Cho K, Hunt CA, Kennedy MB. 1992. The rat brain postsynaptic density fraction contains a homolog of the drosophila discs-large tumor suppressor protein. *Neuron* 9:929-42.

Cho RJ, Campbell MJ, Winzeler EA, Steinmetz L, Conway A, Wodicka L, Wolfsberg TG, Gabrielian AE, Landsman D, Lockhart DJ, Davis RW. 1998. A genome-wide transcriptional analysis of the mitotic cell cycle. *Mol Cell* 2:65-73.

Christy B, Nathans D. 1989. Functional serum response elements upstream of the growth factor-inducible gene zif268. *Mol Cell Biol* 9:4889-95.

Chrivia JC, Kwok RP, Lamb N, Hagiwara M, Montminy MR, Goodman RH. 1993. Phosphorylated CREB binds specifically to the nuclear protein CBP. *Nature* 365:855-9.

Chung KC, Shin SW, Yoo M, Lee MY, Lee HW, Choe BK, Ahn YS. 2000. A systemic administration of NMDA induces immediate early gene pip92 in the hippocampus. *J Neurochem* 75:9-17.

Cole AJ, Saffen DW, Baraban JM, Worley PF. 1989. Rapid increase of an immediate early gene messenger RNA in hippocampal neurons by synaptic NMDA receptor activation. *Nature* 340:474-6.

Collingridge GL, Kehl S, McLennan H. 1983. Excitatory amino acids in synaptic transmission in the Schaffer collateral-commissural pathway of the rat hippocampus. *J Physiol Lond* 334:33-46.

Dash PK, Karl KA, Colicos MA, Prywas R, Kandel ER. 1991. cAMP response element-binding protein is activated by Ca-calmodulin as well as cAMP dependnet protein kinase. *Proc Natl Acad Sci U S A* 88:5061-65.

Davis S, Vanhoutte P, Pages C, Caboche J, Laroche S. 2000. The MAPK/ERK cascade targets both Elk-1 and cAMP response element-binding protein to control long-term potentiation-dependent gene expression in the dentate gyrus in vivo. *J Neurosci* 20:4563-72.

Dawkins JL, Hulme DJ, Brahmbhatt SB, Auer-Grumbach M, Nicholson GA. 2001. Mutations in SPTLC1, encoding serine palmitoyltransferase, long chain base subunit-1, cause hereditary sensory neuropathy type I. *Nat Genet* 27:309-12.

De Smaele E, Zazzeroni F, Papa S, Nguyen DU, Jin R, Jones J, Cong R, Franzoso G. 2001. Induction of *gadd45B* by NF-kB downregulates pro-apoptotic JNK signalling. *Nature* 414:308-13.

De Zeeuw C, Hertzberg E, Mugnaini E. 1995. The dendritic lamellar body: a new neuronal organelle putatively associated with dendrodendritic gap junctions. *J. Neurosci.* 15:1587-604.

De Zeeuw CI, Hoogenraad CC, Goedknegt E, Hertzberg E, Neubauer A, Grosveld F, Galjart H. 1997. CLIP-115, a novel brain-specific cytoplasmic linker protein, mediates the localization of dendritic lamellar bodies. *Neuron* 19:1187-99.

Deisseroth K, Heist EK, Tsien RW. 1998. Translocation of calmodulin to the nucleus supports CREB phosphorylation in hippocampal neurons. *Nature* 392:198-202.

Dickey CA, Loring JF, Montgomery J, Gordon MN, Eastman PS, Morgan D. 2003. Selectively reduced expression of synaptic plasticity-related genes in amyloid precursor protein + presenilin-1 transgenic mice. *J Neurosci* 23:5219-26.

Ding JM, Faiman LE, Hurst WJ, Kuriashkina LR, Gillette MU. 1997. Resetting the Biological Clock: Mediation of Nocturnal CREB Phosphorylation via Light, Glutamate, and Nitric Oxide. *J. Neurosci.* 17:667-75.

Dragunow M, Abraham W, Hughes P. 1996. Activation of NMDA and muscarinic receptors induces nur-77 mRNA in hippocampal neurons. *Brain Res Mol Brain Res* 36:349-56.

Dragunow M, Abraham WC, Goulding M, Mason SE, Robertson HA, Faull RL. 1989. Long-term potentiation and the induction of c-fos mRNA and proteins in the dentate gyrus of unanesthetized rats. *Neurosci Lett* 101:274-80.

Dragunow M, Beilharz E, Mason B, Lawlor P, Abraham W, Gluckman P. 1993. Brain-derived neurotrophic factor expression after long-term potentiation. *Neurosci Lett* 160:232-6.

Dragunow M, Hughes P, Mason-Parker SE, Lawlor P, Abraham WC. 1997. TrkB expression in dentate granule cells is associated with a late phase of long-term potentiation. *Brain Res Mol Brain Res* 46:274-80.

Dutar P, Vaillend C, Viollet C, Billard J-M, Potier B, Carlo AS, Ungerer A, Epelbaum J. 2002. Spatial learning and synaptic hippocampal plasticity in type 2 somatostatin receptor knock-out mice. *Neuroscience* 112:455-66.

Eckhardt M, Bukalo O, Chazal G, Wang L, Goridis C, Schachner M, Gerardy-Schahn R, Cremer H, Dityatev A. 2000. Mice deficient in the polysiayltransferase ST8SialV/PST-1 allow discrimination of the roles of neural cell adhesion molecule protein and polysialic acid in neural development and synaptic plasticity. *J Neurosci* 20:5234-44.

English JD, Sweatt JD. 1996. Activation of p42 mitogen-activated protein kinase in hippocampal long term potentiation. *J Biol Chem* 271:24329-32.

Fagiolini M, Katagiri H, Miyamoto H, Mori H, Grant SGN, Mishina M, Hensch TK. 2003. Separable features of visual cortical plasticity revelaed by N-methyl-D-apartate receptor 2A signaling. *Proc Natl Acad Sci U S A* 100:2854-59.

Fleischmann A, Hvalby O, Jensen V, Strekalova T, Zacher C, Liliana EL, Kvello A, Reschke M, Spanagel R, Sprengel R, Wagner E, Gass P. 2003. Impaired Long-

Term Memory and NR2A-Type NMDA Receptor-Dependent Synaptic Plasticity in Mice Lacking c-Fos in the CNS. *J Neurosci* 23:9116-22.

Forrest D, Yuzaki M, Soares HD, Ng L, Luk DC, Sheng M, Stewart CL, Morgan JI, Connor JA, Curran T. 1994. Targeted disruption of NMDA receptor 1 gene abolishes NMDA response and results in neonatal death. *Neuron* 13:325-38.

Francke U. 1999. Williams-Beuren syndrome: genes and mechanisms. *Hum. Mol. Genet.* 8:1947-54.

French PJ, O'Connor V, Jones MW, Davis S, Errington ML, Voss K, Truchet B, Wotjak C, Stean T, Doyere V, Maroun M, Laroche S, Bliss TV. 2001. Subfield-specific immediate early gene expression associated with hippocampal long-term potentiation *in vivo*. *Eur J Neurosci* 13:968-76.

French PJ, O'Connor V, Voss K, Stean T, Hunt SP, Bliss TV. 2001. Seizure-induced gene expression in area CA1 of the mouse hippocampus. *Eur J Neurosci* 14:2037-41.

Fukaya M, Ueda H, Yamauchi K, Inoue Y, Watabe M. 1999. Distinct spatiotemporal expression of mRNAs for the PSD-95/SAP90 protein family in the mouse brain. *Neurosci Res* 33:111-18.

Gaiddon C, Loeffler JP, Larmet Y. 1996. Brain-derived neurotrophic factor stimulates AP-1 and cyclic AMP-responsive element dependent transcriptional activity in central nervous system neurons. *J Neurochem* 66:2279-86.

Ganetzky B, Robertson GA, Wilson GF, Trudeau MC, Titus SA. 1999. The eag family of K+ channels in Drosophila and mammals. *Ann N Y Acad Sci* 868:356-69.

Garcia JA, Zhang D, Estill SJ, Michnoff C, Rutter J, Reick M, Scott K, Diaz-Arrastia R, McKnight SL. 2000. Impaired Cued and Contextual Memory in NPAS2-Deficient Mice. *Science* 288:2226-30.

Garry EM, Moss A, Delaney A, O'Neill F, Blackemore J, Bowen J, Husi H, Mitchell R, Grant SGN, Fleetwood-Walker SM. 2003. Neuropathic sensitization of behavioral reflexes and spinal NMDA receptor/CaM Kinase II interactions are disrupted in PSD-95 mutant mice. *Curr Biol* 13:321-28.

Gass P, Wolfer DP, Balschun D, Rudolph D, Frey U, Lipp HP, Schutz G. 1998. Deficits in memory tasks of mice with CREB mutations depend on gene dosage. *Learn Mem* 5:274-88.

Gentz R, Rauscher FJ, 3rd, Abate C, Curran T. 1989. Parallel association of Fos and Jun leucine zippers juxtaposes DNA binding domains. *Science* 243:1695-9.

Gewurz H, Zhang XH, Lint TF. 1995. Structure and function of the pentraxins. *Curr Opin Immunol* 7:54-64.

Ghosh A, Ginty DD, Bading H, Greenberg ME. 1994. Calcium regulation of gene expression in neuronal cells. *J Neurobiol* 25:294-303.

Gonzalez GA, Montminy MR. 1989. Cyclic AMP stimulates somatostatin gene transcription by phosphorylation of CREB at serine 133. *Cell* 59:675-80.

Griffith LC, Wang J, Zhong Y, Chun-Fang W, Greenspan RF. 1994. Calcium/calmodulin-dependent protein kinase II and potassium channel

subunit Eag similarly affect plasticity in *Drosophila*. *Proc Natl Acad Sci U S A* 91:10044-48.

Grootjans JJ, Zimmermann P, Reekmans G, Smets A, Degeest G, Durr J, David G. 1997. Syntenin, a PDZ protein that binds syndecan cytoplasmic domains. *Proc Natl Acad Sci U S A* 94:13683-8.

Guzowski JF, Lyford GL, Stevenson GD, Houston FP, McGaugh JL, Worley PF, Barnes CA. 2000. Inhibition of activity-dependent arc protein expression in the rat hippocampus impairs the maintenance of long-term potentiation and the consolidation of long-term memory. *J Neurosci* 20:3993-4001.

Guzowski JF, Setlow B, Wagner EK, McGaugh JL. 2001. Experience-dependent gene expression in the rat hippocampus after spatial learning: a comparison of the immediate-early genes Arc, c-fos, and zif268. *J Neurosci* 21:5089-98.

Hanada K, Hara T, Nishijima M. 2000. D-Serine inhibits serine palmitoyltransferase, the enzyme catalyzing the initial step of sphingolipid biosynthesis. *FEBS Lett* 474:63-5.

Hardingham GE, Arnold FJ, Bading H. 2001. Nuclear calcium signaling controls CREB-mediated gene expression triggered by synaptic activity. *Nat Neurosci* 4:261-7.

Hardingham GE, Bading H. 2003. The Yin and Yang of NMDA receptor signalling. *Trends Neurosci* 26:81-89.

Hardingham GE, Chawla S, Cruzalegui FH, Bading H. 1999. Control of recruitment and transcription-activating function of CBP determines gene regulation by NMDA receptors and L-type calcium channels. *Neuron* 22:789-98.

Hardingham GE, Chawla S, Johnson CM, Bading H. 1997. Distinct functions of nuclear and cytoplasmic calcium in the control of gene expression. *Nature* 385:260-5.

Hardingham GE, Fukunaga Y, Bading H. 2002. Extrasynaptic NMDARs oppose synaptic NMDARs by triggering CREB shut-off and cell death pathways. *Nat Neurosci*.

Harrington CA, Rosenow C, Retief J. 2000. Monitoring gene expression using DNA microarrays. *Curr Opin Micro* 3:285-91.

Hirbec H, Perestenko O, Nishimune A, Meyer G, Nakanishi S, Henley JM, Dev KK. 2002. The PDZ Proteins PICK1, GRIP, and Syntenin Bind Multiple Glutamate Receptor Subtypes. ANALYSIS OF PDZ BINDING MOTIFS. *J Biol Chem* 277:15221-4.

Ho N, Liauw JA, Blaeser F, Wei F, Hanissian S, Muglia LM, Wozniak DF, Nardi A, Arvin KL, Holtzman DM, Linden DJ, Zhuo M, Muglia LJ, Chatila TA. 2000. Impaired synaptic plasticity and cAMP response element-binding protein activation in Ca2+/calmodulin-dependent protein kinase type IV/Gr-deficient mice. *J Neurosci* 20:6459-72.

Hong SJ, Huiwu L, Becker KG, Dawson VL, Dawson TM. 2004. Identification and analysis of plasticity-induced late-response genes. *Proc Natl Acad Sci U S A* 101:2145-50.

Honkaniemi J, Sharp FR. 1999. Prolonged expression of zinc finger immediate-early gene mRNAs and decreased protein synthesis following kainic acid induced seizures. *Eur J Neurosci* 11:10-17.

Hoogenraad CC, Koekkoek B, Akhmanove A, Krugers H, Dortland B, Miedama M, van Alphen A, Kistler WM, Jaegle M, Koutsourakis M, van Camp N, Verhoye M, van der Linden A, Kaverina I, Grosveld F, De Zeeuw CI, Galjart N. 2002. Targeted mutation of *cyln2* in the Williams syndrome critical region links CLIP-115 haploinsufficiency to neurodevelopmental abnormalities in mice. *Nat Genet* 32:116-27.

Hu SC, Chrivia J, Ghosh A. 1999. Regulation of CBP-mediated transcription by neuronal calcium signaling. *Neuron* 22:799-808.

Huang AM, Wang HL, Tang YP, Lee EH. 1998. Expression of integrin-associated protein gene associated with memory formation in rats. *J Neurosci* 18:4305-13.

Huang YY, Kandel ER. 1994. Recruitment of long-lasting protein kinase A dependent long term potentiation in the CA1 region of hippocampus requires repeated tentanization. *Learn Mem* 1:74-82.

Hummler E, Cole TJ, Blendy JA, Ganss R, Aguzzi A, Schmid W, Beermann F, Shutz G. 1994. Targeted mutation of the CREB gene: compensations withing the CREB/ATF family of transcription factors. *Proc Natl Acad Sci U S A* 91:5647-51.

Husi H, Ward MA, Choudhary JS, Blackstock WP, Grant SG. 2000. Proteomic analysis of NMDA receptor-adhesion protein signaling complexes. *Nat Neurosci* 3:661-9.

Impey S, Fong AL, Wang Y, Cardinaux J-R, Fass DM, Obrietan K, Wayman GA, Storm DR, Soderling TR, Goodman RH. 2002. Phosphorylation of CBP mediates transcriptional actiavtion by neural activity and CaM kinase IV. *Neuron* 34:235-44.

Impey S, Mark M, Villacres EC, Poser S, Chavkin C, Storm DR. 1996. Induction of CRE-mediated gene expression by stimuli that generate long-lasting LTP in area CA1 of the hippocampus. *Neuron* 16:973-82.

Impey S, Obrietan K, Wong ST, Poser S, Yano S, Wayman G, Deloulme JC, Chan G, Storm DR. 1998. Cross talk between ERK and PKA is required for Ca2+ stimulation of CREB-dependent transcription and ERK nuclear translocation. *Neuron* 21:869-83.

Inokuchi K, Kato A, Hiraia K, Hishinuma F, Inoue M, Ozawa F. 1996. Increase in activin beta A mRNA in rat hippocampus during long-term potentiation. *FEBS Lett* 382:48-52.

Inokuchi K, Murayama A, Ozawa F. 1996. mRNA differential display reveals Krox-20 as a neural plasticity-regulated gene in the rat hippocampus. *Biochem Biophys Res Commun* 221:430-6.

Jin K, Mao XO, Eshoo MW, Nagayama T, Minami M, Simon RP, Greenberg DA. 2001. Microarray analysis of hippocampal gene expression in global cerebral ischemia. *Ann Neurol* 50:93-103.

Johnston RS, Spiegelman BM, Papaioannou V. 1992. Pleiotropic effects of a null mutation in the c-fos proto-oncogene. *Cell* 71:577-86.

Jones MW, Errington ML, French PJ, Fine A, Bliss TV, Garel S, Charnay P, Bozon B, Laroche S, Davis S. 2001. A requirement for the immediate early gene Zif268 in the expression of late LTP and long-term memories. *Nat Neurosci* 4:289-96.

Jung N, Sun W, Lee H, Cho S, Shim C, Kim K. 1998. Gonadotropin-releasing hormone (GnRH) gene regulation by N-methyl-D-aspartic acid in GT1-1 neuronal cells: differential involvement of c-fos and c-jun protooncogenes. *Brain Res Mol Brain Res* 61:162-9.

Kang H, Sun LD, Atkins CM, Soderling TR, Wilson MA, Tonegawa S. 2001. An important role of neural activity-dependent CaMKIV signaling in the consolidation of long-term memory. *Cell* 106:771-83.

Kato A, Ozawa F, Saitoh Y, Hirai K, Inokuchi K. 1997. vesl, a gene encoding VASP/Ena family related protein, is upregulated during seizure, long-term potentiation and synaptogenesis. *FEBS Lett* 412:183-9.

Kida S, Josselyn SA, de Ortiz SP, Kogan JH, Chevere I, Masushige S, Silva AJ. 2002. CREB required for the stability of new and reactivated fear memories. *Nat Neurosci* 5:348-55.

Kim JE, Lee H-K, Takamiya K, Huganir RL. 2003. The Role of Synaptic GTPase-Activating Protein in Neuronal Development and Synaptic Plasticity. *J Neurosci* 23:1119-24.

Kim JH, Liao D, Lau LF, Huganir RL. 1998. SynGAP: a synaptic RasGAP that associates with the PSD-95/SAP90 protein family. *Neuron* 20:683-91.

Kiss JZ, Wang C, Olive S, Rougon G, Lang J, Baetens D, Harry D, Pralong WF. 1994. Acitivty-dependent mobilisation of the adhesion molecule polysialic NCAM to the cell surface of neurons and endocrine cells. *Embo J* 13:5284-92.

Kogan JH, Frankland PW, Blendy JA, Coblentz J, Marowitz Z, Schutz G, Silva AJ. 1997. Spaced training induces normal long-term memory in CREB mutant mice. *Curr Biol* 7:1-11.

Komiyama NH, Watabe AM, Carlisle HJ, Porter K, Charlesworth P, Monti J, Strathdee DJC, O'Carroll CM, Martin SJ, Morris RGM, O'Dell TJ, Grant SGN. 2002. SynGAP regulates ERK/MAPK signaling, synaptic plasticity and learning in the complex with postsynaptic density 95 and NMDA receptor. *J Neurosci* 22:9721-32.

Konietzko U, Kauselmann G, Scafidi J, Staubli U, Mikkers H, Berns A, Schweizer M, Waltereit R, Kuhl D. 1999. Pim kinase expression is induced by LTP stimulation and required for the consolidation of enduring LTP. *Embo J* 18:3359-69.

Kononen J, Bubendorf L, Kallioniemi A, Barlund M, Schraml P, Leighton S, Torhorst J, Mihatsch MJ, Sauter G, Kallioniemi OP. 1998. Tissue microarrays for high-throughput molecular profiling of tumor specimens. *Nat Med* 4:844-47.

Kornau HC, Schenker LT, Kennedy MB, Seeburg PH. 1995. Domain interaction between NMDA receptor subunits and the postsynaptic density protein PSD-95. *Science* 269:1737-40.

Kutsuwada T, Kashiwabuchi N, Mori H, Sakimura K, Kushiya E, Araki K, Meguro H, Masaki H, Kumanishi T, Arakawa M, et al. 1992. Molecular diversity of the NMDA receptor channel. *Nature* 358:36-41.

Kutsuwada T, Sakimura K, Manabe T, Takamiya K, Katakura N, Kushiya E, Natsume R, Watanabe M, Inoue Y, Yagi T, Aizawa S, Arakawa M, Takahashi T, Nakamura Y, Mori H, Mishina M. 1996. Impairment of suckling response, trigeminal neuron pattern formation, and hippocampal LTD in NMDA receptor e2 subunit mutant mice. *Neuron* 16:333-44.

Lanahan A, Worley P. 1998. Immediate-Early Genes and Synaptic Function. *Neurobiol Learn Mem* 70:37-43.

Leil TA, Ossadtchi A, Cortes JS, Leahy RM, Smith DJ. 2002. Finding new candidate genes for learning and memory. *J Neurosci Res* 68:127-37.

Lein ES, Zhao X, Gage F. 2004. Defining a molecular atlas of the hippocampus using DNA microarrays and high throughput *in situ* hybridisation. *J Neurosci* 24:3879-89.

Lesage F, Lauritzen I, Duprat F, Reyes R, Fink M, Heurteaux C, Lazdunski M. 1997. The structure, function and distribution of the mouse TWIK-1 K+ channel. *FEBS Lett* 402:28-32.

Levenson JM, Choi S, Lee S-Y, Cao YA, Ahn HJ, Worley KC, Pizzi M, Liou H-C, Sweatt JD. 2004. A bioinformatics analysis of memory consolidation reveals involvement of the transcription factor c-Rel. *J Neurosci* 24:3933-43.

Link W, Konietzkl U, Kauselmann G, Krug M, Schwanke B, Frey U, Kuhl D. 1995. Somatodendritic expression of an immediate early gene is regulated by synaptic activity. *Proc Natl Acad Sci U S A* 92:5734-38.

Lyford GL, Yamagata K, Kaufmann WE, Barnes CA, Sanders LK, Copeland NG, Gilbert DJ, Jenkins NA, Lanahan AA, Worley PF. 1995. Arc, a growth factor and activity-regulated gene, encodes a novel cytoskeleton-associated protein that is enriched in neuronal dendrites. *Neuron* 14:433-45.

Ma C, Staudt LM. 2000. Molecular definition of the germinal centre stage of B-cell differentiation. *Philos Trans R Soc Lond B Biol Sci.* 356:83-89.

Marais R, Wynne J, Treisman R. 1993. The SRF accessory protein ELK-1 contains a growth factor-regulated transcriptional activation domain. *Cell* 73:381-93.

Matsuo R, Kato A, Sakaki Y, Inokuchi K. 1998. Cataloging altered gene expression during rat hippocampal long-term potentiation by means of differential display. *Neurosci Lett* 244:173-6.

Matsuo R, Murayama A, Saitoh Y, Sakaki Y, Inokuchi K. 2000. Identification and cataloging of genes induced by long-lasting long-term potentiation in awake rats. *J Neurochem* 74:2239-49.

Matyina A, Kushner SA, Silva AJ. 2002. Genetic Approaches to Molecular and Cellular Cognition: A Focus on LTP and Learning and Memory. *Annu Rev Genet* 36:687-720.

Mayer DJ, Mao J, Holt J, Price DD. 1999. Cellular mechanisms of neuropathic pain, morphine tolerance, and their interactions. *Proc Natl Acad Sci U S A* 96:7731-36.

Mayford M, Bach ME, Huang YY, Wang L, Hawkins RD, Kandel ER. 1996. Contgrol of memory formation through regulated expression of a CaMKII transgene. *Science* 274:1678-83.

Mazzucchelli C, Vantaggiato C, Ciamei A, Fasano S, Pakhotin P, Krezel W, Welzl H, Wolfer DP, Pages G, Valverde O, Marowsky A, Porrazzo A, Orban PC, Maldonado R, Ehrengruber MU, Cestari V, Lipp HP, Chapman PF, Pouyssegur J, Brambilla R. 2002. Knockout of ERK1 MAP kinase enhances synaptic plasticity in the striatum and facilitates striatal-mediated learning and memory. *Neuron* 34:807-20.

Meguro H, Mori H, Araki K, Kushiya E, Kutsuwada T, Yamazaki M, Kumanishi T, Arakawa M, Sakimura K, Mishina M. 1992. Functional characterization of a heteromeric NMDA receptor channel expressed from cloned cDNAs. *Nature* 357:70-4.

Migaud M, Charlesworth P, Dempster M, Webster LC, Watabe AM, Makhinson M, He Y, Ramsay MF, Morris RG, Morrison JH, O'Dell TJ, Grant SG. 1998. Enhanced long-term potentiation and impaired learning in mice with mutant postsynaptic density-95 protein. *Nature* 396:433-9.

Mitsuda N, Ohkubo N, Tamatani M, Lee YD, Taniguchi M, Namikawa K, Kiyama H, Yamaguchi A, Sato N, Sakata K, Ogihara T, Vitek MP, Tohyama M. 2001. Activated cAMP-response element-binding protein regulates neuronal expression of presenilin-1. *J Biol Chem* 276:9688-98.

Mody M, Cao Y, Cui Z, Tay K-Y, Shyong A, Shimizu E, Pham K, Schultz P, Welsh D, Tsien JZ. 2001. Genome-wide gene expression profiles of the developing mouse hippocampus. *Proc Natl Acad Sci U S A* 98:8862-67.

Montminy MR, Sevarino KA, Wagner JA, Mandel G, Goodman RH. 1986. Identification of a cyclic-AMP-responsive element within the rat somatostatin gene. *Proc Natl Acad Sci U S A* 83:6682-6.

Moriyoshi K, Masu M, Ishii T, Shigemoto R, Mizuno N, Nakanishi S. 1991. Molecular cloning and characterization of the rat NMDA receptor. *Nature* 354:31-7.

Morris RG, Anderson E, Lynch GS, Baudry M. 1986. Selective impairment of learning and blockade of long-term potentiation by an N-methyl-D-aspartate receptor antagonist, AP5. *Nature* 319:774-6.

Muda M, Boschert U, Dickinson R, Martinou J-C, Martinou I, Camps M, Schlegel W, Arkinstall S. 1996. MKP-3, a novel cytosolic protein-tyrosine phosphatase that exemplifies a new class of mitogen-activated protein kinase phosphatase. *J Biol Chem* 271:4319-26.

Muller D, Wang C, Skibo G, Toni N, Cremer H, Calaora V, Rougon G, Kiss JZ. 1996. PSA-NCAM is required for activity-induced synaptic plasticity. *Neuron* 17:413-22.

Murphy TH, Worley PF, Nakabeppu Y, Christy B, Gastel J, Baraban JM. 1991. Synaptic regulation of immediate early gene expression in primary cultures of cortical neurons. *J Neurochem* 57:1862-72.

Naeve GS, Ramakrishnan M, Kramer R, Hevroni D, Citri Y, Theill LE. 1997. Neuritin: a gene induced by neural activity and neurotrophins that promotes neuritogenesis. *Proc Natl Acad Sci U S A* 94:2648-53.

Nagai T, Yamada K, Kim HC, Kim YS, Noda Y, Imura A, Nabeshima Y, Nabeshima T. 2003. Cognition impairment in the genetic model of aging klotho gene mutant mice: a role of oxidative stress. *Faseb J* 17:50-2.

Nagarajan R, Svaren J, Le N, Araki T, Watson M, Milbrandt J. 2001. EGR2 mutations in inherited neuropathies dominant-negatively inhibit myelin gene expression. *Neuron* 30:355-68.

Nedivi E, Hevroni D, Naot D, Israeli D, Citri Y. 1993. Numerous candidate plasticity-related genes revealed by differential cDNA cloning. *Nature* 363:718-22.

Newton SS, Collier EF, Hunsberger J, Adams D, Terwilliger R, Selvanayagam E, Duman RS. 2003. Gene Profile of Electroconvulsive Seizures: Induction of Neurotrophic and Angiogenic Factors. *J Neurosci* 23:10841-51.

Nguyen PV, Abel T, Kandel ER. 1994. Requirement of a critical period of transcription for induction of a late phase of LTP. *Science* 265:1104-7.

Niethammer M, Kim E, Sheng M. 1996. Interaction between the C terminus of NMDA receptor subunits and multiple members of the PSD-95 family of membrane associated guanylate kinases. *J Neurosci* 16:2157-63.

O'Brien RJ, Xu D, Petralia RS, Steward O, Huganir RL, Worley P. 1999. Synaptic clustering of AMPA receptors by the extracellular immediate-early gene product Narp. *Neuron* 23:309-23.

Paylor R, Johnson RS, Papaioannou V, Spiegelman BM, Wehner JM. 1994. Behavioural assessment of c-fos mutant mice. *Brain Res* 651:275-82.

Platenik J, Kuramoto N, Yoneda Y. 2000. Molecular mechanisms associated with long-term consolidation of the NMDA signals. *Life Sci* 67:335-64.

Qian X, Esteban L, Vass WC, Upadhyaya C, Papageorge AG, Yienger K, Ward JM, Lowy DR, Santos E. 2000. The Sos1 and Sos2 Ras-specific exchange factors: differences in placental expression and signaling properties. *Embo J* 19:642-54.

Qian Z, Gilbert ME, Colicos MA, Kandel ER, Kuhl D. 1993. Tissue-plasminogen activator is induced as an immediate-early gene during seizure, kindling and long-term potentiation. *Nature* 361:453-7.

Rage F, Alonso G, Tapia-Arancibia L. 1993. Stimulatory effect of N-methyl-D-aspartate on somatostatin gene expression in cultured hypothalamic neurons. *Brain Res Mol Brain Res* 17:287-94.

Rahmsdorf H, Schonthal A, Angel P, Litfin M, Ruther U, Herrlich P. 1987. Posttranscriptional regulation of c-fos mRNA expression. *Nucl. Acids. Res.* 15:1643-59.

Reick M, Garcia JA, Dudley C, McKnight SL. 2001. NPAS2: An Analog of Clock Operative in the Mammalian Forebrain. *Science* 293:506-09.

Ressler KJ, Paschall G, Zhou X-L, Davis M. 2002. Regulation of synaptic plasticity genes during consolidation of fear conditioning. *J Neurosci* 22:7892-902.

Rickard JE, Kreis TE. 1996. CLIPs for organelle-microtubule interactions. *Trends Cell Biol* 6:178-83.

Rimini R, Beltrame M, Argenton F, Szymczak D, Cotelli F, Bianchi ME. 1999. Expression patterns of zebrafish sox11A, sox11B and sox21. *Mech Dev* 89:167-71.

Rivera VM, Sheng M, Greenberg ME. 1990. The inner core of the serum response element mediates both the rapid induction and subsequent repression of c-fos transcription following serum stimulation. *Genes Dev* 4:255-68.

Ryseck RP, MacDonald-Bravo H, Mattei MG, Siegfried RL, Bravo R. 1989. Structure, mapping and expression of a growth factor inducible gene encoding a putative nuclear hormonal binding receptor. *Embo J* 8:3327-35.

Sakimura K, Kutsuwada T, Ito I, Manabe T, Takayama C, Kushiya E, Yagi T, Aizawa S, Inoue Y, Sugiyama H. 1995. Reduced hippocampal LTP and spatial learning in mice lacking NMDA receptor epsilon 1 subunit. *Nature* 373:151-5.

Sassone-Corsi P, Visvander J, Ferland L, Mellon PL, Verma IM. 1988. Induction of proto-oncogene fos transcription through the adenylate cyclase pathway: characterization of a cAMP-responsive element. *Genes Dev* 2:1529-38.

Schulze A, Downward J. 2001. Navigating gene expression using microarrays - a technology review. *Nat Cell Biol* 3:E190-E95.

Shan Y, Carlock LR, Walker PD. 1997. NMDA receptor overstimulation triggers a prolonged wave of immediate early gene expression: relationship to excitotoxicity. *Exp Neurol* 144:406-15.

Shaw KN, Commins S, O'Mara SM. 2003. Deficits in spatial learning and synaptic plasticity induced by the rapid and competitive broad-spectrum cyclooxygenase inhibitor ibuprofem are reversed by increasing endogenous brain-derived neurotrophic factor. *Eur J Neurosci* 17:2438-46.

Sheng M, Thompson MA, Greenberg ME. 1991. CREB: A Ca2+ regulated transcription factor phosphorylated by calmodulin-dependent kinases. *Science* 252:1427-30.

Silva AJ, Paylor R, Wehner JM, Tonegawa S. 1992. Impaired spatial learning in alpha-calcium-calmodulin kinase II mutant mice. *Science* 257:206-11.

Smirnova T, Laroche S, Errington ML, Hicks AA, Bliss TV, Mallet J. 1993. Transsynaptic expression of a presynaptic glutamate receptor during hippocampal long-term potentiation. *Science* 262:433-6.

Spellmen P, Rubin GM. 2002. Evidence for large domains of similarly expressed genes in the *Drosophila* genome. *J Biol* 1:5.1-5.8.

Springer JE, Gwag BJ, Sessler FM. 1994. Neurotrophic factor mRNA expression in dentate gyrus is increased following in vivo stimulation of the angular bundle. *Brain Res Mol Brain Res* 23:135-43.

Steward O, Worley PF. 2001. Selective targeting of newly synthesized Arc mRNA to active synapses requires NMDA receptor activation. *Neuron* 30:227-40.

Stork PJS, Schmitt JM. 2002. Crosstalk between cAMP and MAP kinase signaling in the regulation of cell proliferation. *Trends in Cell Biology* 12:258-66.

Strausak D, Mercer JFB, Dieter HH, Stremmel W, Multhaup G. 2001. Copper in disorders with neurological symptoms: Alzheimer's, Menkes, and Wilson diseases. *Brain Research Bulletin* 55:175-85.

Su AI, Cooke MP, Ching KA, Hakak Y, Walker JR, Wiltshire T, Orth AP, Vega RG, Sapinoso LM, Moqrich A, Patapoutian A, Hampton GM, Schultz PG, Hogenesch JB. 2002. Large-scale analysis of the human and mouse transcriptomes. *Proc Natl Acad Sci U S A*:012025199.

Sun P, Enslen H, Myung PS, Maurer RA. 1994. Differential activation of CREB by Ca2+ calmodulin dependent protein kinases type II and IV involves phosphorylation of a site that regulates activity. *Genes Dev* 8:2527-39.

Szekely AM, Barbaccia ML, Costa E. 1987. Activation of specific glutamate receptor subtypes increases c-fos proto-oncogene expression in primary cultures of neonatal rat cerebellar granule cells. *Neuropharmacology* 26:1779-82.

Szekely AM, Costa E, Grayson DR. 1990. Transcriptional program coordination by N-methyl-D-aspartate-sensitive glutamate receptor stimulation in primary cultures of cerebellar neurons. *Mol Pharmacol* 38:624-33.

Takeichi M. 1991. Cadherin cell adhesion receptors as a morphogenetic regulator. *Science* 251:1451-55.

Takekawa M, Saito H. 1998. A family of stress inducible GADD45-like proteins mediate activation of the stress-responsive MTK1/MEKK4 MAPKKK. *Cell* 95:521-30.

Tang Y-P, Shimizu E, Dube GR, Rampon C, Kerchner GA, Zhuo M, Liu G, Tsien JZ. 1999. Genetic enhancement of learning and memory in mice. *Nature* 401:63-69.

Thornalley PJ. 2003. Glyoxalase 1 - Structure, function and a critical role in the enzymatic defenxe against glycation. *Biochemical Society Transactions* 31:1343-49.

Tischkau SA, Gallman EA, Buchanan GF, Gillette MU. 2000. Differential cAMP Gating of Glutamatergic Signaling Regulates Long-Term State Changes in the Suprachiasmatic Circadian Clock. *J. Neurosci.* 20:7830-37.

Tischkau SA, Mitchell JW, Tyan S-H, Buchanan GF, Gillette MU. 2003. Ca2+/cAMP Response Element-binding Protein (CREB)-dependent Activation of Per1 Is Required for Light-induced Signaling in the Suprachiasmatic Nucleus Circadian Clock. *J. Biol. Chem.* 278:718-23.

Tomczak KK, Marinescu VD, Ramoni MF, Sanoudou D, Montanaro F, Han M, Kunkel LM, Kohane IS, Beggs AH. 2004. Expression profiling and identification of novel genes involved in myogenic differentiation. *FASEB J.* 18:403-05.

Topilko P, Schneider-Maunoury S, Levi G, Baron-Van Evercooren A, Chennoufi ABY, Seitanidou T, Babinet C, Charnay P. 1994. Krox-20 controls myelination in the peripheral nervous system. *Nature* 371:796-99.

Treisman R. 1986. Identification of a protein-binding site that mediates transcriptional response of the *cfos* gene to serum factors. *Cell* 46:567-74.

Tsien JZ, Huerta PT, Tonegawa S. 1996. The essential role of hippocampal CA1 NMDA receptor-dependent synaptic plasticity in spatial memory. *Cell* 87:1327-38.

Tsui CC, Copeland NG, Gilbert DJ, Jenkins NA, Barnes C, Worley PF. 1996. Narp, a novel member of the pentraxin family, promotes neurite outgrowth and is dynamically regulated by neuronal activity. *J Neurosci* 16:2463-78.

Uchida N, Honjo Y, Johnson K, Wheelock M, Takeichi M. 1996. The catenin/cadherin adhesion system is localized in synaptic junctions bordering transmitter release zones. *J. Cell Biol.* 135:767-79.

Uemura H, Mizokami A, Chang C. 1994. Identification of a New Enhancer in the Promoter Region of Human TR3 Orphan Receptor Gene. *J. Biol. Chem.* 270:5427-33.

Uwanogho D, Rex M, Cartwright EJ, Pearl G, Healy C, Scotting PJ, Sharpe PT. 1995. Embryonic expression of the chicken *Sox2, Sox3* and *Sox11* genes suggests an interactive role in neuronal development. *Mech Dev* 49:23-36.

Versteeg R, van Schaik BDC, van Batenburg MF, Roos M, Monajemi R, Caron H, Bussemaker HJ, van Kampen AHC. 2003. The human transcriptome map reveals extremes in gene density, intron length, GC content, and repeat pattern for domains of highly and weakly expressed genes. *Genome Res* 13:1998-2004.

Vulpe C, Levinson B, Whitney S, Packman S, Gitschier J. 1993. Isolation of a candidate gene for Menkes disease and evidence that it encodes a copper-transporting ATPase. *Nat Genet* 3:7-13.

Warner LE, Mancias P, Butler IJ, McDonald CM, Keppen L, Koob KG, Lupski JR. 1998. Mutations in the early growth response 2 (EGR2) gene are association with hereditary myelinopathies. *Nat Genet* 18:382-84.

Watson A, Mazumder A, Stewart M, Balasubramanian S. 1998. Technology for microarray analysis of gene expression. *Curr Opp Biotech* 9:609-14.

Wilson TE, Fahrner TJ, Johnston M, Milbrandt J. 1991. Identification of the DNA binding site for NGFI-B by genetic selection in yeast. *Science* 252:1296-300.

Woods DF, Bryant PJ. 1991. The disc-large tumor suppressor gene of Drosophila encodes a guanylate kinase homolog localized at septate junctions. *Cell* 66:451-64.

Wu GY, Deisseroth K, Tsien RW. 2001. Activity-dependent CREB phosphorylation: convergence of a fast, sensitive calmodulin kinase pathway and a slow, less sensitive mitogen-activated protein kinase pathway. *Proc Natl Acad Sci U S A* 98:2808-13.

Xia Z, Dudek H, Miranti CK, Greenberg ME. 1996. Calcium influx via the NMDA receptor induces immediate early gene transcription by a MAP kinase/ERK-dependent mechanism. *J Neurosci* 16:5425-36.

Xing J, Kornhauser JM, Xia Z, Thiele EA, Greenberg ME. 1998. Nerve growth factor activates exreascellular signal regulated kinase and p38 mitogen activated protein kinase pathways to stimulate CREB serine 133 phosphorylation. *Mol Cell Biol* 18:1946-55.

Yamagata K, Andreasson KI, Kaufmann WE, Barnes CA, Worley PF. 1993. Expression of a mitogen-inducible cyclooxygenase in brain neurons: regulation by synaptic activity and glucocorticoids. *Neuron* 11:371-86.

Yamagata K, Andreasson KI, Sugiura H, Maru E, Dominique M, Irie Y, Miki N, Hayashi Y, Yoshioka M, Kaneko K, Kato H, Worley PF. 1999. Arcadlin is a neural activity-regulated cadherin involved in long term potentiation. *J Biol Chem* 274:19473-1979.

Yamagata K, Kaufmann WE, Lanahan A, Papapavlou M, Barnes CA, Andreasson WI, Worley P. 1994. Egr3/Pilot, a zinc finger transcription factor, is rapidly regulated by activity in brain neurons and colocalizes with Egr1/zif268. *Learn Mem* 1:140-52.

Yamagata K, Sanders LK, Kaufmann WE, Yee W, Barnes CA, Nathans D, Worley PF. 1994. rheb, a growth factor- and synaptic activity-regulated gene, encodes a novel Ras-related protein. *J Biol Chem* 269:16333-9.

Yang YH, Speed T. 2002. Design Issues For cDNA Microarray Experiments. *Nat Rev Genet* 3:579-88.

Yin JC, Wallach JS, Del Vacchio M, Wilder EL, Zhou H, Quinn WG, Tully T. 1994. Induction of a dominant negative CREB transgene specifically blocks long-term memory in *Drosophila*. *Cell* 79:49-58.

Zhang J, McQuade JM, Vorhees CV, Xu M. 2002. Hippocampal expression of c-fos is not essential for spatial learning. *Synapse* 46:91-99.

Zhong J, Russell SL, Pritchett DB, Molinoff PB, Williams K. 1994. Expression of mRNAs encoding subunits of the N-methyl-D-aspartate receptor in cultured cortical neurons. *Mol Pharmacol* 45:846-53.

Zhu RL, Graham SH, Jin J, Stetler RA, Simon RP, Chen J. 1997. Kainate induces the expression of the DNA damage-inducible gene, GADD45, in the rat brain. *Neuroscience* 81:707-20.

Zimmermann P, Tomatis D, Rosas M, Grootjans J, Leenaerts I, Degeest G, Reekmans G, Coomans C, David G. 2001. Characterization of syntenin, a syndecan-binding PDZ protein, as a component of cell adhesion sites and microfilaments. *Mol Biol Cell* 12:339-50.

Zirlinger M, Kreiman G, Anderson DJ. 2001. Amygdala-enriched genes identified by microarray technology are restricted to specific amygdaloid subnuclei. *Proc Natl Acad Sci U S A* 98:5270-5.